



CHALMERS
UNIVERSITY OF TECHNOLOGY

Annex 55

Reliability of Energy Efficient Building Retrofitting- Probability Assessment of Performance and Cost (RAP-RETRO)

Probabilistic Tools

HANS JANSSEN

STAF ROELS

LIESJE VAN GELDER

PAYEL DAS

KU Leuven Belgium

KU Leuven Belgium

KU Leuven Belgium

University College London, UK

International Energy Agency



Energy in Buildings and
Communities Programme

Probabilistic Tools

Authors: Hans Janssen, Staf Roels, Liesje Van Gelder, Payel Das

Reviewers: Thomas Bednar, Zoltan Sadovsky

© CARL-ERIC HAGENTOFT AND AUTHORS, 2015

Report 2015:4

ISSN 1652-9162

Department of Civil and Environmental Engineering

Division of Building Technology

Chalmers University of Technology

SE-412 96 Gothenburg

Sweden

Telephone + 46 (0)31-772 1000

© Copyright Chalmers University of Technology, 2015

All property rights, including copyright, are vested in Chalmers University of Technology, Operating Agent for EBC Annex 55, on behalf of the Contracting Parties of the International Energy Agency Implementing Agreement for a Programme of Research and Development on Energy in Buildings and Communities.

In particular, no part of this publication may be reproduced, stored in a retrieval system or transmitted in any form or by any means, electronic, mechanical, photocopying, recording or otherwise, without the prior written permission of Chalmers University of Technology.

Published by Chalmers University of Technology, SE-412 96 Göteborg, Sweden

Disclaimer Notice: This publication has been compiled with reasonable skill and care. However, neither Chalmers University of Technology nor the EBC Contracting Parties (of the International Energy Agency Implementing Agreement for a Programme of Research and Development on Energy in Buildings and Communities) make any representation as to the adequacy or accuracy of the information contained herein, or as to its suitability for any particular application, and accept no responsibility or liability arising out of the use of this publication. The information contained herein does not supersede the requirements given in any national codes, regulations or standards, and should not be regarded as a substitute for the need to obtain specific professional advice for any particular application.

ISSN 1652-9162

Participating countries in EBC:

Australia, Austria, Belgium, Canada, P.R. China, Czech Republic, Denmark, Finland, France, Germany, Greece, Ireland, Italy, Japan, Republic of Korea, the Netherlands, New Zealand, Norway, Poland, Portugal, Spain, Sweden, Switzerland, Turkey, United Kingdom and the United States of America.

Additional copies of this report may be obtained from:

EBC Bookshop

C/o AECOM Ltd

Colmore Plaza

Colmore Circus Queensway

Birmingham B4 6AT

United Kingdom

Web: www.iea-ebc.org

Email: essu@iea-ebc.org

Preface

The International Energy Agency

The International Energy Agency (IEA) was established in 1974 within the framework of the Organisation for Economic Co-operation and Development (OECD) to implement an international energy programme. A basic aim of the IEA is to foster international co-operation among the 28 IEA participating countries and to increase energy security through energy research, development and demonstration in the fields of technologies for energy efficiency and renewable energy sources.

The IEA Energy in Buildings and Communities Programme

The IEA co-ordinates research and development in a number of areas related to energy. The mission of the Energy in Buildings and Communities (EBC) Programme is to develop and facilitate the integration of technologies and processes for energy efficiency and conservation into healthy, low emission, and sustainable buildings and communities, through innovation and research. (Until March 2013, the IEA-EBC Programme was known as the Energy in Buildings and Community Systems Programme, ECBCS.)

The research and development strategies of the IEA-EBC Programme are derived from research drivers, national programmes within IEA countries, and the IEA Future Buildings Forum Think Tank Workshops. The research and development (R&D) strategies of IEA-EBC aim to exploit technological opportunities to save energy in the buildings sector, and to remove technical obstacles to market penetration of new energy efficient technologies. The R&D strategies apply to residential, commercial, office buildings and community systems, and will impact the building industry in five focus areas for R&D activities:

- Integrated planning and building design
- Building energy systems
- Building envelope
- Community scale methods
- Real building energy use

The Executive Committee

Overall control of the IEA-EBC Programme is maintained by an Executive Committee, which not only monitors existing projects, but also identifies new strategic areas in which collaborative efforts may be beneficial. As the Programme is based on a contract with the IEA, the projects are legally established as Annexes to the IEA-EBC Implementing Agreement. At the present time, the following projects have been initiated by the IEA-EBC Executive Committee, with completed projects identified by (*):

- Annex 1: Load Energy Determination of Buildings (*)
- Annex 2: Ekistics and Advanced Community Energy Systems (*)
- Annex 3: Energy Conservation in Residential Buildings (*)
- Annex 4: Glasgow Commercial Building Monitoring (*)
- Annex 5: Air Infiltration and Ventilation Centre
- Annex 6: Energy Systems and Design of Communities (*)
- Annex 7: Local Government Energy Planning (*)
- Annex 8: Inhabitants Behaviour with Regard to Ventilation (*)
- Annex 9: Minimum Ventilation Rates (*)
- Annex 10: Building HVAC System Simulation (*)
- Annex 11: Energy Auditing (*)
- Annex 12: Windows and Fenestration (*)
- Annex 13: Energy Management in Hospitals (*)
- Annex 14: Condensation and Energy (*)
- Annex 15: Energy Efficiency in Schools (*)

- Annex 16: BEMS 1- User Interfaces and System Integration (*)
- Annex 17: BEMS 2- Evaluation and Emulation Techniques (*)
- Annex 18: Demand Controlled Ventilation Systems (*)
- Annex 19: Low Slope Roof Systems (*)
- Annex 20: Air Flow Patterns within Buildings (*)
- Annex 21: Thermal Modelling (*)
- Annex 22: Energy Efficient Communities (*)
- Annex 23: Multi Zone Air Flow Modelling (COMIS) (*)
- Annex 24: Heat, Air and Moisture Transfer in Envelopes (*)
- Annex 25: Real time HVAC Simulation (*)
- Annex 26: Energy Efficient Ventilation of Large Enclosures (*)
- Annex 27: Evaluation and Demonstration of Domestic Ventilation Systems (*)
- Annex 28: Low Energy Cooling Systems (*)
- Annex 29: Daylight in Buildings (*)
- Annex 30: Bringing Simulation to Application (*)
- Annex 31: Energy-Related Environmental Impact of Buildings (*)
- Annex 32: Integral Building Envelope Performance Assessment (*)
- Annex 33: Advanced Local Energy Planning (*)
- Annex 34: Computer-Aided Evaluation of HVAC System Performance (*)
- Annex 35: Design of Energy Efficient Hybrid Ventilation (HYBVENT) (*)
- Annex 36: Retrofitting of Educational Buildings (*)
- Annex 37: Low Exergy Systems for Heating and Cooling of Buildings (LowEx) (*)
- Annex 38: Solar Sustainable Housing (*)
- Annex 39: High Performance Insulation Systems (*)
- Annex 40: Building Commissioning to Improve Energy Performance (*)
- Annex 41: Whole Building Heat, Air and Moisture Response (MOIST-ENG) (*)
- Annex 42: The Simulation of Building-Integrated Fuel Cell and Other Cogeneration Systems (FC+COGEN-SIM) (*)
- Annex 43: Testing and Validation of Building Energy Simulation Tools (*)
- Annex 44: Integrating Environmentally Responsive Elements in Buildings (*)
- Annex 45: Energy Efficient Electric Lighting for Buildings (*)
- Annex 46: Holistic Assessment Tool-kit on Energy Efficient Retrofit Measures for Government Buildings (EnERGo) (*)
- Annex 47: Cost-Effective Commissioning for Existing and Low Energy Buildings (*)
- Annex 48: Heat Pumping and Reversible Air Conditioning (*)
- Annex 49: Low Exergy Systems for High Performance Buildings and Communities (*)
- Annex 50: Prefabricated Systems for Low Energy Renovation of Residential Buildings (*)
- Annex 51: Energy Efficient Communities (*)
- Annex 52: Towards Net Zero Energy Solar Buildings (*)
- Annex 53: Total Energy Use in Buildings: Analysis & Evaluation Methods (*)
- Annex 54: Integration of Micro-Generation & Related Energy Technologies in Buildings
- Annex 55: Reliability of Energy Efficient Building Retrofitting - Probability Assessment of Performance & Cost (RAP-RETRO)
- Annex 56: Cost Effective Energy & CO2 Emissions Optimization in Building Renovation
- Annex 57: Evaluation of Embodied Energy & Greenhouse Gas Emissions for Building Construction
- Annex 58: Reliable Building Energy Performance Characterisation Based on Full Scale Dynamic Measurements
- Annex 59: High Temperature Cooling & Low Temperature Heating in Buildings
- Annex 60: New Generation Computational Tools for Building & Community Energy Systems
- Annex 61: Business and Technical Concepts for Deep Energy Retrofit of Public Buildings
- Annex 62: Ventilative Cooling
- Annex 63: Implementation of Energy Strategies in Communities
- Annex 64: LowEx Communities - Optimised Performance of Energy Supply Systems with

Exergy Principles

Annex 65: Long-Term Performance of Super-Insulating Materials in Building Components and Systems

Annex 66: Definition and Simulation of Occupant Behavior in Buildings

Annex 67: Energy Flexible Buildings

Working Group - Energy Efficiency in Educational Buildings (*)

Working Group - Indicators of Energy Efficiency in Cold Climate Buildings (*)

Working Group - Annex 36 Extension: The Energy Concept Adviser (*)

ANNEX 55, SUBTASK 2

PROBABILISTIC TOOLS

Authors

Hans Janssen
Staf Roels
Liesje Van Gelder
Payel Das

Acknowledgements

Subtask 2 would not have been possible without the many contributions of the Annex 55 participants to our Common Exercises. Our gratitude goes out to Angela Kalagasidis, Carl-Eric Hagertoft, Pär Johansson and Vahid Nik (Chalmers, Sweden), Anker Nielsen (Danish Building Research Institute, Denmark), Carsten Rode (Technical University of Denmark), Christoph Harreither and Paul Wegerer (Vienna University of Technology, Austria), Fitsum Tariku (British Columbia Institute of Technology, Canada), Florian Antretter, Marcus Fink (Fraunhofer, Germany), Henrik Karlsson, Kristina Mjörnell (SP Technical Research Institute of Sweden), Jianhua Zhao (Dresden University of Technology, Germany), Liesje Van Gelder (KU Leuven, Belgium), Mika Saloonvara (Owens Corning, United States), Mike van der Heijden (TU Eindhoven, the Netherlands), Payel Das and Benjamin Jones (University College London, United Kingdom), Simo Illomets (Talinn University of Technology, Estonia).

Table of contents

1	Subtask 2 of Annex 55	1
1.1	Introduction	2
1.1.1	Annex 55 and Subtask 2	2
1.1.2	Sets of probabilistic tools	3
1.2	First illustration	4
1.2.1	Improving a supply network.....	4
1.2.2	The probabilistic assessment	4
1.2.3	Conclusion and continuation.....	5
1.3	Common Exercises.....	6
1.3.1	Common Exercises in Subtask 2	6
1.3.2	Qualitative exploration: CE1.....	6
1.3.3	Uncertainty propagation: CE2	7
1.3.4	Sensitivity analysis: CE3.....	9
1.3.5	Metamodelling method: CE4	10
1.3.6	Economic optimisation: CE5.....	11
1.4	Summary.....	14
1.5	References	15
2	Qualitative exploration.....	16
2.1	Introduction	17
2.1.1	Annex 55 and Subtask 2	17
2.1.2	Qualitative exploration tools.....	17
2.1.3	'Gains and costs' concept.....	19
2.2	Common Exercise 1.....	20
2.2.1	Presentation of Exercise	20
2.2.2	Outcomes from Exercise	20
2.2.3	Discussion of outcomes.....	23
2.3	Conclusions	25
2.4	References	26

3	Uncertainty quantification.....	27
3.1	Introduction	28
3.1.1	Uncertainty quantification for decision making.....	28
3.2	Quantitative methods.....	29
3.2.1	FORM and SORM-methods	29
3.2.2	Monte-Carlo methods	30
3.3	Advanced MC-methods.....	31
3.3.1	Sampling techniques	31
3.3.2	Sampling efficiency and sampling convergence.....	33
3.4	Common Exercise 2.....	35
3.4.1	Presentation of Exercise	35
3.4.2	Outcomes from Exercise	35
3.5	References	36
4	Sensitivity analysis.....	37
4.1	Introduction	38
4.1.1	Sensitivity analysis tools.....	38
4.2	Presentation of methods	39
4.2.1	Introduction.....	39
4.2.2	One-at-a-time methods.....	39
4.2.3	Screening methods.....	40
4.2.4	Correlation-based methods	41
4.2.5	Segmentation-based methods	41
4.2.6	Variance-based methods.....	42
4.3	Evaluation of methods	44
4.3.1	Methodology of evaluation.....	44
4.3.2	Presentation of evaluation	46
4.3.3	Conclusion of evaluation	52
4.4	Conclusions	53
4.5	References	54

5	Metamodelling methods	55
5.1	Introduction	56
5.1.1	Metamodelling methods	56
5.2	Presentation of methods	58
5.2.1	Basic principles	58
5.2.2	Polynomial regression	58
5.2.3	Multivariate adaptive regression splines (MARS)	59
5.2.4	Kriging	60
5.2.5	Neural networks	61
5.3	Evaluation of metamodelling approaches	65
5.3.1	Calculation object	65
5.3.2	Outcomes of the exercise	65
5.3.3	Quality assessment procedure	66
5.3.4	Result comparison	67
5.3.5	Comparison	73
5.4	Conclusions	77
5.5	References	78
6	Economic optimisation	80
6.1	Introduction	81
6.1.1	Background	81
6.2	Presentation of methods	83
6.2.1	Performance criterion	83
6.2.2	Objective function	84
6.2.3	Optimization schemes	86
6.2.4	Application to the renovation of attics	88
6.3	Evaluation of methods	91
6.3.1	Impact of performance criterion	91
6.3.2	Impact of objective function definition	92
6.3.3	Impact of optimization scheme	95
6.4	Discussion and conclusions	97
6.5	References	99

7	Conclusion	102
7.1	Quantification methodology	103
7.1.1	Introduction.....	103
7.1.2	Preprocessing	104
7.1.3	Uncertainty quantification	105
7.1.4	Final optimisation.....	106
7.1.5	Final thought	107
7.2	References	108
	Addenda.....	109
	Addendum 1	110
	Addendum 2	110
	Addendum 3	110
	Addendum 4	110
	Addendum 5	110

1

SUBTASK 2 OF ANNEX 55

Lead authors

Hans Janssen

Staf Roels

1.1 Introduction

1.1.1 Annex 55 and Subtask 2

The importance of identifying, characterising and displaying the uncertainties on the results of analyses and designs of complex systems is progressively more recognised: many regulatory standards and guidelines explicitly demand an uncertainty appraisal as part of a performance assessment of structures, systems and solutions (Helton and Burmaster, 1996). This appraisal of uncertainties is naturally connected to the concepts of ‘reliability’ and ‘robustness’. Reliability can be defined as the probability for the system to function without a failure during a given interval of time, robustness can be described as the persistence of the characteristic behaviour of a system under uncertain conditions. Reliability, in essence, concerns the probability of failure, while robustness more generally relates to the probability of a certain performance level. But both concepts fundamentally require the assessment of probabilities, calling for the application of probabilistic methodologies rather than deterministic techniques. Or, to quote Oberkampf and co-authors (2002), all “realistic modelling and simulation of complex systems must include the non-deterministic features of the system and the environment”.

The appraisal of the life-cycle gains and costs of a building retrofit is an example of such a complex system, in which the non-deterministic features may originate from stochastic variations in materials, workmanship, user behaviour, economic scenarios, ... Annex 55 therefore aims at providing a foundation for the integration of probabilistic approaches in analyses and designs of hygrothermal performances of buildings. This foundation is to consist of four parts:

1. an overall framework and methodology for probabilistic analysis and design in relation to hygrothermal performances of buildings (subtask 3);
2. probabilistic tools that permit qualitative and quantitative assessment of the impacts of the non-deterministic features in these (subtask 2);
3. data sets characterising the stochastic variations of influencing parameters, for use in the qualitative and quantitative methods (subtask 1);
4. guidelines for application of the general framework, probabilistic tools and stochastic inputs for reliability-based analysis and design (subtask 4);

The primary objective of Annex 55’s Subtask 2 therefore is to appraise the advantages and disadvantages of existing probabilistic methods for qualitative and quantitative assessment with relation to their applicability within the particular context of building performance analysis and design. Subtask 2 does hence not intend to develop new probabilistic tools, instead it aims at familiarizing building physical engineers and researchers with the possibilities and limitations of existing probabilistic tools adopted from various other fields. When applied within the overall probabilistic framework of Subtask 3, based on the guidelines for use of Subtask 4, and fed with the stochastic data from Subtask 1, these tools will allow the non-deterministic appraisal of the life-cycle gains and costs of a thermal building retrofit, with attention for both the potential improvement as well as possible degradation resulting from such upgrades of residential buildings.

1.1.2 Sets of probabilistic tools

Five sets of tools are required for probabilistic assessments, each with a distinct purpose:

1. *qualitative exploration*:
to identify all relevant parameters, and the relations between them;
2. *uncertainty propagation*:
to quantify the probabilistic character of the assessment's outcome;
3. *sensitivity analysis*:
to determine the dominant and the non-dominant input parameters;
4. *metamodelling method*:
to formulate a simple surrogate model, to replace the original model;
5. *economic optimisation*:
financial criteria and optimisation schemes to attain the best solution;

The latter may not be a pure probabilistic tool in itself, but there are sufficient implicit links to include it here.

These five sets of probabilistic tools each form the topic of a Common Exercise in Subtask 2, all aiming at evaluating the capabilities and limitations of different available methods. These five sets of probabilistic tools moreover are the respective subject of the following chapters, which constitute the main report for Subtask 2. Below, these five tool sets, and their respective function in any probabilistic assessment, are first illustrated with a clear-cut example from another field, in Section 1.2. Subsequently, the five Common Exercises of Subtask 2 are presented in Section 1.3, each centred on one of the five sets of probabilistic tools.

1.2 First illustration

1.2.1 Improving a supply network

The different sets of the required suite of probabilistic tools are put forward via an easy example from another engineering discipline, a supply system for electricity. This system consists of a turbine, fed by a main fuel and a backup fuel, and distributing electricity via a cable network. The owner of the electricity supply system wants to avoid all expenses related to power outages, but not at all costs of course, since the avoided expenses should be in balance with the investments needed to improve the reliability of the system.

1.2.2 The probabilistic assessment

First, the possible influence factors related to all possible gains and costs of investments to improve the reliability of the electricity supply system are to be identified, via a *qualitative exploration*. As a first step, the analysis focuses on the basic failure modes of the system, the economic aspects are integrated at a later stage. The electricity supply system fails when the consumer no longer receives electricity, which happens if either the cable network is damaged or if the engine is stopped, which in turn is presumed to occur if both main and backup fuel come to depletion. This assessment, merging identification and organisation of hazards, can be presented as a fault tree, tying all elements of the assessment logically together (Figure 1.1).

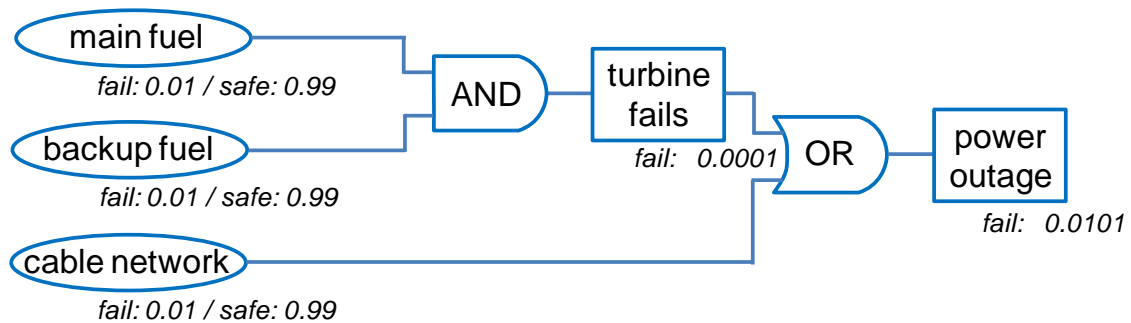


Figure 1.1: Fault tree for the electricity supply network and its primary components

Next, the assessment moves on to *uncertainty propagation*, in which the failure probability of the electricity supply system is explicitly calculated. Based on information on the reliabilities of the fuel supplies and of the cable network, one estimates that each component – main fuel, backup fuel, cable network – has a 1 % chance of failure. So at any moment in time, there is a one percent probability that any of the three components does not deliver. Based on the rules of probability calculus, the probability of engine failure (due to a lack of fuel) becomes 0.0001, and the probability of total system failure become 0.0101. These figures can now be added to the fault tree in Figure 1.1.

After that, the assessment turns to identifying these factors that may have a considerable impact on the failure rate of the electricity supply network, as these are the prime factors to consider when planning an enhancement of the system's reliability. The results of this *sensitivity analysis* are straightforward: reducing the failure probability of the main or backup fuel to zero only has a limited impact (total failure rate 0.01 instead of 0.0101), while decreasing the failure probability of the cable network to zero has a crucial effect (total failure rate 0.0001 instead of 0.0101). In this very simplified case hence, improvements are to concentrate on the cable network rather than the fuel supplies.

At this point in the analysis, one could go back to the start, to further refine the significant influence factors, which is here the failure of the cable network. One could further detail its failure rate, assess the failure rate reductions for different possible measures, document the relevant investment and penalty costs, ... For this example, the additional input data are kept restricted to the gains and costs of possible measures. A 10,000 € investment reduces the failure rate of the cable network to 0.005, while a further reduction to 0.002 would cost an additional 80,000 €, whereas the system failure penalty amounts to 10,000,000 €.

The current example comprises an easy to compute case, which precludes the need for a surrogate model. But, if the quantification of failure rates and its related expenses would require a large computational effort for example, then the formulation of a surrogate model through a *metamodelling method* should be considered. Such a metamodel is a simpler and faster stand-in for the original model, which is hence easier to use in the assessment. To do so, a limited number of scenarios with different input values could be run, and a simple relation between relevant inputs and outputs could be derived, for example with linear regression.

As a final step, the *economic optimisation* can be executed. For this case, only three design options are to be judged: no investment, investing 10,000 €, or investing 10,000 € plus 80,000 €. That first alternative is the neutral choice: nothing lost, nothing gained. The second possibility invests 10,000 € to save 10,000,000 € 0.5 % of the time: the expected value of the costs thus is 10,000 euro, the expected value of the gains is 50,000 €. For the third option these numbers become respectively 90,000 € and 75,000 €. The second possibility thus compares positively to the neutral choice while the third option on the other hand results in a negative balance.

1.2.3 Conclusion and continuation

While this simple example has allowed an introductory explanation of the five primary sets of probabilistic tools, their application to building physical analyses and designs comes with more facets and details, which will be illustrated via more complex thermal building retrofit cases in the following chapters. Before turning to those though, the five Common Exercises of Subtask 2 are concisely presented in Section 1.3 below.

1.3 Common Exercises

1.3.1 Common Exercises in Subtask 2

Subtask 2 of Annex 55 targets the evaluation of the advantages and disadvantages of available methods for probabilistic assessment, categorised in five sets of tools: *qualitative exploration*, *uncertainty propagation*, *sensitivity analysis*, *metamodelling method*, and *economic optimisation*. The appraisal of the five tool sets has been performed via five respective Common Exercises (CE), all of which involved the execution of a particular assignment by multiple Annex participants. Each of these five CE's will come back in the following five chapters, but here an initial presentation is given as a general framework.

1.3.2 Qualitative exploration: CE1

Common Exercise 1 set out to evaluate the capabilities and limitations of qualitative exploration methods within the context of building performance assessments. The CE1 objective was a factor identification and flowchart formation analysis of different post-insulation options for a brick cavity wall, considering both the gains by decreased energy consumption and the costs due to potential hygrothermal damage (see Addendum 1 for more info). Such qualitative exploration could in a next stage support a quantitative comparison.

Figure 1.2 depicts the case considered in CE1: a cavity wall section of a typical mid-century Danish villa is to be thermally upgraded. Three main options exist for the thermal upgrade of this cavity wall: internal insulation, external insulation or cavity filling. Each of these has a different potential efficiency for reduction in building energy consumption and a different potential risk for hygrothermal damages. The primary objective of CE1 was a flowchart for the probabilistic evaluation of the energy consumption and hygrothermal damage. The flowchart should not only identify all factors potentially affecting the energy consumption and hygrothermal damage, but also logically connect all these potential influence parameters to the final estimation of energy consumption and hygrothermal damage. The application and/or evaluation of different methods for factor identification and flowchart formation to that aim then allowed judging the respective advantages and disadvantages of these methods.

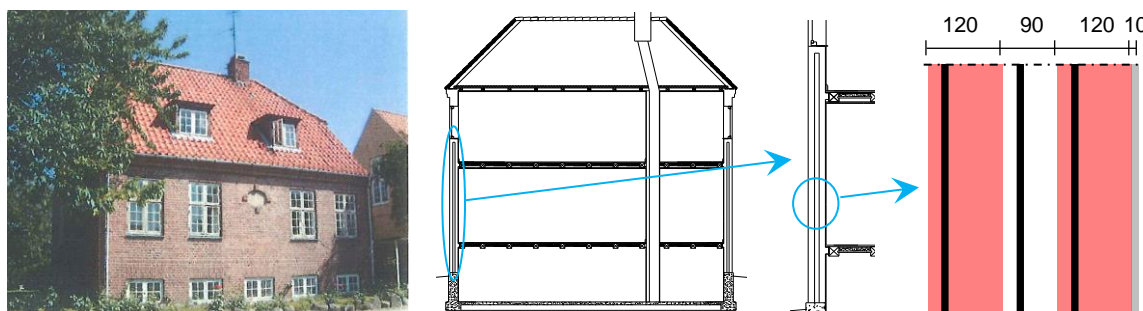


Figure 1.2: Schematic overview of the configuration for CE1.

An exemplary partial outcome of the qualitative exploration analysis is presented in Figure 1.3. This flowchart focuses on one aspect of hygrothermal damage, particularly the deterioration of the interior finishing due to surface condensation and/or mould growth. The flowchart hence identifies all interacting parameters and organizes their interwoven relations. From the chart, it becomes clear that assessing the probability of degradation requires information about the ventilation, the workmanship, ...

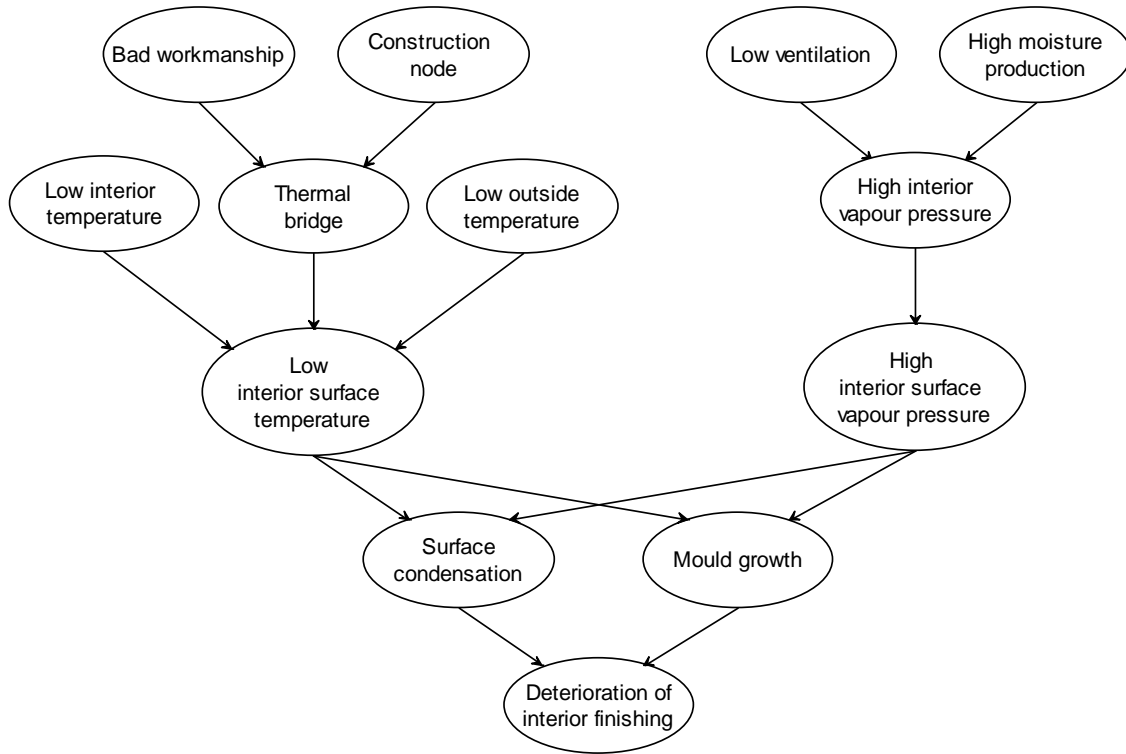


Figure 1.3: Illustrative outcome of CE1 - Bayesian probabilistic net for 'deterioration of interior finishing'

1.3.3 Uncertainty propagation: CE2

The capabilities and limitations of uncertainty propagation methods for building performance applications have been investigated exploratorily in CE2 for a particular retrofitting solution at the building component level. The topic was the probabilistic prediction of energy savings and mould growth for the application of interior insulation on an existing massive masonry wall. To simplify the hygrothermal assessment, a one-dimensional wall section was applied as starting point. This allows investigating different stochastic methodologies for a well-described one-dimensional HAM-problem (HAM: Heat, Air and Moisture), currently typically assessed by deterministic analyses.

Figure 1.4 presents a schematic overview of the problem: an outer brick layer (uniform layer of 29 cm thick) is renovated with interior insulation (6cm) and finished at the inside with a coated gypsum board. The wall is assumed to be perfectly airtight and is submitted to variable indoor and outdoor climates. The hygrothermal material properties of the different layers have been provided (see Addendum 2 for more info), wherein some of them treated as stochastic varia-

bles, with given distribution functions. Also the orientation of the wall and the ventilation rate governing the indoor climate are variable inputs for the assessment. The hygrothermal response of the wall had to be calculated for one year, starting from July 1st until June 30th. To evaluate the benefits and risks of the retrofit measure, both the wall heat loss and the mould growth risk were to be analysed. The thermal performance of the wall was judged by the cumulative heat losses during the month of January calculated at the interior surface. The risk on mould growth had to be judged at the interface between interior insulation and masonry wall. This was based on a simplified mould growth model, inspired by the VTT mould prediction model [Viitanen and Ojanen, 2007], in which a mould growth index is calculated based on the predicted local relative humidity. As output, the evolution of the mould growth index had to be given as a function of time. As an example, figure 1.5 presents the variability of the evolution of the heat losses for the month of January and the increase of the mould growth index over the year, as predicted by one of the participants. The reference case, in which the mean values of the stochastic variables are taken as deterministic values, is plotted in red.

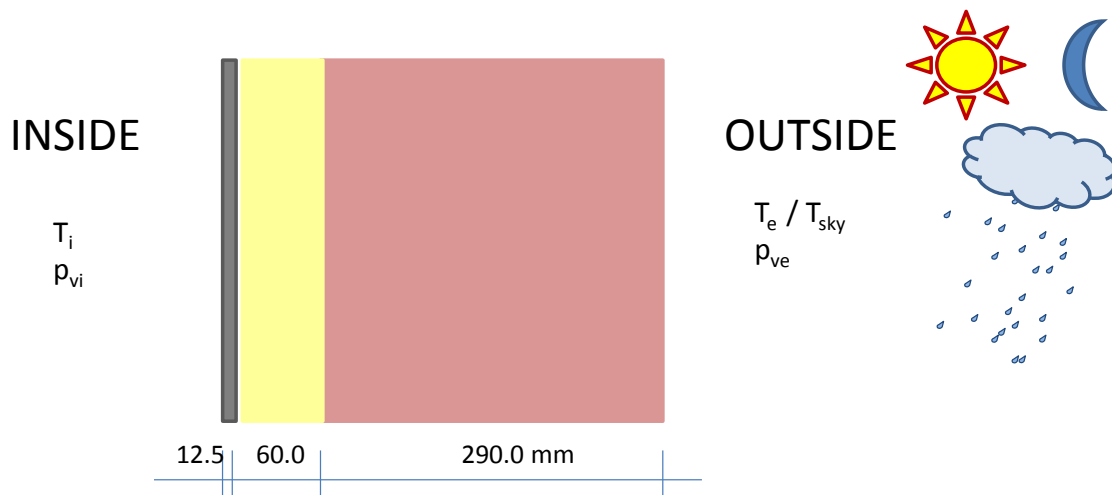


Figure 1.4: Schematic overview of the configuration for CE2.

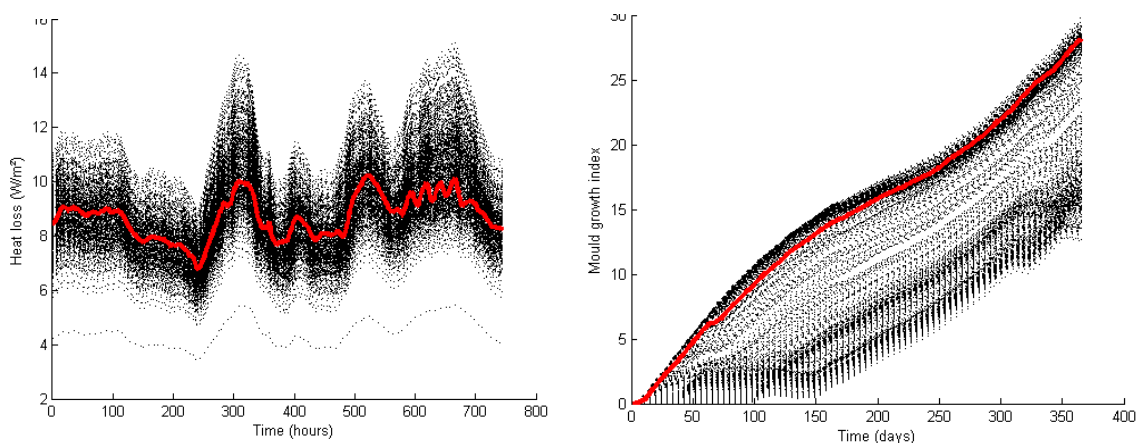


Figure 1.5: Illustrative outcome of CE2 - Predicted cumulative heat loss per m² for January (left), evolution of the mould growth index over the year (right). The reference case is plotted in red.

1.3.4 Sensitivity analysis: CE3

Common Exercise 3 aimed at an evaluation of the capabilities and limitations of sensitivity analysis methods for building performance analysis and design. However, as CE2 had shown that the influence of deviations due to the HAM simulation environment used were bigger than the differences between uncertainty quantification methods, CE3 started with an initial uncertainty propagation component. To avoid interferences caused by differing HAM tools, a common simulation model for a cold attic (Hagentoft, 2011) was used by all participants in the exercise. This cold attic model relates the heat loss to and mould growth in a cold attic to 15 stochastic input parameters, related to climate, material, geometry and construction characteristics.

The topic of CE3 hence was an uncertainty propagation and a sensitivity analysis for the hygrothermal behaviour of cold attics, with as main aims the reintroduction of uncertainty propagation methods and the exploration of sensitivity analysis approaches. The choice of techniques was free for both aspects, and CE3 hence generally targeted a comparison between different methods. The analysis considered the hygrothermal behaviour of a cold attic, for which heat and mass balances were solved in a Matlab model. The model links 15 input parameters to 2 output variables: the cumulated heat loss to the attic and the peak mould growth in the attic (see Addendum 3 for more info). The input parameters are collected in Table 1.1, with their respective probability distributions. Two different distribution types are applied: uniform U(lower limit, upper limit) and normal N(average, standard deviation) distributions.

A typical outcome of the sensitivity analysis is depicted in Figure 1.6, which presents the standardised regression coefficients for the cumulated heat loss to the attic. It becomes clear that this heat loss is primarily governed by the ceiling's U-value and the roof's R-value, and to a lesser degree by indoor temperature and ceiling leakage area. Other parameters, especially these not included in the graph, do not impact the heat loss significantly.

Table 1.1: variable input parameters, .m-file symbol, probability distribution

Area of ceiling and roof (m ²)	U(50,200)
Length of building (eave side) (m)	U(7,20)
Height of building H (m)	U(4,8)
Leakage area per m ² of ceiling (m ² /m ²)	U(0.001,0.05)**
Venting area per meter eave (m ² /m)	U(0.001,0.05)
Indoor temperature (°C)	N(20,1.5)
Indoor moisture supply (kg/m ³)	N(0.005,0.002)
Year of climate data used (-)	U(1,30)*
Orientation of one of eave sides (-)	U(0,180)
U-value of the ceiling (W/m ² K)	U(1,5)**
Resistance of roof insulation (m ² K/W)	U(0,1)
Thickness of wooden underlay (m)	U(0.010,0.020)
Thermal conductivity of wood (W/mK)	N(0.13,0.02)
Vapour diffusivity of wood (m ² /s)	N(10 ⁻⁶ ,2 10 ⁻⁷)
Initial relative humidity of wood (-)	U(0.5,0.9)

**only discrete integers **excessively high values*

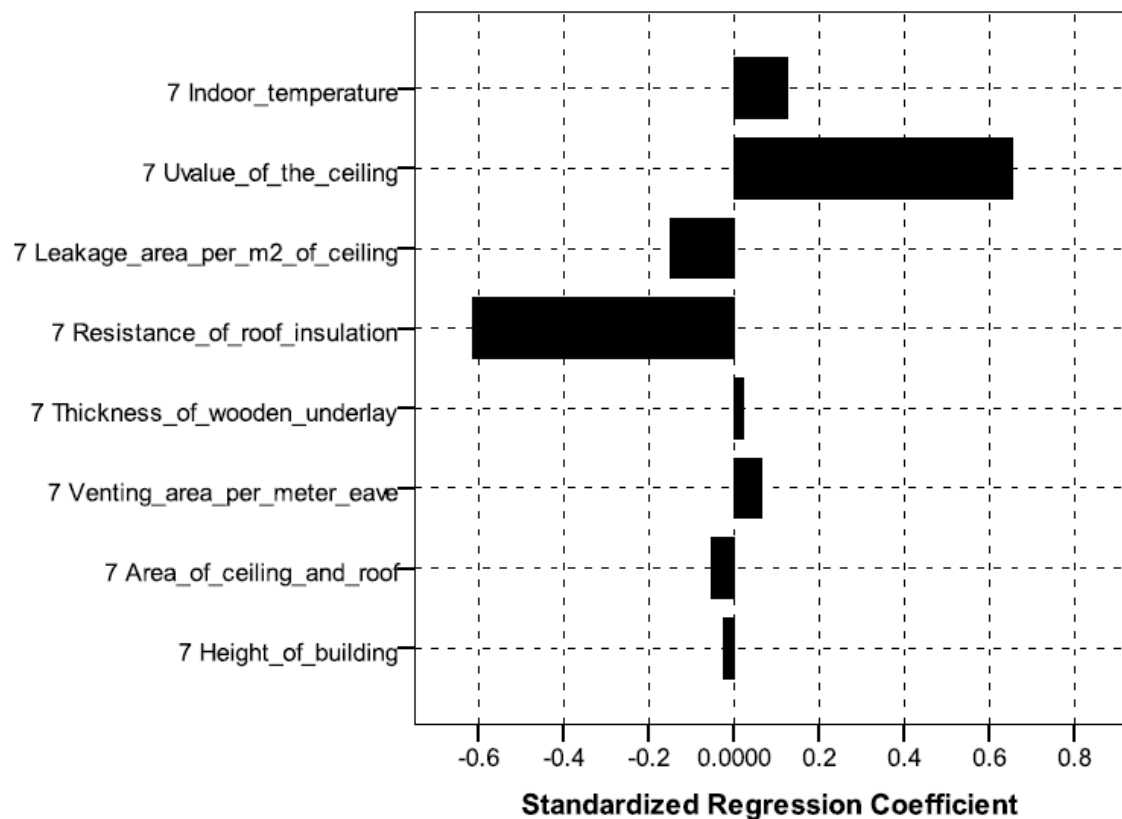


Figure 1.6: Illustrative outcome of CE3 – Standardised regression coefficients for the relation between the cumulated heat loss and the 15 input parameters. Non-mentioned parameters do not have any significant impact.

1.3.5 Metamodelling method: CE4

The capabilities and limitations of metamodelling methods for surrogate simulation for building performance assessments have been examined empirically in CE4, again via the cold attic model employed in CE3. Metamodelling techniques are a crucial element of probabilistic tools, as the execution time for the deterministic core model often is a restrictive factor. This implies that only a small number of runs are actually feasible, which obstructs most standard methods for uncertainty propagation, sensitivity analysis or performance and robustness optimization. To resolve this, an approximate surrogate model – or metamodel – is derived from a small set of initial results, which is then applied instead of the original model for the further investigation and/or optimization. The main aim of CE4 was thus to explore the effectiveness and efficiency of different meta-modelling methods. As simulation time is a primary motivation for metamodelling though, the impact of the initial set size formed an important auxiliary focal point.

In this CE, the main aim of the metamodelling efforts was ‘design space approximation’: the goal was to obtain a quicker approximate model to stand in for the original model, mimicking the original model as good as possible over the entire parameter space. The quality of the resulting metamodels was assessed by comparing their outcomes to the outcomes of the original model at 100 reference points in the parameter space. These 100 reference points were however not be used in the development of the metamodel (see Addendum 4 for more info).

Two results of the metamodelling exercise are shown in Figure 1.7, which demonstrates the fine agreement for the cumulated heat loss (CHL) and the less nice concurrence for the peak mould growth (PMG). On the vertical axes, the original model results are shown, versus the metamodel results on the horizontal axes.

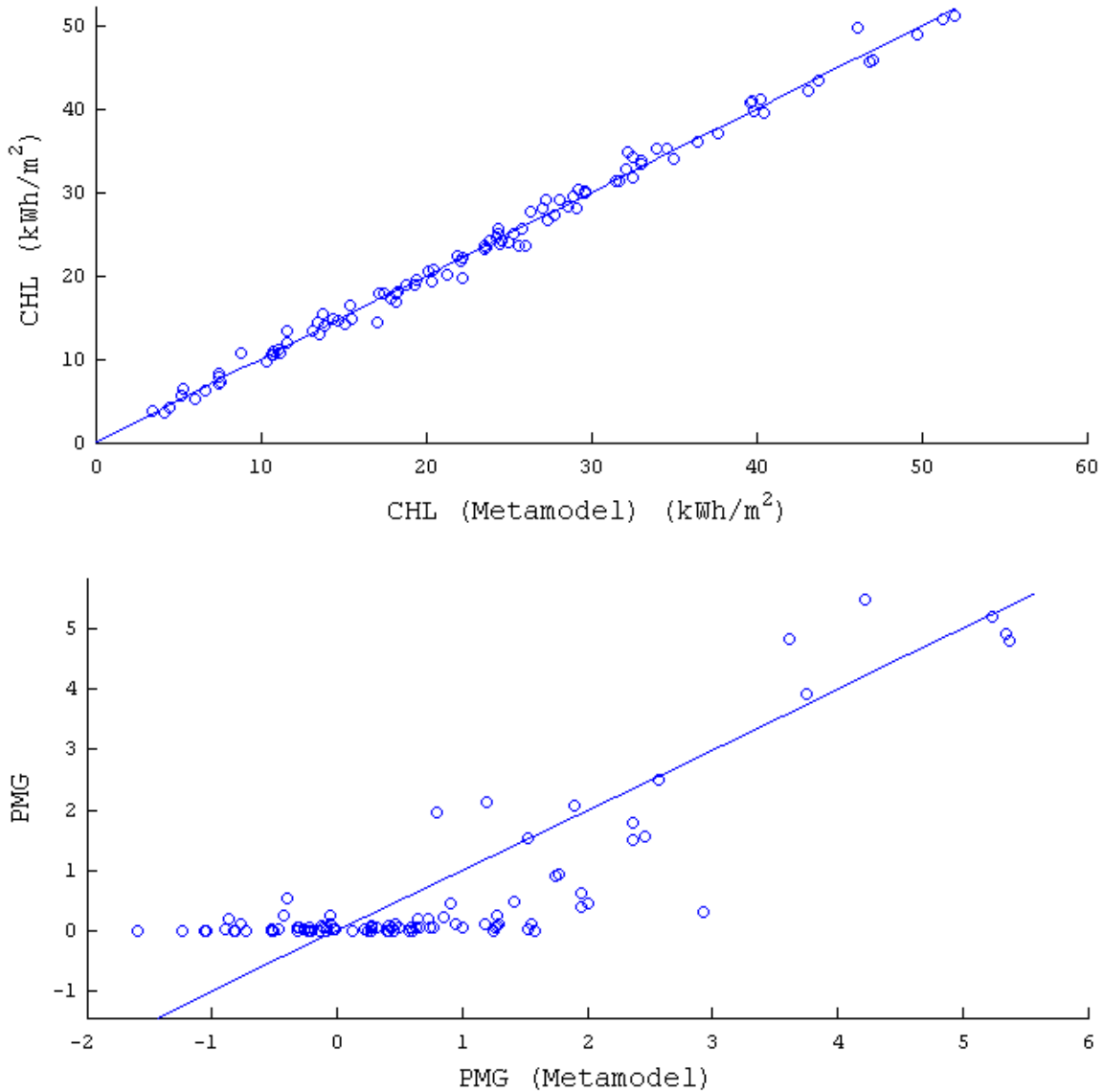


Figure 1.7: Illustrative outcome of CE4 – Comparison of results of original model and metamodel for cumulated heat loss (top) and peak mould growth (bottom).

1.3.6 Economic optimisation: CE5

In the last common exercise CE5 the developed methodology was applied in a generic way by making decisions on retrofitting measures for a typical building stock and from an economic perspective. To do so, participants were asked to ‘take up’ the function of a consultant for an ESCO (Energy Saving Company) that will renovate the attics of 237 dwellings in a neighbourhood. To limit the work load, the same cold attic model of CE3 and CE4 is used, but instead of the earlier cumulative heat loss and peak mould growth indicators, the overall cost is consider-

ed the main performance criterion. Different renovation measures (such as adding attic floor insulation, increasing air tightness of ceiling, closing ventilation gaps,...) could be applied (and if relevant combined), but of course each renovation measure corresponds to a certain cost, will result in certain benefits (energy savings) and may result in hygrothermal risks (mould growth). Goal of the common exercise was to come up with the renovation measure (applicable to all dwellings) that results in the largest overall profit within a timespan of ten years.

The original state of the building was described by probability density functions of all variable input parameters as in CE3 (see Table 1.1). For the different renovation measures, optimal target values had to be determined. For each target value, the finally obtained value was presumed to have a normal distribution around this target value due to uncertainties in workmanship. Of course, each of these renovation measures corresponds to a certain cost, as given in Table 1.2.

Table 1.2: costs related to the different renovation measures

renovation measure	cost	
1.insulating attic floor	$8.0+1.2*(1/U_c^{new} - 1/U_c^{old})$	euro/m ²
2. increasing air tightness of attic floor	$5.0+3.0*10^{-7}/A_c^{new}$	euro/m ²
3.sealing ventilation gaps at the eaves	$12.0 + 3.0*10^{-4}/A_e^{new}$	euro/m
Repair cost if PMG > 5	58.0	euro/m ²

The largest overall profit within a time span of 10 years had to be evaluated based on the net present value (NPV), simplified to:

$$NPV = -I_0 - I_M + \sum_{i=1}^{10} \frac{\Delta K_E (1 + r_E)^i}{(1 + a)^i}$$

in which I_0 corresponds to the initial investment of the renovation measure, I_M is the maintenance cost, ΔK_E the change in annual energy costs due to the renovation measure, r_E the inflation corrected mean annual increment in energy cost ($0 < r_E < 1$) and a the inflation corrected present value factor ($0 < a < 1$). Detailed information on all input parameters and variations are given in Addendum 5.

As increasing the insulation level of the attic floor can be seen as the first and easiest choice for an ESCO to apply, participants were requested to determine first the optimal U-value of the ceiling when no other renovation measures are applied. As an example the graph at the top of Figure 1.8 shows the outcome as determined by one of the participants, both when only the benefits are taken into account (indicated as 'no repair costs') as well as when the repair costs for attics with mould growth is incorporated in the NPV (indicated as 'with repair costs'). The bottom graph depicts the corresponding cumulative distribution function of the dwelling stock with and without repair costs, as well as the cdf of the most optimal renovation scenario for all dwellings. This kind of figures clearly illustrates the advantages of the developed probabilistic methodology. Further information and interpretation can be found in Chapter 6.

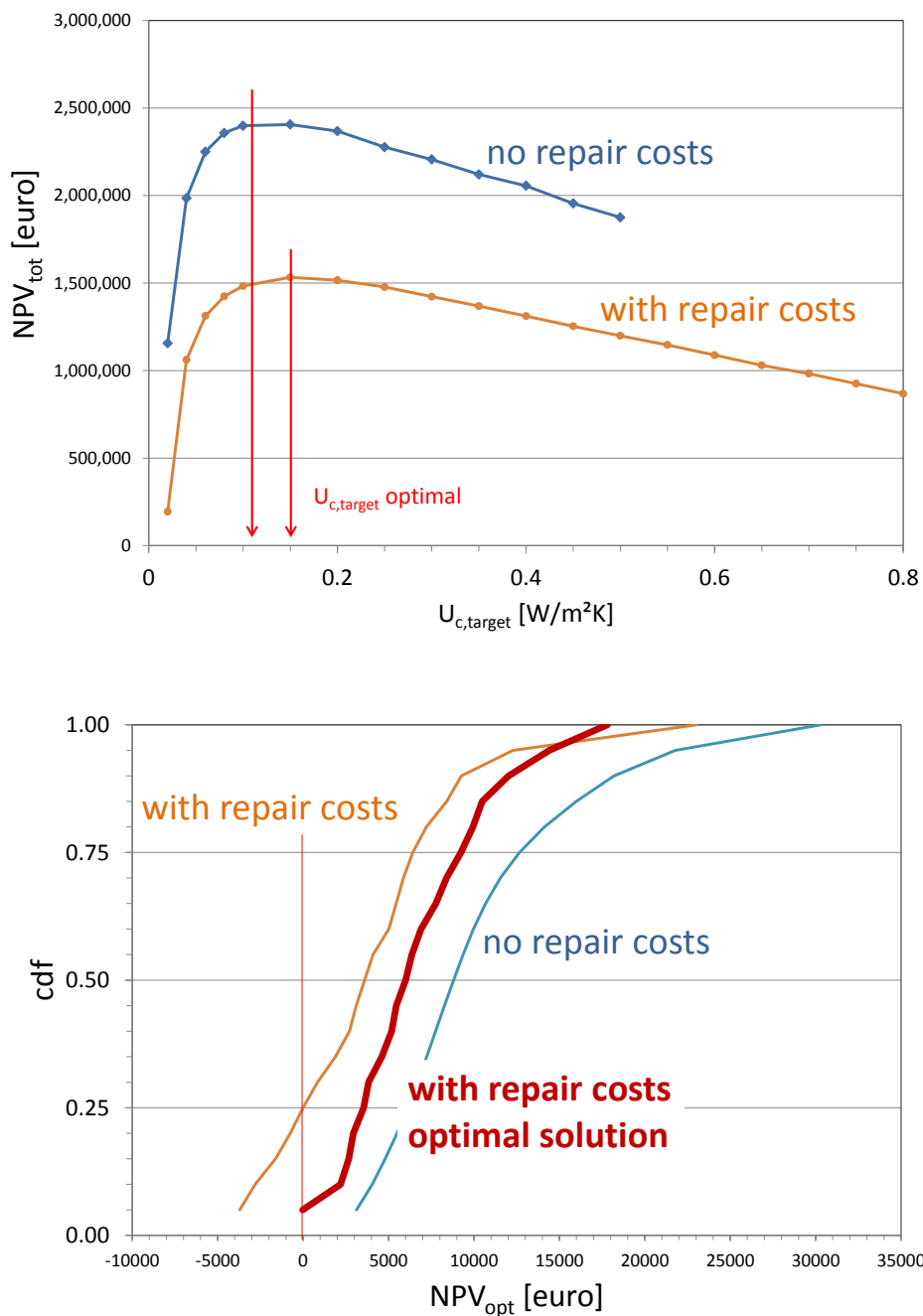


Figure 1.8: Illustrative outcome of CE5 – The total NPV (sum for all dwellings and over a time span of ten years) as a function of the target U-value of the ceiling when applied to all 237 dwellings (top) and corresponding cdf of the NPV for each dwelling for the optimal solutions (bottom).

1.4 Summary

In this chapter a concise introduction on probabilistic tools was given. The five primary sets of probabilistic tools: *qualitative exploration*, *uncertainty propagation*, *sensitivity analysis*, *meta-modelling* and *economic optimisation* have been presented and illustrated via an easy example from another engineering discipline. Hereafter, the different Common Exercises of Subtask 2 have been shortly presented. Each of these Common Exercises went more in detail on one of the five sets. This way the application of typical probabilistic tools to hygrothermal analysis and design of building retrofits could be investigated. In Chapters 2 to 6, each set of tools is investigated and illustrated in more detail, to finally come to a conclusive quantification methodology in Chapter 7.

1.5 References

Hagentoft C.-E (2011). Probabilistic analysis of hygrothermal conditions and mould growth potential in cold attics. Impact of weather, building system and construction design characteristics, in Proceedings of the 12th International Conference on Durability of Building Materials and Components, Porto, Portugal.

Helton J.C. and Burmaster D.E. (1996). Guest editorial: treatment of aleatory and epistemic uncertainty in performance assessments for complex systems. *Reliability Engineering and System Safety* 54:91-94.

Oberkampf W.L., DeLand S.M., Rutherford R.M., Diegert K.V. and Alvin K.F. (2002). Error and uncertainty in modeling and simulation. *Reliability Engineering and System Safety* 75:333-357.

Van Gelder L., Janssen H. and Roels S. (2014). Probabilistic design and analysis of building performances: methodology and application example. *Energy and Buildings* 79:202-2011.

Viitanen H. and Ojanen T. (2007). Improved model to predict mould growth in building materials, in Proceedings of 10th International Conference on Thermal Performance of the Exterior Envelopes of Whole Buildings, Clearwater Beach, Florida, USA.

2

QUALITATIVE EXPLORATION

Lead author

Hans Janssen

2.1 Introduction

2.1.1 Annex 55 and Subtask 2

The prime objective of Annex 55's Subtask 2 is to appraise the advantages and disadvantages of existing probabilistic methods for qualitative and quantitative assessment with regard to their applicability within the particular context of building performance analysis and design. Five sets of tools have been identified for probabilistic assessments, each with a distinct goal:

1. *qualitative exploration*:
to identify all relevant parameters, and the relations between them;
2. *uncertainty propagation*:
to quantify the probabilistic character of the assessment's outcome;
3. *sensitivity analysis*:
to determine the dominant and the non-dominant input parameters;
4. *metamodelling method*:
to formulate a simple surrogate model, to replace the original model;
5. *economic optimisation*:
financial criteria and optimisation schemes to attain the best solution;

These five sets of probabilistic tools each form the topic of a Common Exercise in Subtask 2, all aiming at evaluating the capabilities and limitations of different available methods. These five sets furthermore are the respective subject of this and the next chapters, which constitute the main report for Subtask 2.

2.1.2 Qualitative exploration tools

This chapter focuses on *qualitative exploration*, the first set from the mentioned suite of tools. The application of these *qualitative exploration* tools to a hygrothermal analysis or design case has a double objective: *factor identification* and *flowchart formation*. The *factor identification* is to map out all relevant parameters that may affect the outcome of the analysis or design under consideration, while the *flowchart formation* is to establish all relations between the parameters and outcomes which are part of the assessment.

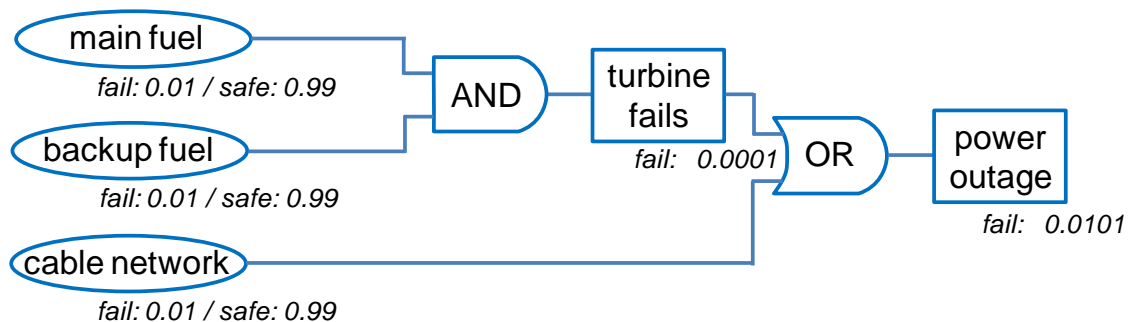


Figure 2.1: Fault tree for the electricity supply network and its primary components

Qualitative techniques for probabilistic assessment mainly stem from the risk assessment field, and therefore often take the narrower focus on *hazard identification* and *hazard organisation*. These two aspects of qualitative exploration have already been illustrated in Section 1.2.2, the results of which are brought back in Figure 2.1. The hazard identification indicated the turbine, the main fuel, the backup fuel and the cable network as potential causes of failure. The hazard organisation demonstrated the different causal relations between those factors, for example illustrated by the turbine failure resulting from the simultaneous depletion of main and backup fuel.

Different hazard identification methods have sprouted from different engineering fields, but all are founded on similar concepts. They aim at assessing which hazards may jeopardize the system, which causes can lay at the origin of the hazards, and which impacts could result from the hazards. Combining the probability of the cause with the criticality of the impact moreover allows a qualitative ranking of the hazards. Selected examples of hazard identification methods are: preliminary hazard analysis, failure modes and effects analysis, hazard and operability studies, risk screening sessions, ... Further detail and background on these methods can be found in (Stewart and Melchers, 1997).

Having identified the possible hazards, and their causes and impacts, logical trees may be used to represent and analyse the relations between hazards, causes and impacts. The main aim of these hazard organisation methods is the mapping of all these relations, to allow further qualitative and/or quantitative examinations of the system. Again, different fields have developed different methods, but again, they all share one prime feature, which is to logically connect different events in that hazard/cause/impact scheme. Selected examples of hazard organisation methods are: event trees, fault trees, cause-consequence charts, bayesian probabilistic nets, ... (Stewart and Melchers, 1997).

The qualitative techniques for probabilistic assessment thus target: 1) the detection of all possible hazards, causes and impacts, and the parameters interacting in those, and 2) the synthesis of all relations between the hazards, causes, impacts and interacting parameters. Such hazard identification and organisation is a crucial initial feature of any risk assessment, as none of the following stages can be completed – or even just make sense – without this first step. Careful execution of this qualitative exploration is therefore essential, since the neglect of any hazard, cause, impact or relation directly affects the overall dependability of the analysis, and thus the reliability of the considered structure.

Overall, the desired outcome of the qualitative exploration is a lucid and logical representation of the considered risk assessment, in support for consecutive qualitative or quantitative analyses. The example in Figure 2.1 illustrates such ‘lucid and logical representation’ and ‘support for consecutive analyses’: the logical relations between different hazards, causes and impacts are evident, and a consecutive assessment of the various risks is straightforward. A similar approach and methodology is equally applicable though to more complex and multifaceted configurations, like oil pipelines (Yuhua and Datao, 2005), power systems (Volkanovski et al., 2009), nuclear reactors (Kumawat et al., 2013), among other cases.

2.1.3 'Gains and costs' concept

In many engineering disciplines, the reliability of a certain system is assessed via its probability of failure. Consequent to that train of thought, risk assessment indeed focuses on the hazards, causes and impacts in relation to such failure. In hygrothermal building performance engineering on the other hand, there often are no strict transitions from 'functional' to 'non-functional'. Instead, thermal retrofits aim at positive effects on health, comfort, durability and sustainability, while hygrothermal failures affect these aspects negatively. When analysing and designing building performances, it is hence more appropriate to consider 'gains and costs' instead of 'no failure or failure'. These gains and costs are preferably expressed in financial terms, see Chapter 6, but other indirect expressions can equally be employed.

The extension from the narrower 'hazards, causes, impacts' idea to the wider 'gains and costs' concept is straightforward. To reflect the more universal nature of the qualitative approaches with respect to hygrothermal building performances, we have opted for discarding the original risk-based terminology. Instead, *factor identification* and *flowchart formation* are put forward, as they have a more universal character. The applicability of currently available factor identification and flowchart formation methods for building performance analysis and design is investigated in Section 2.2 below. Our findings are based on the outcomes of Common Exercise 1, which examined thermal renovation solutions for walls. It is observed that even simple cases involve a multitude of interacting factors, with complex and entwined relations between them. This renders the flowchart formation a daunting task, and direct further quantification far from easy.

2.2 Common Exercise 1

2.2.1 Presentation of Exercise

Common Exercise 1 has already been presented in Section 1.3.2, and all details can be found at that location. The primary objective of Common Exercise 1 is to judge the applicability of existing techniques for factor identification and flowchart formation in a building performance context. To that aim, participants are requested to execute the factor identification and flowchart formation for the gains and costs related to the thermal retrofit of a brick cavity wall by means of cavity, interior or exterior insulation. In essence, the outcome of this *qualitative exploration* should support the future quantification of these gains and costs, which should in turn allow a comparison of the relative performances of the three retrofit options, and ultimately a decision on which solution shows most potential. To limit the complexity, gains are simplified to improvements in energy efficiency, costs are condensed to the extent of hygrothermal damages.

The formal deliverables of the Exercise are:

- an overview of all interacting parameters that may affect the set gains and costs;
- a flowchart indicating the logical relations between parameters and gains and costs;
- comments on the overall capabilities and limitations of the applied methods for factor identification and flowchart formation.

2.2.2 Outcomes from Exercise

Six solutions for ST2-CE1 were received. The solutions of Carsten Rode (Technical University of Denmark), Kristina Mjörnell (SP Technical Research Institute of Sweden) and Christoph Harreither (Vienna University of Technology, Austria) focus primarily on factor identification, while the submissions of Simo Illomets (Talinn University of Technology, Estonia), Angela Kalagasidis (Chalmers, Sweden) and Liesje Van Gelder (KU Leuven, Belgium) concentrate mainly on flowchart formation. The aim here is not to represent the complete solutions, but instead to make a synthesis of their findings and comments only.

2.2.2.1 Factor identification

2.2.2.1.1 Observations from participants

A first important observation, made by many participants, is that even fairly simple analyses involve a significant number of interacting parameters. Carsten Rode limits his analysis to a factor identification in relation to potential moisture-related durability problems. For the case of interior insulation only, he identifies more than 10 potential hazards, ranging from rain penetration over beam end decay to differential movements. When including the two alternatives, this inventory of hazards would expand even further. For each hazard, a diversity of interacting parameters is put forward, going from geometries and dimensions over material and component properties to workmanship issues. Similar extensive surveys of interacting factors are observed in the solutions from all other participants.

Moreover, most of the risk-oriented factor identification methods classify the interacting parameters into a limited number of levels, typically along the lines of the actual hazards, their potential causes and their possible consequences. Liesje Van Gelder attempts such classification in relation to ‘deterioration of interior finishing’ as hazard, see Figure 2.2. Potential causes are surface condensation and mould growth, where the latter in turn stems from the combination of mould spores in the air, low surface temperature and high surface vapour pressure. The low surface temperature can be the effect of the low outside temperature, thermal bridging or low inside temperature; and so on. This multitude of interacting parameters does therefore result in a multitude of levels in the factor identification and subsequent flowchart formation.

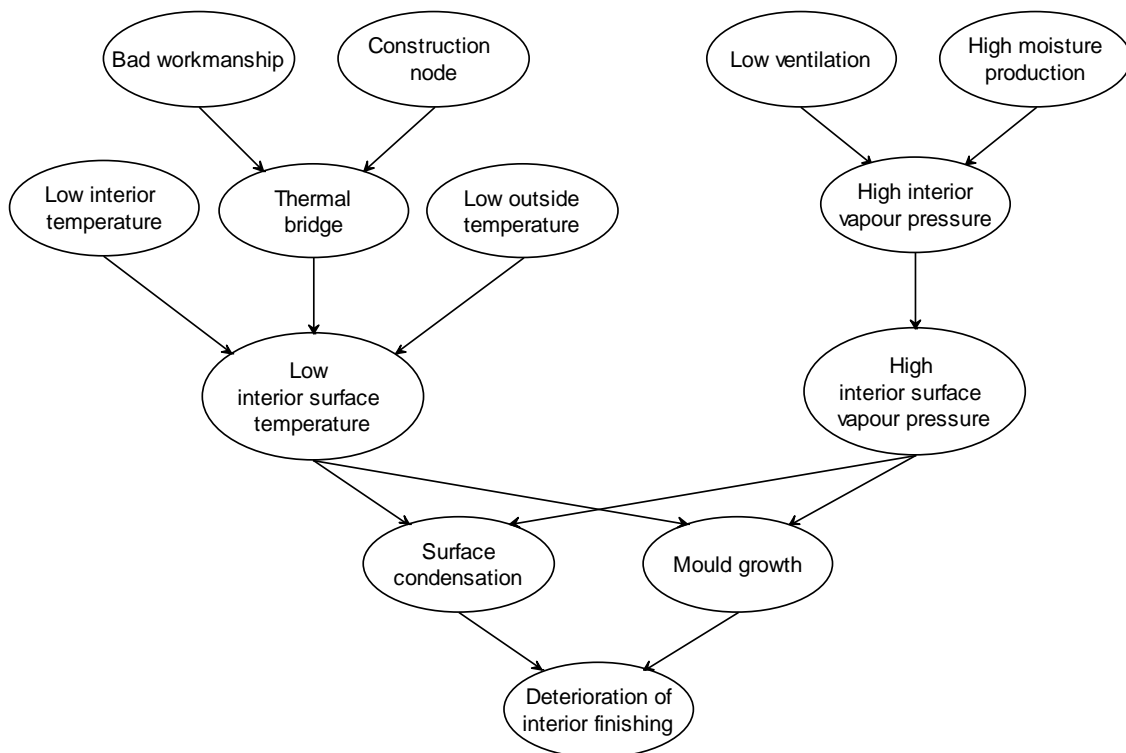


Figure 2.2: Bayesian probabilistic net for ‘deterioration of interior finishing’ (adapted from Figure 2 in Liesje Van Gelder’s solution)

2.2.2.1.2 Observations from subtask leaders

Most of the solutions report the work of an individual researcher, or exceptionally the work of a small group of researchers. Although many intentionally reduce the objective of their analysis to limit the required efforts, there is sufficient overlap between different participants’ solutions for a comparison. This comparison points out that there is a large disparity between the solutions: each participant arrives at identifying factors that no other participant points at, implying that each participant also lacks factors that are correctly identified by other participants. A correct factor identification necessitates much expertise and an open mind, which can most probably be more easily established by a larger group, rather than by an individual researcher. In other engineering branches, such factor identification is indeed commonly undertaken by a group of engineers (Faber, 2009).

In many solutions, participants stay close to the original risk-centred concept, thus focusing on potential hazards and their causes and impacts. Liesje Van Gelder, in relation to mould growth owing to excessive interior vapour pressure, identifies ‘low ventilation’ as a potential cause and hence as interacting parameter, see Figure 2.2. The insufficiency of ventilation is a rather relative concept though, since it depends on various other parameters, and hence cannot be easily judged. Besides, when it comes to the energy consumption, such ‘low ventilation’ may actually prove beneficial. The ‘hazard-cause-impact’ train of thought, typical for standard risk assessments, consequently may bring about a judgmental bias, hampering the precision of the factor identification. For the case in Figure 2.2, the ‘low ventilation’ should simply have been identified as ‘ventilation’, to be quantified for both the costs and the gains.

2.2.2.2 Flowchart formation

2.2.2.2.1 Observations from participants

It is widely accepted that a breakdown of a system is often not the result of a failure of a single component, but rather stems from a sequence of negative events (Faber, 2009). In ‘standard’ configurations, this sequence can however be broken down easily into single events, each with a probability of failure or non-failure. With respect to the probabilistic assessment of building performances, on the other hand, the gains and costs are determined by a multitude of interwoven events, frequently of coupled, non-linear and time-dependent nature. Angela Kalagaidis exemplifies this with microbiological growth on the exterior rendering, see Figure 2.3, which depends on moisture content, temperature, daylight availability, The latter interacting parameters cannot be reduced to distinct events with a certain failure probability, but have to be assessed as an interacting set of parameters.

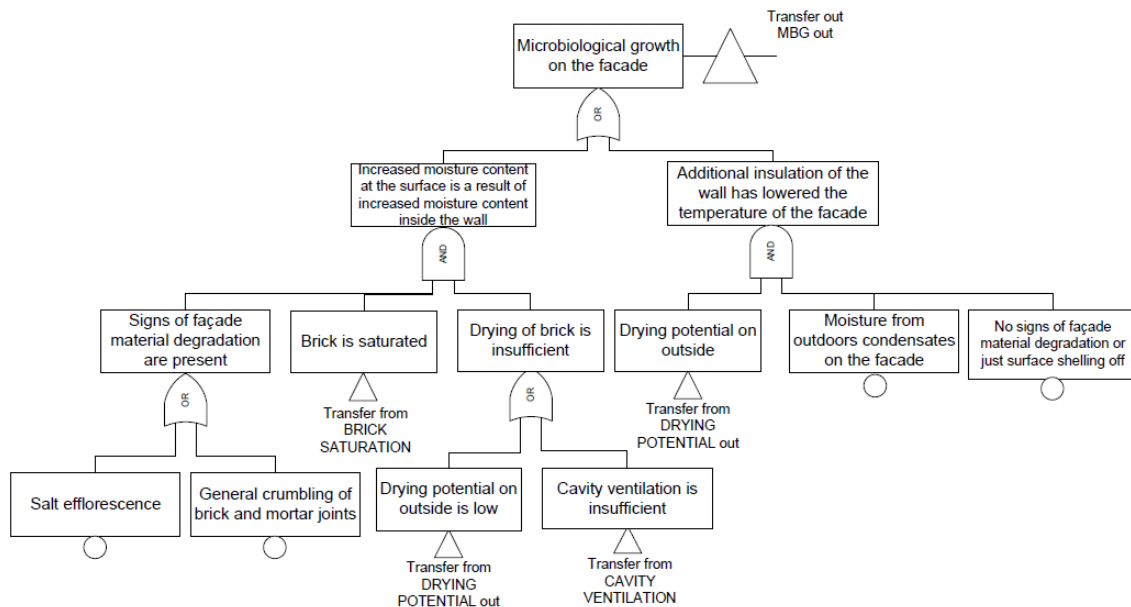


Figure 2.3: Event tree net for ‘microbiological growth on the facade’ (taken from Figure 12 in Angela Kalagaidis’ solution)

Moreover, the performance criteria for the gains and costs related to building performance assessments can neither be straightforwardly reduced to a functional versus non-functional idea. Microbiological growth on the facade does typically not yield structural damage, but just leads to a maintenance cost for the building owner. Reduced energy consumption is a similar example of such gradual performance criteria. Furthermore, as both gains and costs are of interest, some interacting parameters may have opposite meanings for different gain and cost aspects. For example, the ‘additional insulation of the wall’, see Figure 2.3, may indeed promote microbiological growth and consequently increase the costs, it will on the other hand equally add to the gains by reduced transmission losses. This, together with the complex interaction between parameters, often leads to extensive, multi-faceted and interwoven flowcharts.

2.2.2.2.2 Observations from subtask leaders

The comments made for ‘factor identification’ remain valid here as well. The solutions submitted by the participants show a significant disparity with respect to the overall contents, specific details and overall applicability of their flowcharts. Again, the high amount of expertise needed favours collective approaches over individual efforts. The hazard-cause-impact thinking equally affects the flowchart formation. For example in the third layer of the right-hand-side branch in Figure 2.3, both ‘drying potential on outside’ and ‘moisture from outdoors condensates on the facade’ appear as separate processes. These should be interpreted as concurrent causes for microbiological growth on the facade, in the combination of excessive surface condensation and moderate surface evaporation. However, both can actually be substituted by ‘surface moisture content’ as the interacting parameter. Similarly, most of the left-hand-side branch in Figure 2.3 can be condensed to that same ‘surface moisture content’ parameter. The correct identification of the interacting parameters and the processes that determine them – surface moisture content is influenced by moisture exchanges with the interior and exterior environments – would strongly reduce the density and complexity of the resulting flowcharts.

2.2.3 Discussion of outcomes

The prime objective of Common Exercise 1 was to judge the applicability of existing techniques for factor identification and flowchart formation in a building performance context. In essence, the *qualitative exploration* should result in a lucid and logical representation of the considered assessment, in support of a consecutive assessment of expected gains and costs.

Several reservations are put forward:

- separate researchers or engineers may come to deviating results in the factor identification and flowchart formation; such can be resolved by performing the qualitative exploration with a larger group of experts.
- the factor identification and flowchart formation results quickly become very complex and involved, partially due to a too hazard-focused approach; this can be eased by use of correct concepts, rigorous procedures and appropriate software.

These reservations are not new, and can be addressed as stated. In various other engineering fields, qualitative exploration based on factor identification and flowchart formation is successfully applied to very large configurations, such as oil pipelines (Yuhua and Datao, 2005), power systems (Volkanovski et al., 2009), nuclear reactors (Kumawat et al., 2013), ...

Such large systems justify an allocation of significant resources for the probabilistic assessment in general and the qualitative exploration in particular. Unfortunately, this is not the case for a 'simple' thermal retrofit of a building, which is commonly designed by an engineer or architect and executed by a building contractor. These limited resources form an important bottle-neck for the applicability of existing techniques for qualitative exploration in the context of building performance analysis and design.

However, the core barriers for a copy-roll forward of existing techniques into the probabilistic assessment of building performances are the issue of gradual gains and costs – instead of strict failure probabilities –, and the complex and interwoven relations between gains, costs and interacting parameters. These lead to the observation that the resulting flowcharts no longer allow a direct further quantification, thus defying their primary purpose. And without their support for quantification intents, their value for probabilistic assessment can be questioned.

2.3 Conclusions

The core objective of Annex 55's Subtask 2 is to evaluate the advantages and disadvantages of existing methods for probabilistic assessment when applied to building performance analysis and design. Five sets of tools are needed for probabilistic assessments: *qualitative exploration*, *uncertainty propagation*, *sensitivity analysis*, *metamodelling method*, and *economic optimisation*. This chapter focused on *qualitative exploration*, which has the double objective of *factor identification* and *flowchart formation*. *Factor identification* is to map out all relevant parameters for the case considered, while *flowchart formation* is to establish all relations between parameters for the case considered. *Qualitative exploration* thus targets the identification of all parameters involved and their logic interrelations.

Factor identification and *flowchart formation* tools were adopted from the field of risk assessment, which however have a narrower focus on hazard identification and hazard organisation. Respective examples of these tools are preliminary hazard analysis, failure modes and effects analysis, risk screening sessions, ... and event trees, cause-consequence charts, bayesian probabilistic nets. As most of these methods stem from the risk assessment field, they aim at evaluating the probability of failure, with a fairly strict limit between functional and non-functional. Such firm distinction is however not suitable for hygrothermal building performances, where a far more nuanced and gradual performance evaluation is required, which is accommodated by opting for the more general concept of gains and costs.

The overall applicability and the inherent (dis)advantages of factor identification and flowchart formation methods was judged via a comparative analysis of wall post-insulation solutions in a Common Exercise. Several reservations were distilled from the six submitted responses:

- the factor identification and flowchart formation results quickly become very complex and involved;
- separate researchers or engineers may come to differing results in the factor identification and flowchart formation;
- the concept of gains and costs, and their complex and interwoven relations with other parameters, complicate further quantitative evaluation.

The first two can be countered respectively by adopting correct concepts, rigorous procedures and appropriate software, and by performing the qualitative exploration with a larger group of experts, as is state-of-the-art in many other risk assessment applications. These typically consider large systems though – like oil pipelines, power systems, nuclear reactors, ... –, where significant resources are allocated for the probabilistic assessment in general and the qualitative exploration in particular. The more limited resources typically available for thermal retrofits of buildings hence form an important bottle-neck for the applicability of existing techniques for qualitative exploration in the context of building performance analysis and design. The last reservation is even more critical however. Due to the gradual and complex nature of typical building performance criteria, and their interwoven and multifaceted relation with interacting parameters, the resulting flowcharts do not allow easy further quantification, defying their primary aim. And without this support for quantification, their value can be questioned.

2.4 References

Faber M.H. (2009). Lecture notes on 'Risk and Safety in Engineering', ETH, Zurich, Switzerland, www.ibk.ethz.ch/emergitus/fa/education/ws_safety/Non_printable_script.pdf, last accessed on April 15 2014.

Kumawat H.L., Singh O.P. and Munshi P. (2013). Uncertainty evaluation of reliability of safety grade decay heat removal system of Indian prototype fast breeder reactor. *Annals of Nuclear Energy* 62:242-250.

Stewart M. and Melchers R.E. (1997). Probabilistic risk assessment of engineering structures. Chapman & Hall, London, United Kingdom.

Volkanovski A., Cepin M. and Mavko B. (2009). Application of the fault tree analysis for assessment of power system reliability, *Reliability Engineering and System Safety* 94:1116-1124.

Yuhua D. and Datao Y. (2005). Estimation of failure probability of oil and gas transmission pipelines by fuzzy fault tree analysis, *Journal of Loss Prevention in the Process Industries* 18:83-88.

3

UNCERTAINTY QUANTIFICATION

Lead author

Staf Roels

3.1 Introduction

3.1.1 Uncertainty quantification for decision making

Where factor identification and flowchart formation (see Chapter 2) reveal the interacting factors determining the benefits and risk of hygrothermal retrofits, quantitative methods are necessary to steer the decision making. The aim of uncertainty quantification is to determine to what extent the outcome(s) will vary if some of the input parameters, be it material properties, boundary conditions, future scenarios,... are not exactly known. Due to complexity and computational cost, a quantitative probabilistic analysis is often performed on well defined (sub)problems and if relevant the results can be fed into a global flowchart. Well-defined here means that all input parameters and requested output parameters are expected to be identified, even though the actual distribution of the input parameters might be lacking. A quantitative method then will predict the variation of the different outcomes based on the stochastic variation of the input parameters. In most building physics applications, the benefits and risk are determined by multiple sources of uncertainty, such as the building geometry and exact composition, the impact of workmanship, the physical properties of the components, the boundary and initial conditions, etc... Determining the relative impact of the multiple sources of uncertainty on the obtained response is then also a prerequisite to come to effective retrofit strategies. Uncertainty quantification in combination with sensitivity analysis (see Chapter 4) will help to identify and manage the priorities and to reduce sources of uncertainty.

Though some examples of other methods for uncertainty quantification in building physics applications can be found in literature and have also been presented in free papers during the Annex-meetings – such as the first-order and second order reliability methods (FORM/SORM) – in the common exercises typically Monte Carlo methods have been used. The Monte Carlo method makes use of (optimised quasi-) random sampling, with the prediction of the outcome given by a numerical tool, similar as the one used for a deterministic prediction. These deterministic models can be quite elaborated (a lot of building physics applications are solved using finite element or finite volume discretisation) and as such might hamper a stochastic analysis due to computational costs. To overcome this, surrogate or so-called meta-models can be used, as will be elaborated upon in Chapter 5.

The next section of this chapter will give a brief overview of different quantitative methods available in literature. The specific focus of this chapter is to decide on which are applicable for hygrothermal retrofitting problems. As was shown by the common exercises, due the time-dependent and highly nonlinear behaviour of many retrofitting problems, Monte Carlo shows to be the most promising technique. Since the Monte Carlo method is a simulation based technique, an important aspect will be the calculation efficiency, which is largely determined by the sampling scheme. This will be discussed in Section 3.3. Addendum 2 presents CE2 of ST2 which was an exploratory exercise on uncertainty quantification for analysing benefits and risks of a retrofitting measure.

3.2 Quantitative methods

Uncertainty quantification for reliable energy efficient building retrofitting is a typical example of so-called forward uncertainty propagation. In forward uncertainty propagation we are interested in the quantification of the uncertainty of the outputs as a result of possible variance of the input parameters. This type of uncertainty quantification is especially used in reliability engineering, often to predict failure probabilities, but can as well be used to assess the probability distribution function of the outputs. With respect to energy retrofitting measures, the latter is e.g. of help to predict the (financial) benefits of a renovation measure, while the first could be used to assess related risks as mould growth, wood rot, structural damage,...

Although several probabilistic approaches exist to evaluate uncertainty propagation, in building physics mainly examples of most probable point based methods (first and second order reliability methods) and simulation based methods or sampling methods (Monte Carlo simulations) are found.

3.2.1 FORM and SORM-methods

First order and second order reliability methods are very common in structural reliability analysis. These methods compute the probability of an event (in structural reliability often failure) by means of idealisation of the limit state function. To do so, the probability density functions of all random variables are first approximated by equivalent normal distributions. Hence, the space of the random variables is transformed into a space of standard normal variables. In this transformed space of standard normal variables, the point of minimum distance between the origin and the limit state surface is searched and the failure probability is calculated corresponding to the (approximated) failure surface near this point. In the FORM method (First Order Reliability Method) the failure surface is approximated by a hyper plane tangent to the surface of failure. If this linear approximation is not sufficient, higher order approximations of the failure surfaces can be used. The Second Order Reliability Method for example approximates the failure surface by a quadratic surface at the design point.

FORM- and SORM are analytical and approximate methods which turned out to be very efficient compared to simulation methods, as long as the number of variables is not too high. Furthermore, the random variables need to be continuous and also the failure surface must be a smooth and continuous surface. Compared to structural reliability analysis though, the probabilistic assessment of energetic renovation measures of buildings is seldom determined by a failure criterion. Mostly an economic optimisation is the ambition and even if (moisture) damage can occur, it is rarely handled as a strict failure criterion, but more often described as a possible additional repair cost. As a result, although some applications of FORM and SORM in building physics can be found in literature (Pietrzyk and Hagentoft, 2008) and also have been presented at Annex-meetings, the methods showed to be not applicable for typical renovation design and building physics performance assessment as dealt with in the common exercises.

3.2.2 Monte-Carlo methods

While FORM and SORM analyses are typically used to estimate the probability density function at specific points of interest (often the tail of the distribution function), Monte Carlo methods are mainly used to build the entire probability density function and to assess global uncertainty and sensitivity. Monte Carlo methods consist of sampling input variables according to their probabilistic characteristics and feeding them into the calculation tool to predict the corresponding output parameters. In this way, a sample of responses is obtained. It is obvious that the quality of the outcome (the pdf of the output sample) is dependent on the number of simulations carried out and the sampling scheme used (the representation of the original distribution by the sampling). To assess whether the number of simulation runs is sufficient the convergence of some statistical values, as mean, variance,... of the output parameters can be investigated for different truncation levels.

Main advantage of the Monte-Carlo method is that the method can be applied to all kind of problems using both static or dynamic simulation models and for all kind of probabilistic variables (be it continuous or discrete). Major drawback is that, to increase the quality of the output, the method often requires a large number of simulation runs, making it almost impossible to apply when model runs are expensive in computing or labour costs. To overcome this, recently a number of sampling techniques, such as: importance sampling, adaptive sampling, stratified sampling, latin hypercube sampling,... have been developed that achieve the same level of accuracy in output performance while using fewer runs than the basic random sampling. As an alternative – and often in combination – also metamodeling is introduced in which the original time consuming model is replaced in the Monte-Carlo loops by a fast surrogate model. The surrogate or metamodel actually approximates the response surface by a simple mathematical model, such as linear regression planes, polynomials, neural networks,... hence avoiding the problem of long calculation times. The next paragraph will go a bit more in depth on the more efficient sampling methods. Metamodeling will be dealt with in Chapter 5.

3.3 Advanced MC-methods

The common exercises of Annex 55 showed that Monte Carlo simulations are often the only way to assess and quantify uncertainty and robustness of reliable energy efficient building retrofitting. As most studies are based on transient non-linear hygrothermal simulations, the need for cost efficient, optimised sampling schemes is clear. In this section, some of the most common sampling schemes for Monte Carlo simulations are described ranging from basic random sampling towards more optimised space filling designs. As the question ‘When is the size and quality of the sampling set sufficient?’ remains one of the key issues, evaluating sampling efficiency and sampling convergence will be discussed as well.

3.3.1 Sampling techniques

3.3.1.1 Basic random sampling

Basic random sampling (BRS) is the simplest sampling technique to randomly assign values to the different input parameters. When applying basic random sampling, every new value of an input parameter is only determined by the statistical distribution of this parameter, not on values already selected. In addition, basic random sampling does not require determining in advance how many samples will be used. As such, basic random sampling is a simple technique (a random number generator and the input distribution suffice to make the design), but it is also computationally expensive as often many runs are needed to sample the parameter space in a representative way. Figure 3.1, taken from (Janssen, 2013), shows that a BRS-design is typically neither space filling nor provides non-collapsing sampling points.

3.3.1.2 Latin Hypercube sampling

Compared to basic random sampling, Latin Hypercube sampling (LHS) reduces the computational time by improving the non-collapsing property of the design. To do so, the distribution of each input variable is subdivided into n strata with equal probability. Each stratum is sampled randomly once. Hence, the input variables are chosen randomly, but no longer independently of each other. This means that in practice, one first has to decide on n , the number of sample points to generate in the design and then subdivides the input range of each variable into this number of subsets. LHS-designs are still fairly easy to generate, but though they improve in general the space filling character of the design, the basic Latin Hypercube sampling mainly focusses on the fact that the design is non-collapsing. This, however, does not automatically guarantees an optimal distribution of sampling points in the parameter space, and in principle still poorly space filling designs are possible as illustrated in Figure 3.1 (top right).

3.3.1.3 Space filling design

To improve the space filling character of the design, several modification of the basic LHS-method can be found in literature. Best known are the distance-based design methods, which

try to optimise the multidimensional distances between the different sampling points. This can e.g. be done by maximising the minimal distance between sampling points (the so-called maximin criterion) or by minimising the maximal distance between the sampling points (the minimax criterion). As an alternative also (nearly) uniform designs can be used. These designs try for a set of sampling points to minimise the global deviation from a perfectly uniform sampling design. Compared to basic random sampling and basic Latin Hypercube sampling, space filling designs result in much more optimal designs as can be seen in Figure 3.1 (bottom), but generating the designs is a challenging task, with a complexity increasing with the size of the design space.

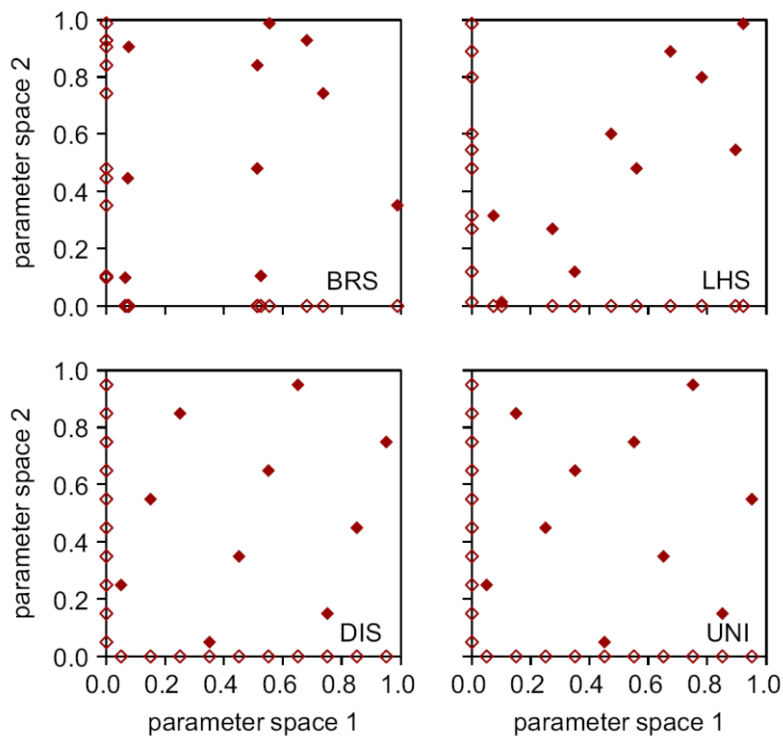


Figure 3.1: Sampling designs for basic random sampling (top left), Latin Hypercube sampling (top right) and distance based (bottom left) and uniform (bottom right) space filling designs. Figure taken from (Janssen, 2013).

Note that Latin Hypercube sampling in general and most space filling designs subdivide the input space a priori and that the number of Monte Carlo runs is determined by this subdivision. Whereas with a traditional sequential sampling, as in basic random sampling, Monte Carlo loops are run in a sequence, one at a time and each new sampling point can be added based on the information already obtained in the previous runs. As sequential sampling has some advantages (e.g. combined with a convergence criterion), it can be interesting to run the Latin Hypercube sampling in batches corresponding to (a multiple of) the number of strata in the Latin Hypercube design space to allow sequential sampling.

3.3.2 Sampling efficiency and sampling convergence

As investigating the reliability of building retrofitting measures is often based on time consuming simulations, the above mentioned advanced sampling techniques are all introduced to reduce the number of runs needed to bring the variance on the outcomes below an acceptable value. This is referred to as increasing the **sampling efficiency**. At the same, it is clear that flexible sampling methods that can easily be stopped or prolonged based on a convergence criterion can also significantly reduce the necessary calculation time. This requires though, a reliable assessment of the **sampling convergence** during the calculations.

One of the misconceptions present amongst the Annex-participants at the start of the project was the idea that the number of runs in a Monte Carlo simulation is dependent on the number of input parameters. Investigating sampling convergence in the Common Exercises showed that the needed number of runs can be output dependent (e.g. mould growth versus heat loss) but is not dependent on the number of input variables. As such, a problem with one input variable might need as many runs as a problem with more than twenty input variables. An interesting study on this topic, comparing the sampling efficiency and sampling convergence of different sampling techniques for building physics applications has been presented at one of the Annex-meetings and is more extensively documented in (Janssen, 2013). The study uses the fourth benchmark exercise from the HAMSTAD-project (Hagentoft et al, 2004) as an exemplary building physics application. This benchmark case evaluates the hygrothermal response of a massive brick wall with interior finishing. The uncertainty on cumulative heat losses and moisture gains is evaluated with the hygrothermal properties of the brick wall and the surface coefficients as input variables. Sampling efficiency and sampling convergence are studied for four different sampling strategies: basic random sampling, basic Latin Hypercube sampling and two space filling designs, the maximin and a uniformity-based design.

Sampling efficiency is evaluated for all four sampling strategies by comparing the predicted mean value μ and standard deviation σ of the heat losses and moisture gains to a reference solution. Figure 3.2 shows the results for the cumulative heat losses. It is clear that Latin Hypercube sampling substantially reduces the deviation from the reference solutions in comparison to the results of the basic random sampling. Combining LHS with a space filling design furthermore significantly enhances the sampling efficiency. Relative to basic random sampling, on average 10 times less runs are needed with the LHS-design to achieve the same accuracy of mean value and standard deviation. The maximin design and the uniformity-based design further improve the sampling efficiency with a factor 7 and 10, respectively. Note that the results presented in Figure 3.2 also falsify the idea that the accuracy does not improve much above 100 runs, as often put forward in literature. For all sampling strategies a continued decrease of the relative deviations from the reference solution is found with increasing number of runs.

The study furthermore presents a kind of bootstrapping approach based on replicated Latin Hypercube designs to run LHS in sequential mode, introducing the possibility to halt the simulations when sufficient accuracy has been attained. As convergence criterion the internal standard deviations on the resulting mean value μ and standard deviation σ of the different subgroups is used. It is shown that this is a reliable estimate for the root-mean-square

deviations from the reference solution. More details on the method can be found in (Janssen, 2013).

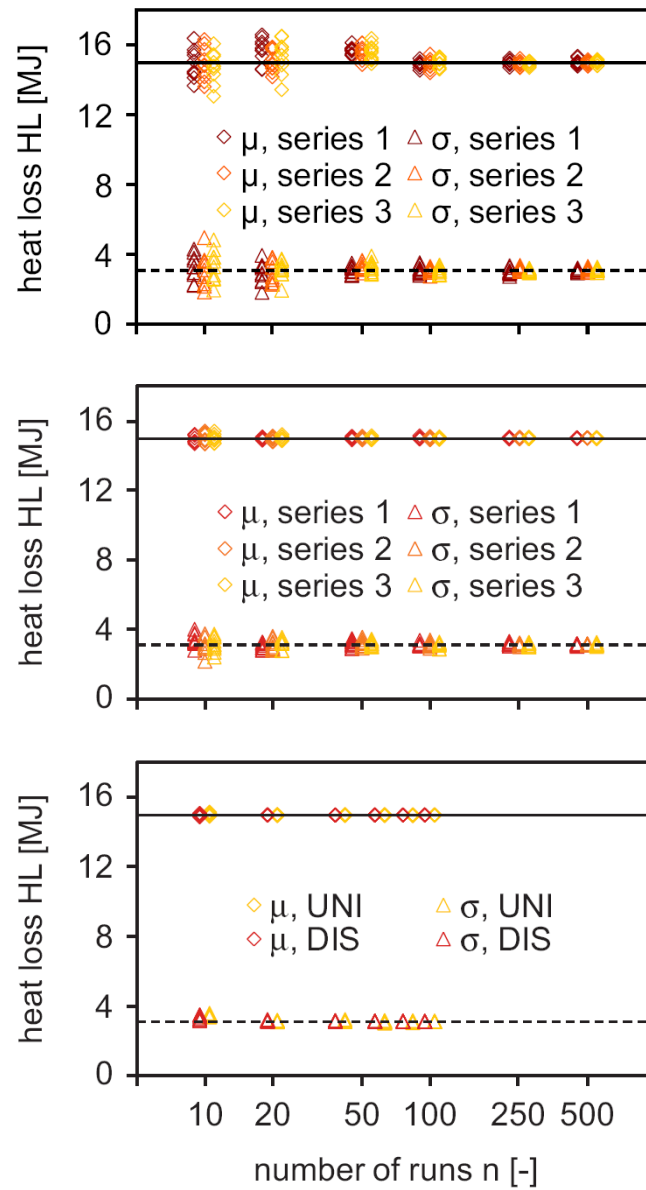


Figure 3.2: Predicted mean value and standard deviation for basic random sampling (top), latin hypercube sampling (middle) and space filling designs (bottom). The black lines correspond to the reference solution. Figures taken from (Janssen, 2013).

3.4 Common Exercise 2

3.4.1 Presentation of Exercise

Complementary to the first common exercise in ST2, which aimed at an exploration of qualitative probabilistic tools (see Addendum 1), CE2 investigated quantitative probabilistic tools applicable on a smaller scale. The subject of CE2 was the probabilistic prediction of energy savings and hygrothermal risk for a specific retrofitting measure at the building component level: the application of interior insulation on an existing massive wall. The CE is described in more detail in Section 1.3 and in Addendum 2.

The formal deliverables of the exercise are:

- the predicted evolution of the heat losses through the wall during the month of January, both for the deterministic case (determined by the mean input values) as well as for the different stochastic runs;
- the evolution of the mould growth index as a function of time over the year, again both for the deterministic case as well as for the different stochastic runs.

3.4.2 Outcomes from Exercise

Nine solutions for ST2-CE2 were received. The solutions of Anker Nielsen (Danish Building Research Institute, Denmark) and Florian Antretter (Fraunhofer, Germany) were more a sensitivity analysis than an uncertainty quantification. Pär Johansson (Chalmers, Sweden), Fitsum Tariku (British Columbia Institute of Technology, Canada) and Paul Wegerer (Vienna University of Technology, Austria) performed a parametric study to assess the impact of the uncertainty of the input parameters on the outcome. The other four results by Carl-Eric Hagentoft (Chalmers, Sweden), Hans Janssen (DTU, Denmark), Liesje Van Gelder (KU Leuven, Belgium) and Jianhua Zhao (TUDresden, Germany) performed Monte Carlo simulations to quantify the uncertainty. In the latter case, both basic random sampling, Latin Hypercube sampling and space filling designs have been applied.

Although the aim of the common exercise was an exploration of different quantitative probabilistic tools, it is difficult to compare the results as the deterministic case showed already significant deviations between the different solutions. Furthermore, several participants limited the stochastic analysis to a first parametric study, making it unable to assess and compare the predicted mean value and standard deviation. Therefore, it was decided to use a fixed simulation tool (the Matlab-model for the Swedish attic case) in the next common exercises. In these common exercises, several participants further examined uncertainty quantification and Monte Carlo sampling efficiency.

3.5 References

Hagentoft C.-E., Kalagasidis A.S., Adl-Zarrabi B., Roels S., Carmeliet C., Hens H., Grunewald J., Funk M., Becker R., Shamir D., Adan O., Brocken H., Kumaran K. and Djebbar R. (2004). Assessment method of numerical prediction models for combined heat, air and moisture transfer in building components: benchmarks for one-dimensional cases. *Journal of Thermal Envelope and Building Science* 27: 327-352.

Janssen H. (2013). Monte-Carlo based uncertainty analysis: sampling efficiency and sampling convergence. *Reliability Engineering and System Safety* 109:123-132.

Pietrzyk K. and Hagentoft C.-E. (2008). Reliability analysis in building physics design. *Building and Environment* 43:558-568.

4

SENSITIVITY ANALYSIS

Lead author

Hans Janssen

4.1 Introduction

4.1.1 Sensitivity analysis tools

This chapter discusses *sensitivity analysis*, the third set from the mentioned suite of tools. The application of these sensitivity analysis tools aims at distinguishing the dominant from the non-dominant input parameters, wherein (non-)dominance relates to the respective impact on the resulting outcomes of the probabilistic assessment. This distinction is crucial in many respects: such dominant parameters can be applied as design parameters, they should be accounted for in a surrogate model and they should be properly characterised with regard to their variability.

Sensitivity analysis is the evaluation of how the uncertainty in the output of a model or system can be attributed to different sources of uncertainty in its inputs (Saltelli et al., 2008). Sensitivity analysis can therefore be useful for many aims, such as (Wikipedia, 2014a):

- model simplification: fixing inputs that have no effect on the output, or identifying and removing redundant parts of the model or system structure;
- error identification: searching for errors in the model or system by tracing unexpected relationships between inputs and outputs;
- robustness evaluation: testing the robustness of the outcomes of a model or system in the presence of uncertainty;
- uncertainty reduction: identifying model inputs that cause significant variability of the output and should therefore be further evaluated if the robustness is to be increased;
- optimisation or filtering: finding regions in the space of input factors for which the model or system output meets some optimality criterion;

Given its wide range of uses, the literature provides numerous techniques for sensitivity analysis: examples can be found in (Saltelli et al., 2008; Wikipedia, 2014; Hamby, 1994; Hamby, 1995; Helton and Davis, 2002; Lomas and Eppel, 1992) among others. With respect to the objectives of Subtask 2 of Annex 55, this chapter judges the capabilities and limitations of (a selection of) these sensitivity analysis approaches, via their application for the hygrothermal behaviour of a cold attic in Common Exercise 3. Initially, in Section 4.2, the applied methods are presented, secondly, in Section 4.3, their merits and flaws are discussed, and finally, in Section 4.4, conclusions are formulated.

4.2 Presentation of methods

4.2.1 Introduction

A vast array of sensitivity analysis methods is available in the literature; see for example (Saltelli et al., 2008; Wikipedia, 2014; Hamby, 1994; Hamby, 1995; Helton and Davis, 2002; Lomas and Eppel, 1992), among many others. In this section, only the methods applied in relation to Common Exercise 3 are presented, and this selection is therefore by no means complete. The selected methods can be categorised into five distinct classes: one-at-a-time, screening, correlation-based, segmentation-based and variance-based methods.

4.2.2 One-at-a-time methods

The simplest approach to sensitivity analysis is to alter one input parameter at a time – while maintaining the other factors at their nominal values – and observe the impact of such change on the resulting outcome. The impact may then be expressed with different indicators:

- basic:
$$S_{x_i} = Y_{x_{i,max}} - Y_{x_{i,min}} \quad (4.1)$$

- sensitivity index:
$$S_{x_i} = \left(Y_{x_{i,max}} - Y_{x_{i,min}} \right) / Y_{x_{i,max}} \quad (4.2)$$

- elasticity index:
$$S_{x_i} = \left(Y_{x_{i,max}} - Y_{x_{i,avg}} \right) / \left(x_{i,max} - x_{i,avg} \right) \quad (4.3)$$

with x_i the considered input parameter, $x_{i,max/min/avg}$ referring to its largest, smallest and average value considered, S_{x_i} the sensitivity of the output to input parameter x_i , $Y_{x_{i,max/min/avg}}$ the output value for the different values of input parameter x_i . In these, the largest and smallest values applied for x_i are typically located around the 1- and 99-percentile, for both uniformly and normally distributed parameters. Commonly reported advantages of these one-at-a-time techniques are their simplicity and efficiency.

A typically mentioned shortcoming is however that they only sample a limited part of the input space, by using a limited number of input parameter levels while also maintaining all other parameters at their nominal values. The former restriction can be addressed by selecting several equiprobable values for the input parameter, and computing the sensitivity based on the average variation of the resulting outcome. Two possible – and strongly related – indicators are:

- mean square impact:
$$S_{x_i} = \sum_{j=1}^k \left(Y_{x_{i,j}} - Y_{x_{i,avg}} \right)^2 \quad (4.4)$$

- standard deviation:
$$S_{x_i} = \text{std} \left(Y_{x_{i,j}} \right) \quad (4.5)$$

with $x_{i,j}$ the k selected equiprobable values for the input parameter and std the standard deviation. This extension of course significantly inflates the computational cost, while the sampling of the input space still remains relatively restricted.

4.2.3 Screening methods

To address that limited sampling of the entire input space, screening methods can be applied, wherein the one-at-a-time changes are abandoned in favour of more advanced sampling schemes. Typical examples are the fractional factorial design and the elementary effects method. In the former, two levels are defined for each input parameter, normally $x_{i,max}$ and $x_{i,min}$. A fractional factorial design with k runs for the considered parameters with two levels each is then taken as the sampling design, and the sensitivity is expressed as:

$$S_{x_i} = \left| \text{avg}(Y_{x_{i,max}}) - \text{avg}(Y_{x_{i,min}}) \right| / 2 \quad (4.6)$$

hence indicating the distance between the average output values for respectively the high and the low levels of each considered input parameter. An example of a fractional factorial design for a problem with 15 input parameters is shown in Figure 4.1.

The elementary effects method instead makes use of a (limited) number of levels for the input parameters. Starting from an initial random combination of input parameter values, only one parameter is modified from one simulation to the next, and a total of k runs is performed. The sensitivity is then expressed as:

$$S_{x_i} = \text{avg}(d_{x_i}) \quad \text{with} \quad d_{x_i} = \left| Y_{x_i+\Delta} - Y_{x_i} \right| / \Delta \quad (4.7)$$

In this expression, d_{x_i} hence indicates the normalised output difference between two consecutive simulations wherein x_i is the parameter that changes its value with a step Δ . Figure 4.2 depicts a characteristic elementary effects sampling design for a 5-parameter-problem. More info on the elementary effects method can be found in (Morris, 1991; Campolongo et al., 2007).

	x_1	x_2	x_3	x_4	x_5	x_6	x_7	x_8	x_9	x_{10}	x_{11}	x_{12}	x_{13}	x_{14}	x_{15}
Run 1	-1	-1	-1	-1	1	1	1	1	1	1	-1	-1	-1	-1	1
Run 2	1	-1	-1	-1	-1	-1	-1	1	1	1	1	1	1	-1	-1
Run 3	1	-1	1	1	-1	1	1	-1	-1	1	-1	-1	1	-1	-1
Run 4	1	1	-1	-1	1	-1	-1	-1	-1	1	-1	-1	1	1	1
Run 5	-1	-1	1	-1	1	-1	1	-1	1	-1	1	-1	1	1	-1
Run 6	1	-1	1	-1	-1	1	-1	-1	1	-1	-1	1	-1	1	1
Run 7	-1	1	1	-1	-1	-1	1	1	-1	-1	-1	1	1	-1	1
...	1 = $x_{i,max}$; -1 = $x_{i,min}$							

Figure 4.1: exemplary fractional factorial design for a 15-parameter problem with two levels

parameters	Run 1	Run 2	Run 3	Run 4	Run 5	Run 6
Height of ...	5.33	8	8	8	8	8
Area of ...	100	100	200	200	200	200
Orientation ...	120	120	120	0	0	0
Venting ...	0.05	0.05	0.05	0.05	0.017	0.017
Length of ...	20	20	20	20	20	11.33

Figure 4.2: exemplary elementary effects method trajectory for a 5-parameter problem

4.2.4 Correlation-based methods

Where the methods above make use of (fairly) simple sampling designs, from here on Monte Carlo sampling designs are applied, be it random, latin hypercube or optimised latin hypercubes (see Chapter 3). The data available to the sensitivity analysis methods thus becomes more exhaustive, specifically k samples from the distributions of the input parameters and k corresponding values of the resulting outcomes. These give a (much) more representative sampling of the input and output space, and should therefore allow for a better evaluation of the (non-)dominance of parameters. The sensitivity indicators introduced above can however no longer be applied. Instead, based on the k values of the input parameters and corresponding output, sensitivity can equally be investigated via correlations between output and input. Typical techniques in this respect are Pearson's product-moment correlation and Spearman's rank correlation and linear regression.

The Pearson coefficient is a measure of the linear correlation between two variables, giving values from +1 (full positive correlation) over 0 (no correlation) to -1 (full negative correlation):

$$S_{x_i} = \left(\sum_{j=1}^k (x_{i,j} - \text{avg}(x_i))(Y_j - \text{avg}(Y)) \right) / \sqrt{\sum_{j=1}^k (x_{i,j} - \text{avg}(x_i))^2 (Y_j - \text{avg}(Y))^2} \quad (4.8)$$

The Pearson coefficient implicitly assumes linear relationships between input and output. This constraint is avoided by used of the Spearman coefficient, for which the values of $x_{i,j}$ and Y_j are replaced with their ranks in their specific populations. The Spearman coefficient however still implicitly requires monotonous relations between input and output.

Alternatively, the correlation between input and output can be assessed via the linear regression coefficients. Fitting a linear relation between input parameters and resulting outcome:

$$Y = \alpha_0 + \alpha_1 x_1 + \dots + \alpha_k x_k \quad (4.9)$$

with α_j the regression coefficients, allows derivation of the sensitivity indicators as the standardised regression coefficients:

$$S_{x_i} = \alpha_i \cdot \text{std}(x_i) / \text{std}(Y) \quad (4.10)$$

wherein standardisation is implemented to avoid wrongly estimated sensitivities for input parameters with low average and/or standard deviation. For an optimal result, iterative pruning is recommended, during which irrelevant parameters are iteratively eliminated from the linear regression model until only significant parameters remain. An extension to standard linear regression is rank regression, which has however not been applied in the framework of the analysis here. Analogous to the Pearson and Spearman coefficients, constraints related to monotonicity and/or linearity are equally valid here.

4.2.5 Segmentation-based methods

To circumvent these constraints of monotonicity and/or linearity of the correlation and/or regression coefficients, more advanced methods are needed. Typically, these are based on segmentation or variance. First, the segmentation-based techniques are discussed.

Segmentation-based sensitivity analysis techniques split the set of k inputs or outputs into different segments and evaluate whether the corresponding output or input segments stem from the same population: the larger the degree of dissimilarity between the distributions for each of the segments, the larger the sensitivity. Two tests are typically applied in this respect: Kolmogorov-Smirnov (KS) and Kruskal-Wallis (KW).

For KS the set of k outputs is divided into two segments with respectively the values below and above the output's median. The two parallel segments of the input parameter are then judged on whether they have a similar distribution, with the sensitivity expressed as:

$$S_{x_i} = \max \left(\left| \text{cdf} \left(x_{i,Y_{\text{top}}} \right) - \text{cdf} \left(x_{i,Y_{\text{bottom}}} \right) \right| \right) \quad (4.11)$$

with cdf the cumulative probability density distribution, $Y_{\text{top/bottom}}$ the segments of respectively the over- and below-median output values, and $x_{i,Y_{\text{top/bottom}}}$ the corresponding input parameter values. For more information, see (Hamby, 1994).

For KW, each set of k values for the considered input parameter is split into a (limited) number of equiprobable segments, and their corresponding output values are categorised analogously. The probability that the different sets of output values stem from different populations is then a measure for the sensitivity:

$$S_{x_i} = 1 - p \left(Y_{x_{i,1..k/m}}, Y_{x_{i,k/m..2k/m}}, \dots \text{ from same population} \right) \quad (4.12)$$

with m the number of segments, $Y_{x_{i,1..k/m}}$ the set of output values in segment 1, $Y_{x_{i,k/m..2k/m}}$ the set of output values related to segment 2, ...

Finally, scatterplots can equally be considered a segmentation-based method, however evaluated qualitatively rather than quantitatively. This approach applies plots of the k output values in function of the k values for the input parameter, to visually judge the (dis)similarity between the output populations for different segments of the input parameters. Scatterplots could also be considered a correlation-based method, wherein the sensitivity is deemed higher when a more well-defined visual relation between input and output is obtained.

4.2.6 Variance-based methods

The methods introduced above all yield a single sensitivity indicator for each input parameter, hence representing the total effect of the variability of the input parameter on the variation of the resulting outcomes. When decomposition into direct and interactive influences is desired, variance-based methods provide a possible approach.

Variance-based sensitivity analysis aims at decomposing the variance of the output of the model or system into fractions which can be attributed to separate and/or combined inputs. For example, given a model with two inputs and one output, one might find that 70% of the output variance is caused by the variance in the first input, 20% by the variance in the second, and 10% due to Interactions between the two (Wikipedia, 2014b). These percentages can be interpreted as measures of sensitivity. Variance-based sensitivity analysis is moreover attractive as it judges sensitivity across the whole input space and can easily deal with nonlinear responses.

Basically hence, a decomposition of the variance of the output is the target:

$$\text{var}(Y) = \sum_{i=1}^d V_i + \sum_{i < j}^d V_{ij} + \dots + V_{12\dots d} \quad (4.13)$$

from which sensitivity indicators can be deduced as first order effects (the primary impact of the parameter itself):

$$S_{x_i} = V_i / \text{var}(Y) \quad (4.14)$$

or total order effects (including all interactions with other parameters):

$$S_{x_i} = \left(V_i + \sum_{j=1}^d V_{ij} + \dots + V_{12\dots d} \right) / \text{var}(Y) \quad (4.15)$$

with var the variance and V the partial variances.

In a linear systems, the coefficients of determination r^2 between the output and the different inputs provide such variance decomposition. For more general systems, several other methods are available (Saltelli et al., 2008), amongst which the Fourier amplitude sensitivity test (FAST) method (Saltelli et al., 1999). Unfortunately, this report does not lend itself to a detailed presentation, as this would lead us too far. The general principles, and their implementation in FAST, can be found in the literature.

4.3 Evaluation of methods

4.3.1 Methodology of evaluation

The capabilities and limitations of the different sensitivity analysis methods introduced above are appraised via application for a hygrothermal performance analysis. Firstly the calculation object is introduced, subsequently the processing of the results is discussed.

4.3.1.1 Calculation object

The evaluation of the sensitivity analysis techniques is executed via Common Exercise 3. This Common Exercise centres on the hygrothermal performance of a cold attic. A matlab model is provided, wherein the relevant heat, air and moisture balances to determine the hygrothermal conditions in the cold attic are solved. More information can be found in the instruction document in Section 1.7. Simulations typically cover one year and result in hourly values for the hygrothermal conditions in the attic and the hygrothermal flows to and from the attic. These are transformed to two particular outputs: the cumulated heat loss (CHL) in January, and the peak mould growth (PMG) over the year.

The hygrothermal performances of the cold attic depend on 15 stochastic input parameters, which are brought together in Table 4.1 with their probability distributions. Two different distribution types are applied: U(niform)(lower limit, upper limit) and N(ormal)(average, standard deviation) distributions. The aim of CE3 is hence to determine the (non-)dominance of these 15 input parameters with respect to CHL and PMG, once for a case wherein the climate year is fixed, once for a case where the climate year is variable.

Table 4.1: variable input parameters, probability distribution

Area of ceiling and roof (m ²)	U(50,200)
Length of building (eave side) (m)	U(7,20)
Height of building (m)	U(4,8)
Leakage area per m ² of ceiling (m ² /m ²)	U(0.001,0.05)**
Venting area per meter eave (m ² /m)	U(0.001,0.05)
Indoor temperature (°C)	N(20,1.5)
Indoor moisture supply (kg/m ³)	N(0.005,0.002)
Year of climate data used (-)	U(1,30)*
Orientation of one of eave sides (-)	U(0,180)
U-value of the ceiling (W/m ² K)	U(1,5)**
Resistance of roof insulation (m ² K/W)	U(0,1)
Thickness of wooden underlay (m)	U(0.010,0.020)
Thermal conductivity of wood (W/mK)	N(0.13,0.02)
Vapour diffusivity of wood (m ² /s)	N(10 ⁻⁶ ,2 10 ⁻⁷)
Initial relative humidity of wood (-)	U(0.5,0.9)

**only discrete integers **excessively high values*

4.3.1.2 Evaluation method

Application of each of the sensitivity analysis techniques put forward above results in sensitivity indicators for 14 input parameters. The sensitivity to the climate year is not assessed, since it cannot be reliably quantitatively characterised. For the CHL in the fixed-climate-scenario for example, the resulting Spearman coefficients are depicted in Figure 4.3. In a next step, these results are transformed, first by taking absolute values of the sensitivity indicators and second by dividing all sensitivity indicators by the largest sensitivity indicator, see Figure 4.4.

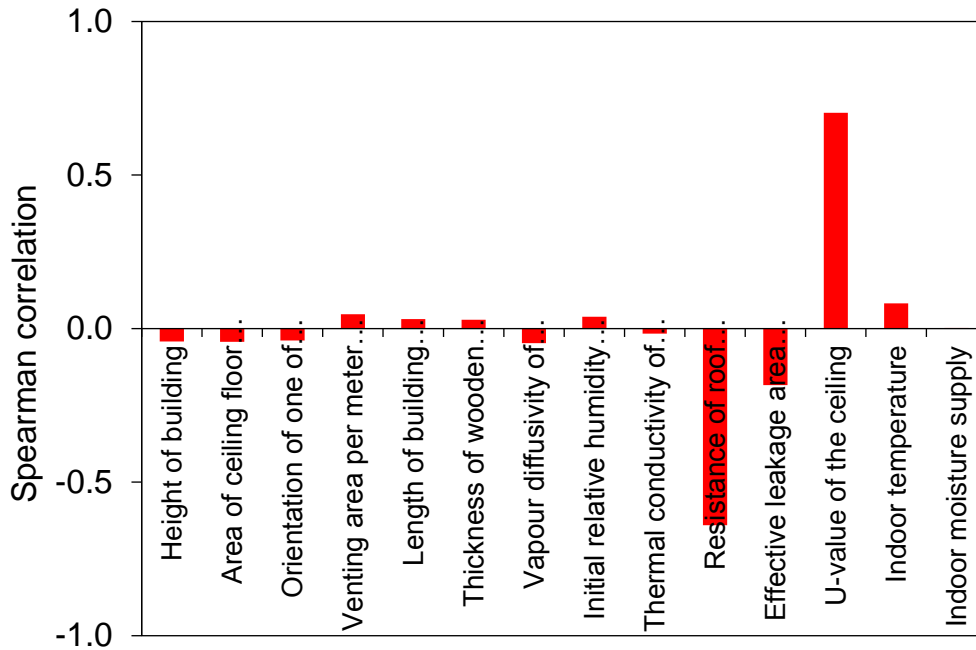


Figure 4.3: Spearman correlation coefficients for the cold attic case with fixed climate year

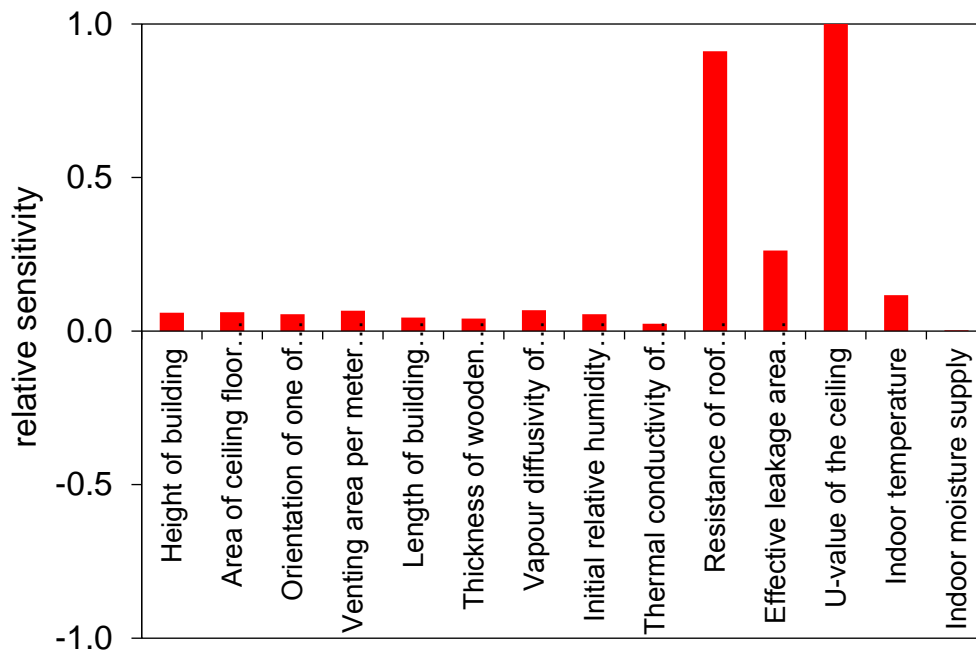


Figure 4.4: Normalised Spearman coefficients for the cold attic case with fixed climate

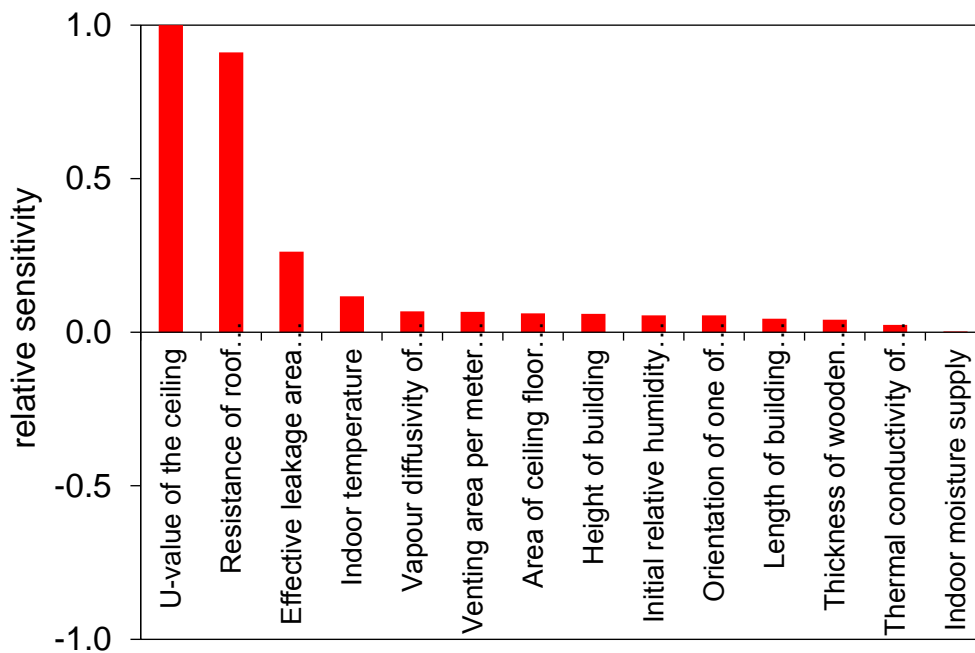


Figure 4.5: Ordered normalised Spearman coefficients for the cold attic case with fixed climate

Ultimately these positive and relative sensitivity indicators are ordered along the large to small order resulting from the Spearman coefficients, see Figure 4.5, wherein the Spearman results are hence accepted as the reference outcomes. The entire transformation and ordering allows easy comparison of the different methods, as they all originally produce sensitivity indicators of different sign and magnitude. The only method excluded from this analysis is ‘scatterplots’, as these do not lead to quantified sensitivity indicators. The scatterplots will however be judged complementarily.

4.3.2 Presentation of evaluation

In the end, the collection of sensitivity analysis methods presented above can be boiled down to these twelve distinct methods and/or indicators:

- differential sensitivity analysis, 2 points, indicator basic (eq. 4.1)
- differential sensitivity analysis, 2 points, indicator sensitivity index (eq. 4.2)
- differential sensitivity analysis, 2 points, indicator elasticity index (eq. 4.3)
- differential sensitivity analysis, 30 points, indicator standard deviation (eq. 4.5)
- fractional factorial design, indicator average impact (eq. 4.6)
- elementary effects method (EEM), indicator average impact (eq. 4.7)
- linear regression, indicator standardised regression coefficients (eq. 4.10)
- Pearson’s coefficient, indicator moment correlation coefficient (eq. 4.8)
- Spearman’s coefficient, indicator rank correlation coefficient (eq. 4.8 with ranks)
- Kolmogorov-Smirnov, indicator maximal distance (eq. 4.11)
- Kruskal-Wallis, indicator different-population-probability (eq. 4.12)
- Fourier amplitude sensitivity test (FAST), indicator total effect (eq. 4.15)

The comparison of their outcomes is founded on the solutions for Common Exercise 3, nine of which were received, as contributed by Mika Saloonvara (Owens Corning, USA), Marcus Fink & Florian Antretter (Fraunhofer, Germany), Payel Das & Benjamin Jones (University College London), Liesje Van Gelder (KU Leuven, Belgium), Fitsum Tariku (British Columbia Institute of Technology, Canada), Mike van der Heijden (TU Eindhoven, the Netherlands), Vahid Nik (Chalmers, Sweden), Pär Johansson (Chalmers, Sweden), and Henrik Karlsson (SP, Sweden). The complete solutions are not included here, instead we will make a synthesis of their findings and comments only. Where appropriate, all solutions made use of Monte Carlo sampling to obtain sets of input parameters and related outputs, for which different contributors used different sampling designs. In a preliminary analysis however, the equivalency of their uncertainty and sensitivity results has been verified and all sensitivity indicators should be sufficiently reliable for further analysis here.

4.3.2.1 Fixed-climate case

For the fixed-climate case, ten out of the twelve methods mentioned previously are employed, only the elementary effects method and the Fourier amplitude sensitivity test are not included. The collected relative sensitivities resulting from these 10 methods are presented in Figure 4.6 for CHL and Figure 4.7 for PMG.

It is clear that most of the methods produce consistent results, but it is similarly evident that a few methods come to deviating outcomes, with specifically over- and underestimations of the actual sensitivities. For example, the 'DSA, 2 pts, basic' method gives a high sensitivity to non-dominant parameters, while the 'DSA, 2 pts, elastic.' method yields a low sensitivity for dominant parameters.

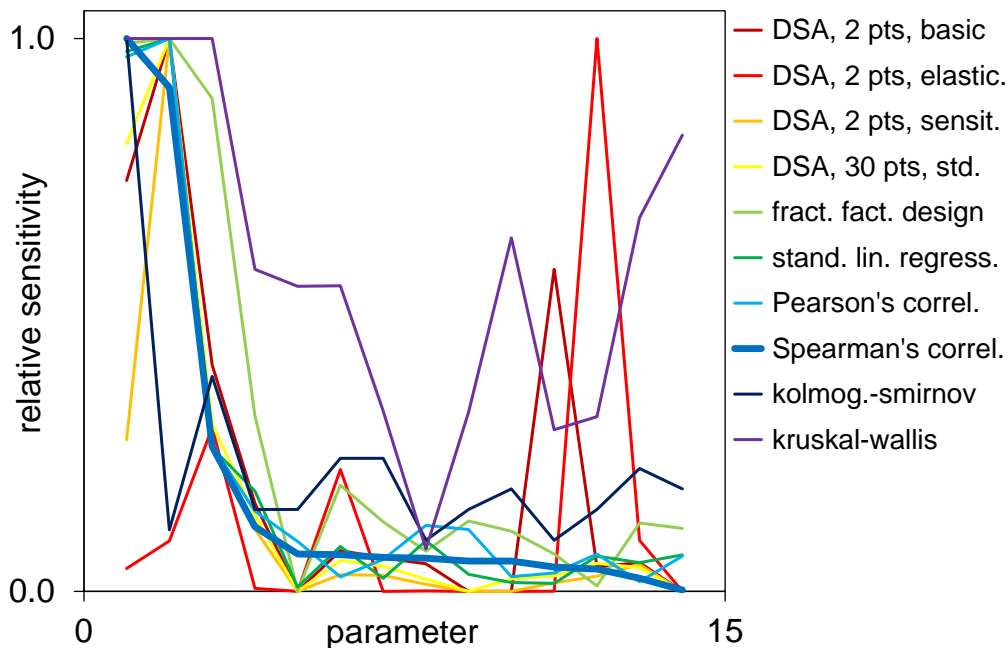


Figure 4.6: Relative sensitivities for CHL (the significant parameters 1 to 4 are U-value of ceiling, resistance of roof, effective leakage area, indoor temperature).

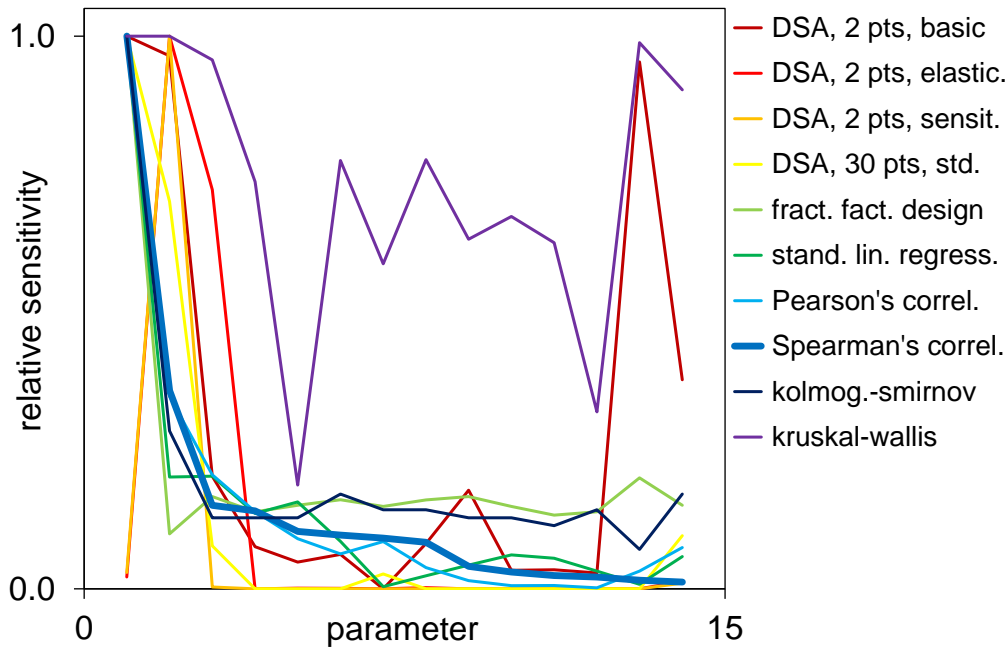


Figure 4.7: Relative sensitivities for PMG (the significant parameters 1 to 3 are indoor moisture supply, indoor temperature and resistance of roof).

The ‘DSA, 30 pts, std.’, ‘fract. fact. design’, ‘stand. lin. regress.’, ‘Pearson’s correl.’ and ‘Spearman’s correl.’ identify the U-value of the ceiling, the resistance of the roof, the effective leakage area, the indoor temperature and the indoor moisture supply, the indoor temperature, the resistance of the roof as the dominant variables for respectively CHL and PMG. These are, based on the physics, the plausibly significant input parameters, and the five mentioned sensitivity analysis methods can thus be considered as reliable. The other five methods, on the contrary, need to be deemed undependable. This is a common conclusion for the DSA methods based on two points, but somewhat surprising for the segmentation-based methods Kolmogorov-Smirnov and Kruskal-Wallis. No effort has however been undertaken to explain those observations for the latter two methods.

The CHL scatterplots in Figure 4.8 also identify U-value of the ceiling, the resistance of the roof, the effective leakage area and the indoor temperature as dominant variables, while the other scatterplots (not shown) indicate the insignificance of the other input parameters. It should be noted though that the identification of effective leakage area and indoor temperature – secondarily dominant input parameters – remains ambiguous.

Based on Figures 4.6 to 4.8, the reliable methods can be reduced to:

- differential sensitivity analysis, 30 points, indicator standard deviation (eq. 4.5)
- fractional factorial design, indicator average impact (eq. 4.6)
- linear regression, indicator standardised regression coefficients (eq. 4.10)
- Pearson’s coefficient, indicator moment correlation coefficient (eq. 4.8)
- Spearman’s coefficient, indicator rank correlation coefficient (eq. 4.8 with ranks)
- *scatterplots*

bearing in mind that EEM and FAST have not been assessed yet.

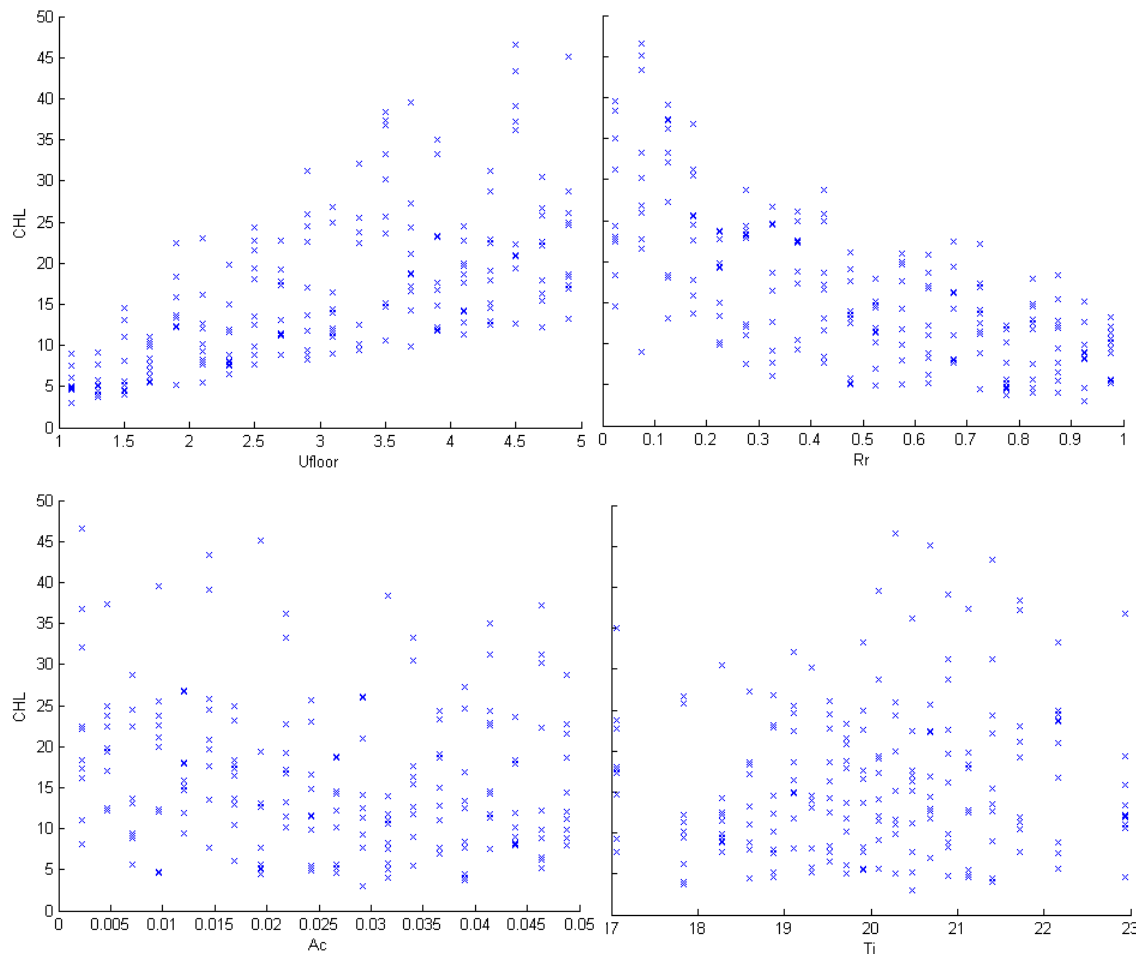


Figure 4.8: Scatterplots of CHL in function of U-value of ceiling (top left), resistance of roof (top right), effective leakage area (bottom left) and indoor temperature (bottom right).

4.3.2.2 Variable-climate case

For the variable-climate case, only the six methods deemed reliable above are further evaluated, complemented by the elementary effects method and the Fourier amplitude sensitivity test, the results of which can be found in Figure 4.9 and Figure 4.10. The ‘DSA, 30 pts., std.’ obviously falls through. In order to calculate the sensitivities under variable climates, the method can only be applied by randomly varying the climate year while doing the one-at-a-time variations of the other parameters, and naturally, this invalidates the method. Also the ‘fract. fact. design’ is cracking up, given its underestimation of the second significant parameter for PMG. Moreover, as the sampling design only applies a lower and upper limit, the complete variability of the climate can fundamentally not be accounted for. All other techniques appear to remain reliable, although some question marks surround the FAST results. Further analysis does reveal though that the relatively high sensitivities for the relatively non-dominant parameters are primarily a consequence of incorporating the interaction effects. If solely the main order is used, the agreement with the other methods improves vastly. This however nullifies the primary advantage of the FAST approach, as it now does not result in any valuable additional information while requiring far more runs than all other methods. One can moreover wonder where information on such interactions actually finds relevant applications.

As before, the scatterplots (not shown here) allow identification of the main dominant input parameters, but remain more ambiguous when it comes to secondarily dominant parameters.

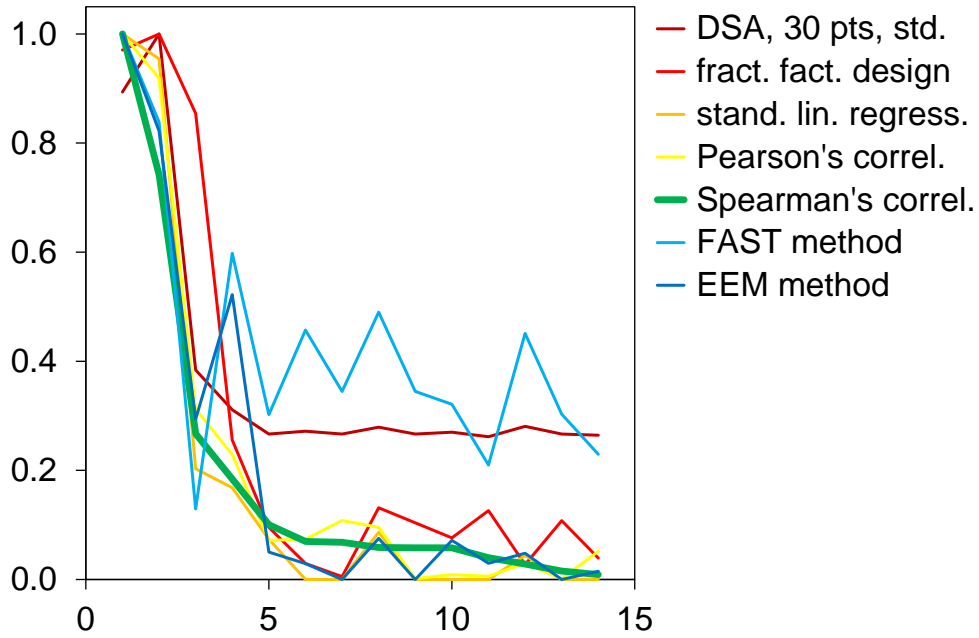


Figure 4.9: Relative sensitivities for CHL (the significant parameters 1 to 4 are U-value of ceiling, resistance of roof, effective leakage area, indoor temperature).

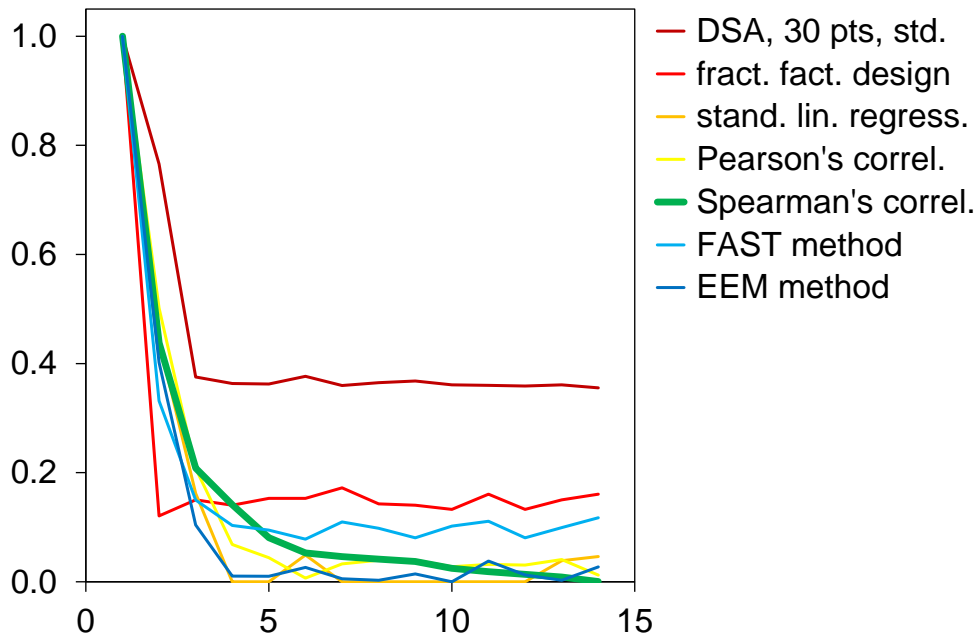


Figure 4.10: Relative sensitivities for PMG (the significant parameters 1 to 3 are indoor moisture supply, indoor temperature and resistance of roof).

Based on Figures 4.9 and 4.10, the reliable methods can be reduced to:

- linear regression, indicator standardised regression coefficients (eq. 4.10)
- Pearson’s coefficient, indicator moment correlation coefficient (eq. 4.8)
- Spearman’s coefficient, indicator rank correlation coefficient (eq. 4.8 with ranks)
- elementary effects method (EEM), indicator average impact (eq. 4.7)
- Fourier amplitude sensitivity test (FAST), indicator *first* order (eq. 4.14)
- *scatterplots*

4.3.2.3 Influence of sample size

As a final element in this evaluation, the impact of the sample size is investigated for a selected number of methods, specifically the Pearson’s coefficient, the elementary effects method, the Fourier amplitude sensitivity test and the scatterplots. One illustration is shown in Figure 4.11, which depicts the variation of the Pearson’s coefficients for CHL with the number of samples in the supporting Monte Carlo analysis. It is obvious that significant evolutions take place when increasing the number of runs. The same observation is made for the other methods, and care should thus be taken with the number of samples applied to quantify the sensitivity indicators. For that reason hence, statistical validation of the resulting sensitivity indicators is essential, to confirm the dependability of the obtained (non-)dominant input parameters. That specific aspect has not been elaborated further in Annex 55, but more information is available in the literature (see e.g. Van Gelder et al., 2014).

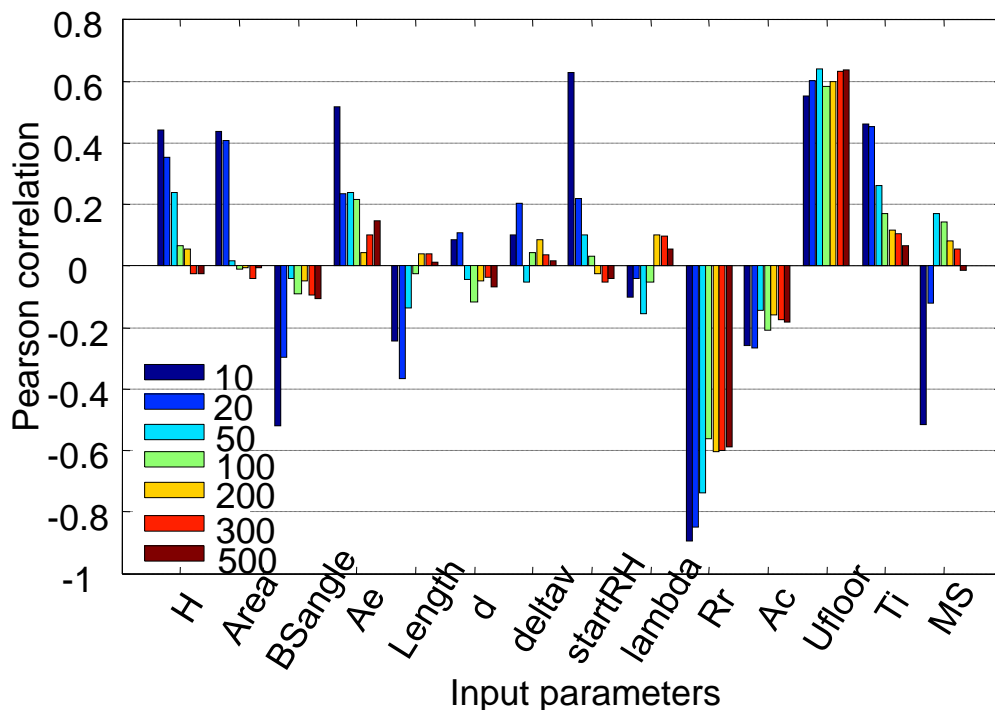


Figure 4.11: Variation of the CHL Pearson’s coefficients with the sample size.

4.3.3 Conclusion of evaluation

Our assessment, based on the specific example of the hygrothermal performances of a cold attic, has revealed that only six of the original twelve methods can be considered reliable:

- linear regression, indicator standardised regression coefficients (eq. 4.10)
- Pearson's coefficient, indicator moment correlation coefficient (eq. 4.8)
- Spearman's coefficient, indicator rank correlation coefficient (eq. 4.8 with ranks)
- elementary effects method (EEM), indicator average impact (eq. 4.7)
- Fourier amplitude sensitivity test (FAST), indicator **first** order (eq. 4.14)
- *scatterplots*

Each of these comes with disadvantages though:

- **linear (rank) regression coefficients**
 - linear regression coefficients presume linear relations between input and output
 - linear rank regression coefficients presume monotonous relations between input and output
- **Pearson's & Spearman coefficients**
 - Pearson's coefficients presume linear relations between input and output
 - Spearman's coefficients presume monotonous relations between input and output
- **elementary effects method**
 - the actual distribution of the input parameter is not taken into account
 - relative to other methods, far more runs are needed to come to stable results
- **Fourier amplitude sensitivity test**
 - the reliability of the sensitivities can be weak for discrete input variables
 - relative to other methods, far more runs are needed to come to stable results
- **scatterplots**
 - interpretation of scatterplots is subjective and at times ambiguous
 - no quantified sensitivity indicators are available, rating is hence difficult

4.4 Conclusions

The core objective of Annex 55's Subtask 2 is to evaluate the advantages and disadvantages of existing methods for probabilistic assessment when applied to building performance analysis and design. Five sets of tools are needed for probabilistic assessments: *qualitative exploration*, *uncertainty propagation*, *sensitivity analysis*, *metamodelling method*, and *economic optimisation*. This chapter focused on techniques for sensitivity analysis, which target the identification of the dominant and non-dominant input parameters, wherein (non-)dominance relates to the respective influence on the resulting outcomes of the probabilistic assessment. This identification is crucial in many respects: such dominant parameters can be applied as design parameters, they should be accounted for in a surrogate model and they should be properly characterised with regard to their variability.

The literature on sensitivity analysis provides a vast array of different approaches, which can be classified into one-at-a-time, screening, correlation-based, segmentation-based and variance-based methods. Twelve methods have been evaluated in this chapter, wherein at least one example from each category. While the list of potential sensitivity analysis methods is far larger, the selected techniques give a fine overview of the different approaches. The assessment of their respective capabilities and limitations has been based on application to a hygrothermal performance assessment of a cold attic in the framework of Common Exercise 3. The target of this Common Exercise was to identify which of the fifteen stochastic input parameters of this problem have a (non-)dominant influence on the two resulting outcomes, the cumulated heat loss and the peak mould growth.

Different participants of the Common Exercise applied different methods based on different sampling techniques. The equivalency of their resulting sensitivity indicators was however verified, and after normalisation and ordering the different outcomes could be reliably compared. This comparison was based on a fixed-climate and a variable-climate case, wherein the correct identification of (non-)dominant parameters was the primary objective. The assessment showed that only the following methods led to reliable results:

- linear regression, indicator standardised regression coefficients (eq. 4.10)
- Pearson's coefficient, indicator moment correlation coefficient (eq. 4.8)
- Spearman's coefficient, indicator rank correlation coefficient (eq. 4.8 with ranks)
- elementary effects method (EEM), indicator average impact (eq. 4.7)
- Fourier amplitude sensitivity test (FAST), indicator first order (eq. 4.14)
- *scatterplots*

Our final recommendation would be the combined use of Spearman's coefficients and scatterplots. The former is very easy in application, given its implementation in multiple software environments. And contrary to the EEM and FAST approaches, far less runs are required to come to reliable results. Moreover, these runs can be based on standard Monte Carlo sampling, the approach that also underpins uncertainty quantification (see Chapter 3) and metamodel development (see Chapter 5). The complementary use of scatterplots, which can be deduced from the same sampling data, sidesteps the monotonicity restriction of the Spearman's coefficients.

4.5 References

Campolongo F., Cariboni J. and Saltelli A. (2007). An effective screening design for sensitivity analysis of large models. *Environmental Modelling and Software* 22:1509-1518.

Hamby D.M. (1994). A review of techniques for parameter sensitivity analysis of environmental models. *Environmental Monitoring and Assessment* 32:132-154.

Hamby D.M. (1995). A comparison of sensitivity analysis techniques. *Health Physics* 68:194-204.

Helton J.C. and Davis F.J. (2002). Illustration of sampling-based methods for uncertainty and sensitivity analysis. *Risk Analysis* 22:591-622.

Lomas K.J. and Eppel H. (1992). Sensitivity analysis techniques for building thermal simulation programs. *Energy and Buildings* 19:21-44.

Morris M.D. (1991). Factorial sampling plans for preliminary computational experiments. *Technometrics* 33:161-174.

Saltelli A., Ratto M., Andres T., Campolongo F., Cariboni J., Gatelli D., Saisana M. and Tarantola S. (2008). *Global sensitivity analysis: the primer*. John Wiley and Sons, West Sussex, England.

Saltelli A., Tarantola S. and Chan K.P.S. (1999). A quantitative model-independent method for global sensitivity analysis of model output. *Technometrics* 41:39-56.

Van Gelder L., Janssen H. and Roels S. (2014). Probabilistic design and analysis of building performances: methodology and application example. *Energy and Buildings* 79:202-2011.

Wikipedia (2014a). Sensitivity analysis. http://en.wikipedia.org/wiki/Sensitivity_analysis, last accessed on April 14 2014.

Wikipedia (2014b). Variance-based sensitivity analysis. http://en.wikipedia.org/wiki/Variance-based_sensitivity_analysis, last accessed on April 14 2014.

5 METAMODEL- LING METHODS

Lead author

Liesje Van Gelder

5.1 Introduction

5.1.1 Metamodelling methods

Monte Carlo analyses proved to be very helpful for uncertainty quantification (Chapter 3) and sensitivity analysis (Chapter 4) for performance and robustness optimisation (Chapter 6). In order to perform these probabilistic assessments, a simulation model is needed and is run for several settings of the input parameters. Standard methods as explained and applied in previous mentioned chapters require tens or even millions of such simulation runs. Depending on the complexity of the simulation model, the execution time of one simulation can take from a few seconds to even some days. This implies that often only a small number of deterministic runs is feasible, thus hindering the application of the standard methods. The execution time of these simulation models is thus unfortunately a restrictive factor.

Instead of using these time inefficient simulation models for such probabilistic assessments, the use of metamodels can be considered. Such a metamodel mimics the original simulation model via a simplified mathematical model: the simulation outputs can be approximated with high confidence as illustrated in Figure 5.1, comparing the CHL for Common Exercise 4 (see Addendum 4) as predicted by one of the metamodels and the reference simulation. A simulation run then only takes a fraction of the original simulation time, hence allowing significant computational savings. In order to formulate such a model, a limited number of input combinations is run in the original model. The input/output combinations are then used to statistically fit the coefficients of these mathematical functions. This results in an independent model to estimate new input/output combinations within the range of the sampled combinations.

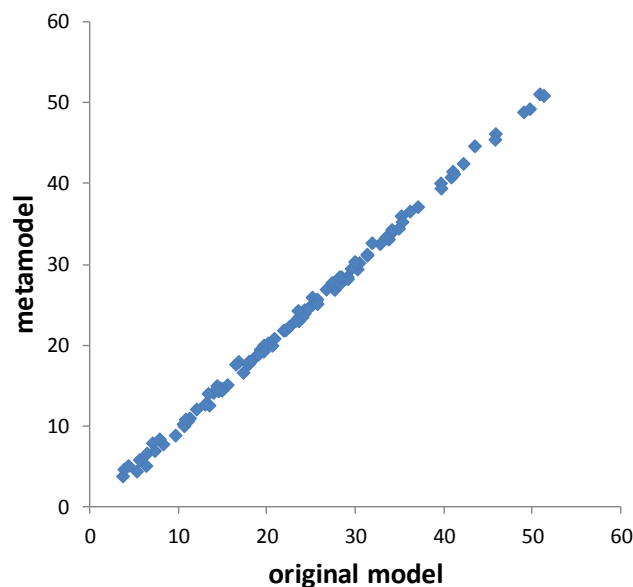


Figure 5.1: Metamodel example.

Numerous methods for metamodeling are available in literature. This chapter will explain and evaluate only polynomial regression, multivariate adaptive regression splines (MARS), kriging and neural networks to decide on which are most reliable, as explored in Common Exercise 4 of Subtask 2. Furthermore, one of the important aspects is the influence of the sample size on the different methods, as this will determine the feasibility and calculation efficiency. Therefore, methods with good approximation ability using only a few samples are preferable.

5.2 Presentation of methods

5.2.1 Basic principles

Metamodels are formulated by fitting a mathematical function to input/output combinations. To create this set of input/output combinations, the original model is run for a sample of input parameters. These combinations are called the training set. When multiple output parameters are considered, each output parameter is usually modelled separately, although it is possible with some methods to fit them simultaneously. In general, all input and output data is standardised to overcome the influence of the parameter units. This is done by transforming the data to zero mean and unit variance, also known as calculating the z-score. Standardisation can reduce calculation time and errors.

In metamodeling, the training data can be perfectly fit, while unseen data are not approximated well at all, especially for larger training sets. This phenomenon is called overfitting and emphasises the importance of testing the model performance on unseen data, as will be done in Section 5.3. Extra input/output combinations, the validation set, are therefore created and used to compare the predictions of the metamodel with the original model output.

Overfitting can be avoided by reducing model complexity during the training stage. For that purpose the Euclidian norm of the coefficients vector can be limited through *regularisation*, as is done in polynomial regression (5.2.2), radial basis function networks (5.2.5.1) and sigmoidal transfer function networks (5.2.5.2). Alternatively, the generalisation ability can be improved by reducing the number of coefficients of a complex model, what is called *pruning*, as is done in polynomial regression (5.2.2) and the multivariate adaptive regression splines method (5.2.3). A *model selection criterion* to trade off model complexity against goodness-of-fit can be used as well, as applied in multivariate adaptive regression splines (5.2.3) and radial basis function networks (5.2.5.1). Finally, the whole sample set can be divided into *training*, *validation* and *testing data*. The training data and validation data is then used to train the model, while the testing data is used to compare different models, as in done in sigmoidal transfer function networks (5.2.5.2). Dividing into training and testing samples is done multiple times in cross-validation, as in polynomial regression (5.2.2).

5.2.2 Polynomial regression

Polynomial regression is one of the most common metamodeling techniques: it fits an n^{th} order polynomial between the sampled input and output data. In general, the model is a function of the form

$$\underline{y} = b_0 + \sum_{n=1}^m \sum_{i=1}^k b_{ni} x_i^n + \sum_{n=1}^m \sum_{p=1}^m \sum_{i=1}^k \sum_{j=1}^k b_{npj} x_i^n x_j^p \quad (5.1)$$

with \underline{y} is the estimated output parameter, x the input parameter values, k the number of input parameters, m the order of the polynomial and b the regression coefficients (Jin et al. 2001). These coefficients are determined with the least squares method.

This method can be optimised to avoid overfitting, as in Tikhonov regularisation (Wikipedia 2013). Not only are the summed squares of the errors minimised, but this sum is extended to penalise large coefficients. Therefore, the least square cost function is modified by an additional term which aims at keeping the norm of the solution vector small. This extra term is the squared norm of the regression coefficients multiplied with a regularisation factor, which is selected based on cross-validation. This cross-validation is performed by dividing the training data set into several segments.

One of the advantages of polynomial regression is that the regression coefficients can be used directly in sensitivity analysis (Chapter 3). The metamodel is easy to understand as well. Unfortunately, the disadvantage is that the calculation time exponentially increases with the number of input parameters and the order of the polynomial. Furthermore, more training data is recommended when the order and the dimension increases. In fact, the number of initial samples should be higher than the number of regression coefficients (Johnson et al., 2010). The latter can be avoided by pruning. As will be seen in the application of this method however, good models can be obtained for underdetermined problems as well.

First, second and third order polynomials are studied in this chapter. For example, a fourth order polynomial with 14 input parameters would have 3600 coefficients. Hence, this is computationally expensive and ideally needs more than 3600 training samples. A fifth order polynomial would even have 11628 coefficients. The Matlab extension *polyfitn* (D'Errico, 2012) is used for fitting the polynomial models. To avoid overfitting for larger training sets, this algorithm is adjusted by means of the Tikhonov regularisation. For smaller training sets, the *stepwisefit* function (Mathworks, 2013) is also used, which adds and removes terms from the input vector based on their statistical significance to reduce the number of coefficients (pruning).

5.2.3 Multivariate adaptive regression splines (MARS)

Multivariate adaptive regression splines (MARS) can be seen as an extension of polynomial regression. The models are also of the form

$$\underline{y} = \sum_{i=1}^k c_i B_i(x) \quad (5.2)$$

with \underline{y} the estimated output parameter, x the input parameter values, k the number of basis functions B_i and c_i the weight factors (Friedman 1991, Jin et al. 2001). In contrast to polynomial regression, non-linearities between output and input can be taken into account because of the use of hinge functions. A hinge function has the form $\max(0, x - \text{constant})$ or $\max(0, \text{constant} - x)$ and thus produces a kink. The basis functions in (5.2) are a constant, a hinge function, or a product of hinge functions to take interactions into account (Wikipedia 2014).

Both the hinge functions and weight factors have to be determined, which is done through a forward selection and backward deletion iterative approach. In the forward phase, basis functions giving largest reduction of training error are added. This phase ends when

- the (change in) training error becomes small,
- the user-defined maximum number of terms is reached,

- or more weight factors than training samples are expected in the next iteration.

Typically an overfit model is the result. In the backward phase the model is pruned by trading off goodness-of-fit against model complexity. The least effective terms are deleted one by one to improve the generalisation ability (Jekabsons 2011, Wikipedia 2014).

The major advantages of the MARS technique are that the model construction is very time-efficient and easy to understand. Unfortunately, the accuracy for smaller training sets seems to be low.

Both piecewise-linear and piecewise-cubic models are created in this chapter with the Matlab toolbox *ARESLab* (Jekabsons 2011). The latter can have basis functions that are a product of two hinge functions. In R, MARS modelling can be done with the *mda* package (Hastie et al., 2013). It seems that for small sample sizes the R code is better. The model settings are all default except for the maximal number of parameter interactions, which is set equal to the number of parameters, to allow more model complexity. The maximum number of terms can be changed to increase the complexity as well.

5.2.4 Kriging

Kriging has its origin in the field of geostatistics and interpolates the value of a random field at an unobserved location from observations at nearby locations. The models are of the form

$$\underline{y} = \sum_{i=1}^k b_i f_i(x) + Z(x) \quad (5.3)$$

with \underline{y} the estimated output parameter, x the input parameter values, k the number of fixed polynomial functions f_i , b_i the regression coefficients and Z a realisation of a stochastic process with mean zero and spatial correlation function given by

$$\text{cov}[Z(x_i), Z(x_j)] = \sigma^2 R(x_i, x_j) \quad (5.4)$$

where σ^2 is the process variance and R the correlation. The first term is analogous to the polynomial regression and provides a global model, while the second term interpolates the different sampled data points (Simpson et al., 2001). The coefficients are determined with the least squares method, analogously to polynomial regression.

The major disadvantage of this method is, as for polynomial regression, the curse of dimensionality. As numerous regression coefficients need to be calculated for high orders and several input parameters, the calculation time can be very long. Furthermore, the method is complicated and mistakes are therefore possible. Moreover, Jin et al. (2001) state that kriging does not perform well if the model is noisy because of the interpolation technique.

Several correlation functions can be applied, such as exponential, linear, spherical, cubic and spline. However, the Gaussian correlation function is most frequently used. First and second order models are studied with Matlab toolbox *DACE* (Nielsen et al., 2002). An initial guess on the correlation function parameters and lower and upper bounds must be provided. However, it is not clear how to determine these. Therefore, the same values as in the user manual

example can be taken: initial guess 10, lower bound 0.1 and upper bound 20 for all parameters. In R, the kriging function is supplied by the *fields* package (Furrer et al., 2013).

5.2.5 Neural networks

A neural network is composed of an interconnected group of artificial neurons. In this chapter, multilayer perceptrons are used. These are structures consisting of several layers: input layer, output layer and multiple hidden layers with neurons, as illustrated in Figure 5.2. The neurons contain the ‘transfer functions’. Each neuron is associated with a weight and possibly also a bias, which are trained by least-squares minimisation (Simpson et al., 2001).

One of the advantages of neural networks is that the calculation time is not increasing exponentially with the amount of input parameters. Therefore, this method is often used for high-dimensional problems. The disadvantage of this technique is that it is difficult to select the best settings because of the multiple layers. Two categories of constructions are explored in this chapter: radial basis function network and sigmoidal transfer function networks.

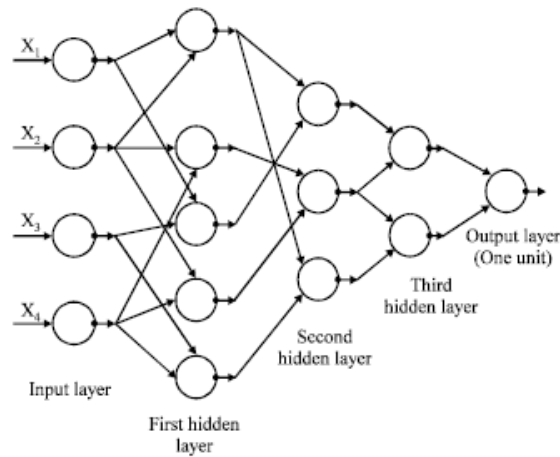


Figure 5.2: Neural network with three hidden layers (Galkin and Lowell, 2013).

5.2.5.1 Radial basis function networks (RBF)

Radial basis function networks are single hidden layer neural networks as illustrated in Figure 5.3. Each of the n components of the input vector x feeds forward to m n -dimensional basis functions h_j whose outputs are linearly combined with weights w_j into the network output $f(x)$.

A radial basis function network is thus of the form

$$f(x) = \sum_{j=1}^m w_j h_j(x) \quad (5.5)$$

and a typical Gaussian basis function is of the form

$$h_j(x) = \exp\left(-\frac{\|x - c_j\|^2}{r_j^2}\right) \quad (5.6)$$

with c_j the center and r_j the radius of basis function h_j (Orr, 1996). Other basis functions are available as well, like the Cauchy, the multiquadric and the inverse, as illustrated in Figure 5.4. All functions are applied in this chapter.

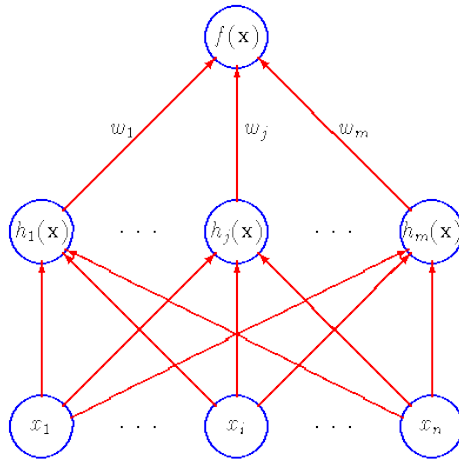


Figure 5.3: Radial basis function network (Orr, 1996).

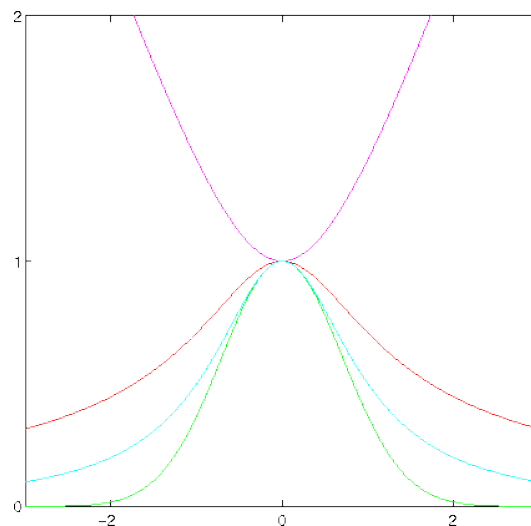


Figure 5.4: Radial basis functions with center 0 and radius 1: Gaussian (green), Cauchy (cyan), multiquadric (magenta) and inverse (red). (Orr, 1996).

Both weights and centers and radii of basis functions have to be determined. According to (Orr, 1999), the centers of the basis functions are generally equal to the input matrix. Each basis function center is thus n -dimensional and has many basis functions (or neurons) as initial samples can be created. The radii are for each dimension generally chosen equal to the span of the training set inputs (maximal value minus minimal value). Each basis function thus has the same radius. Preferably, a scale factor is applied to this radius to avoid underfitting. Therefore scale factors between 10% and 100% with steps of 10% are selected in this chapter. Each scale factor is used to create a network and the network with the lowest model selection score (eg. generalised cross-validation) is selected (Orr, 1996).

Either a forward selection or a ridge regression can be performed to select some of the available basis functions (including a bias unit), similar to the MARS method. A forward selection compares models made up of different subsets of basis functions and thus selects the number of hidden nodes. Basis functions that most reduce the sum-squared-error are added one by one, until the model selection criterion score stops decreasing to avoid too complex models. Weight factors are determined based on the sum-squared-error as well. Ridge regression selects all available basis function and augments the sum-squared-error with an extra term penalising large weights, to avoid overfitting analogously to regularised polynomial regression (Orr, 1996).

The RBF networks are implemented with the *RBF* toolbox in Matlab (Orr, 1999).

5.2.5.2 Sigmoidal transfer function network

These networks consist of a first layer with input neurons, a final layer with output neurons, and any number of hidden layers in between. The transfer functions in all layers are sigmoidal except the final layer, which is linear. A weighted sum of the input parameter values x_i with weights w_i and a bias value β feeds forward to m sigmoid functions (Figure 5.5) in a feed forward construction. This is repeated if there are more hidden layers, and then outputs of the final hidden layer y are linearly combined with a bias and weights w_j into the network output $f(x)$ (Simpson et al., 2001). With a cascade forward construction, connections are also possible between non-adjacent layers.

The output of the sigmoidal transformation of the j^{th} neuron is given by

$$y_j(\eta) = \frac{2}{1 + \exp(-2\eta)} - 1 \quad (5.7)$$

with y the output, and η the value going into the neuron (Figure 5.5). Tan-sigmoidal functions are used in this chapter and illustrated in Figure 5.5.

This network is similar to the radial basis function network, but the transfer functions are different, more hidden layers are possible, and the input parameter values are weighted. The initial samples are divided into three subsets:

- 70% is used as the training set to determine weights and biases
- 15% is used as a validation set, used during training to overcome overfitting
- 15% is used as a test set to determine the optimal combination of neural network architecture and training algorithm.

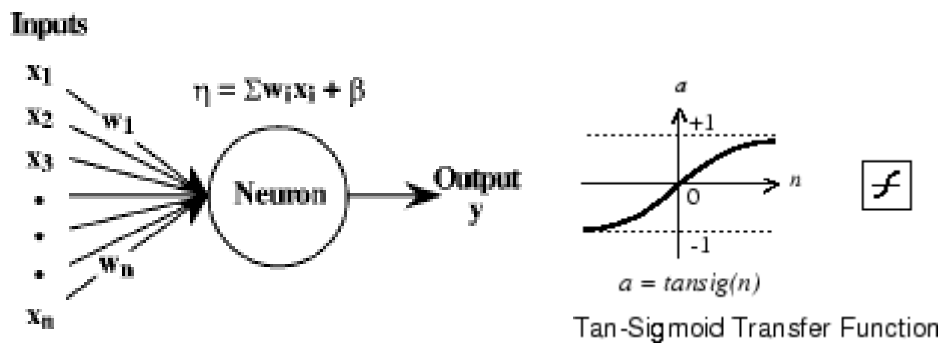


Figure 5.5: Neuron in neural network (Simpson et al., 2001) (left) and tan-sigmoid transfer function (Mathworks, 2014a) (right).

Another approach is also used to determine the optimal combination of network architecture and training algorithm: instead of using a model selection criterion to trade off model complexity against goodness-of-fit, all combinations of the following are explored:

1. Network type [feed forward, cascade forward]
2. Number of hidden layers [1,2]
3. Number of neurons per hidden layer (assumed to be the same per layer) [1,2,...,20]
4. Training algorithm [Levenberg-Marquardt, Bayesian regularization]

The Bayesian regularisation training algorithm only needs a training set and test set, and therefore the validation set is added to the training set. To determine the optimal combination, the mean squared error performance criterion is used on the test set. The neural networks were created using the Matlab Neural Network toolbox (Mathworks, 2014b).

5.3 Evaluation of metamodelling approaches

5.3.1 Calculation object

Comparison of the different metamodelling methods and the impact of sample sizes was the aim of Common Exercise 4 (see Addendum 4). The considered calculation tool in this common exercise is the *Matlab cold attic model* which determines hygrothermal performances of cold attics, as already described in Chapter 1. This model includes wind-pressure and thermal-stack induced attic ventilation, thermal and hygric inertia of finishing materials in the attic, and long- and short-wave radiation on exterior surfaces. 14 different input parameters – material properties, component characteristics, geometric dimensions – are used to compute two performance criteria: the cumulated heat loss through the ceiling in January (*CHL* [kWh/m²]), and the yearly peak mould growth index for the wooden underlay (*PMG* [-]). The input parameters are collected in Table 5.1 with their probability distributions and are coded to easily use them in metamodelling.

Table 5.1: Variable input parameters.

Input parameter	Distribution*	Code
Height of building (m)	U(4,8)	X1
Area of ceiling floor and roof (m ²)	U(50,200)	X2
Orientation of one of eave sides (-)	U(0,180)	X3
Venting area per meter eave (m ² /m)	U(0.001,0.05)	X4
Length of building (eave side) (m)	U(7,20)	X5
Thickness of wooden underlay (m)	U(0.010,0.020)	X6
Vapour diffusivity of wood (m ² /s)	N(10 ⁻⁶ , 2 10 ⁻⁷)	X7
Initial relative humidity of wood (-)	U(0.5,0.9)	X8
Thermal conductivity of wood (W/mK)	N(0.13,0.02)	X9
Resistance of roof insulation (m ² K/W)	U(0,1)	X10
Effective leakage area of ceiling (m ²)	U(10 ⁻⁵ , 5 10 ⁻⁵)	X11
U-value of the ceiling (W/m ² K)	U(0.2,5)	X12
Indoor temperature (°C)	N(20,1.5)	X13
Indoor moisture supply (kg/m ³)	N(0.005,0.002)	X14

* Explanation of symbols:

$U(x_{low}, x_{upp})$: uniform distribution with x_{low} the lower and x_{upp} the upper limit

$N(x_{avg}, x_{std})$: normal distribution with x_{avg} the average and x_{std} the standard deviation

5.3.2 Outcomes of the exercise

Three solutions for Common Exercise 4 were received, as contributed by Marcus Fink & Florian Antretter (Fraunhofer, Germany), Payel Das (University College London) and Liesje Van Gelder (KU Leuven, Belgium). Different participants use different sampling schemes in their solutions. To reliably compare the different metamodelling techniques, in this chapter all samples are provided by optimised Latin Hypercube Sampling schemes, as this guarantees a uniform sampling of the probability space.

5.3.3 Quality assessment procedure

Metamodels for CHL and PMG are formulated as described in 5.2 based on five different initial sample sizes: 5, 15, 50, 150 and 2000 training samples. The models based on 2000 training samples can be considered as the foundation for creating the best possible metamodels. To assess the quality of the developed metamodels, a set of 100 validation samples is used. Both Root Mean Squared Errors (RMSE) and Maximum Absolute Errors (MAE) between the original and predicted outputs are calculated as

$$RMSE = \sqrt{\frac{\sum_{t=1}^n y_t - \underline{y}_t}{n}} \quad (5.8)$$

$$MAE = \max(|y_1 - \underline{y}_1|, |y_2 - \underline{y}_2|, \dots, |y_n - \underline{y}_n|) \quad (5.9)$$

with y_t the original output, \underline{y}_t the predicted output and n the number of validation samples. These indicators are compared for the metamodeling techniques and sample sizes. The RMSE indicates the overall approximation ability of the metamodel; the lower the value, the better the approximation, as can be seen in Figure 5.6 for two of the following metamodels. The MAE indicates the maximal error that can be expected and is indicated in Figure 5.6 as well. Furthermore, as cumulative distribution functions (CDF) are used in probabilistic analysis and design, the CDFs of the validation set are compared with the CDFs of the predicted outputs. This can also indicate whether the metamodels over- or underestimate the original outputs.

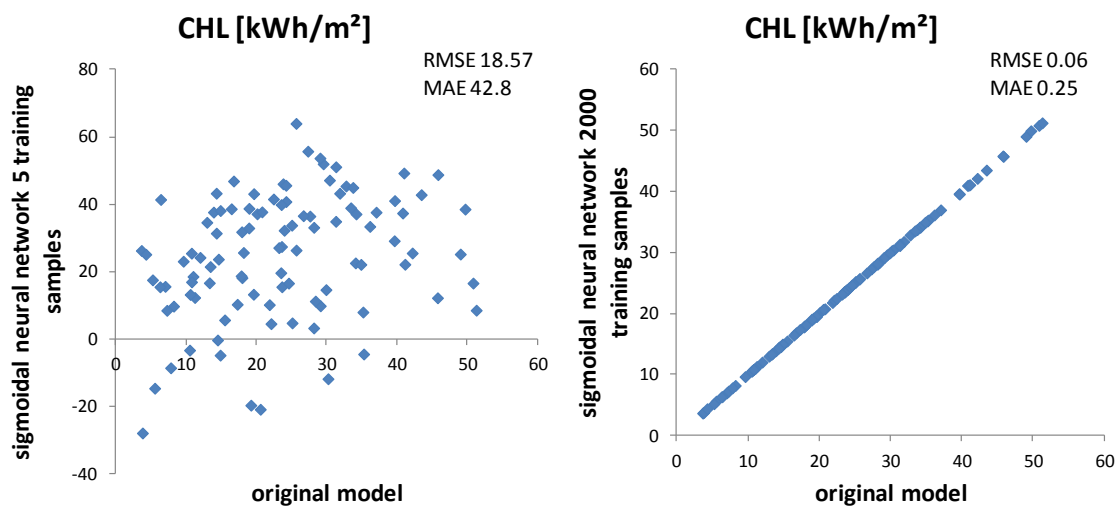


Figure 5.6: Scatter plots of reference solution and two of following metamodels with RMSE and MAE indicated.

5.3.4 Result comparison

5.3.4.1 Polynomial regression

For comparison of first, second and third order regularised polynomial regression models, RMSE and MAE are presented in Figure 5.7 for CHL and in Figure 5.8 for PMG. These figures show the results for several initial sample sizes. As discussed before, more samples than coefficients are preferred. Hence, the underinformed models can be slightly improved by reducing the number of coefficients as shown for the second order models. For example, no interaction terms are taken into account for the metamodels based on 5 and 15 training samples.

Figure 5.9 shows the CDFs of the validation output data in comparison with the predicted outputs of the first, second and third order polynomial regression models based on 2000 initial samples. RMSE, MAE and CDFs all indicate that a third order polynomial can approximate the original model the best. A second order model is however a better choice because of the reduced number of coefficients. Furthermore, it performs only slightly worse than the third order model.

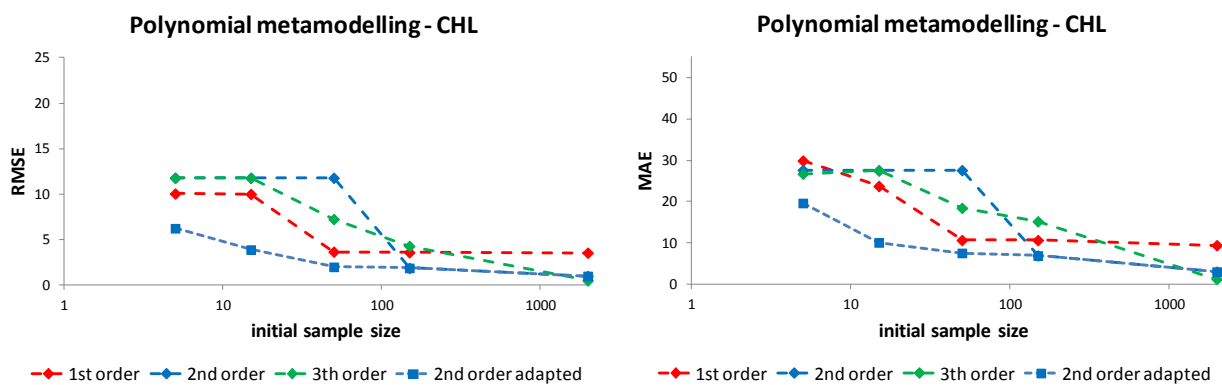


Figure 5.7: Comparison RMSE and MAE of validation data and regularised polynomial regression models for CHL.

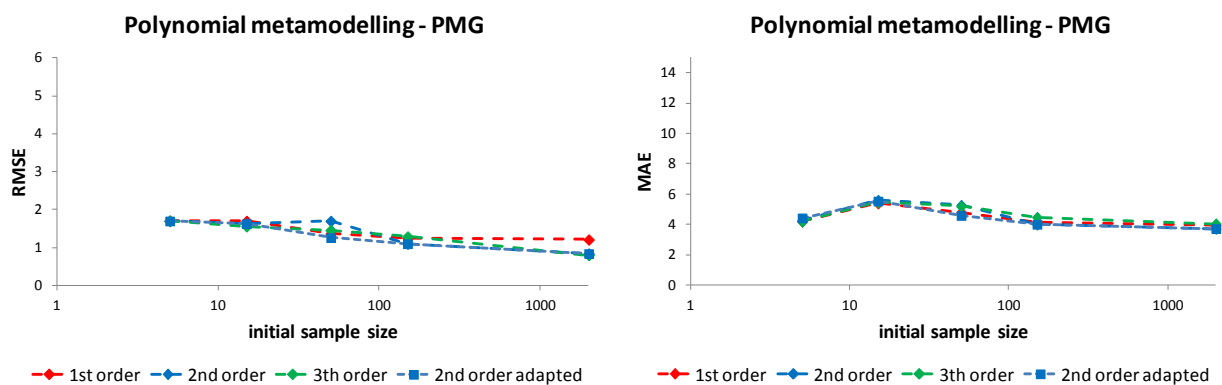


Figure 5.8: Comparison RMSE and MAE of validation data and regularised polynomial regression models for PMG.

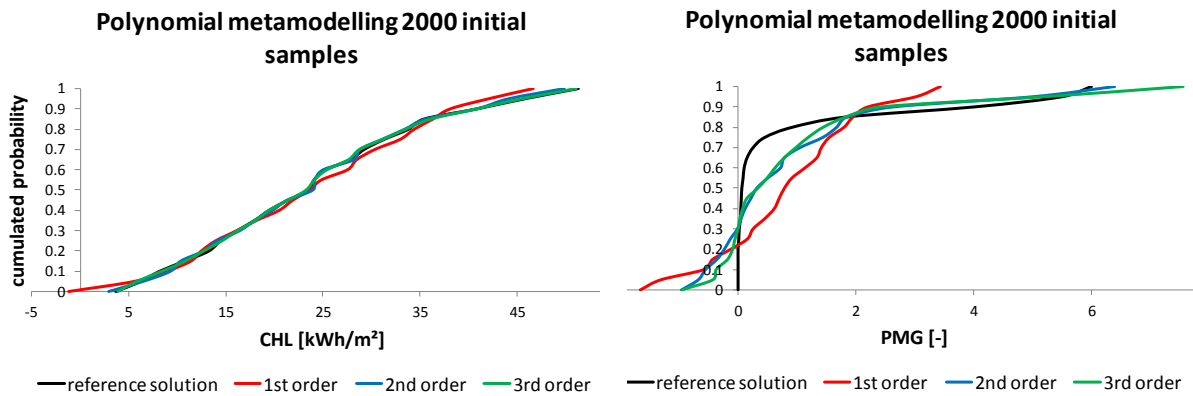


Figure 5.9: Cumulative distribution functions for reference solution and polynomial metamodelling based on 2000 initial samples.

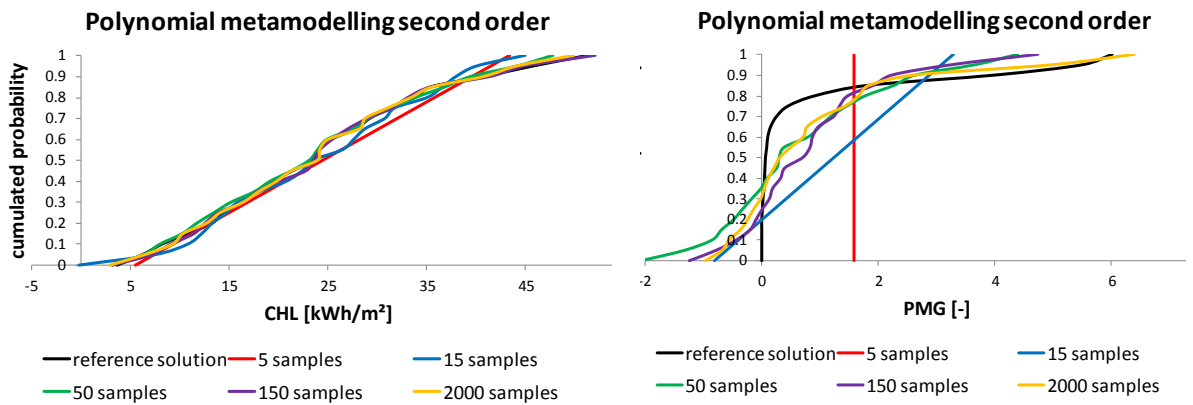


Figure 5.10: Cumulative distribution functions for reference solution and second order polynomial metamodelling based on several initial sample sizes.

Figure 5.10 shows the CDFs for the improved second order polynomial regression with different initial sample sizes. All initial sizes can result in acceptable second order polynomial models for CHL, if of course the number of estimated coefficients is lower than the sample size. The PMG model is much harder to approximate for polynomial regression models. One can also see that the PMG model makes an overestimation for low values.

5.3.4.2 Multivariate adaptive regression splines (MARS)

For comparison of first and second order MARS models, RMSE and MAE are presented in Figure 5.11 for CHL and Figure 5.12 for PMG. Both figures show the results for several initial sample sizes. Figure 5.13 shows the CDFs for first and second order MARS models based on 2000 initial samples in comparison with the original model for the validation set. RMSE, MAE and CDFs all indicate that a second order MARS model is slightly better to approximate the original model than a first order model.

Figure 5.14 shows the CDFs for second order MARS models with different initial sample sizes. When more samples than input parameters are available, the results are satisfying. The CHL model is easier to mimic than the PMG model and one can see that the PMG makes an overestimation for low values.

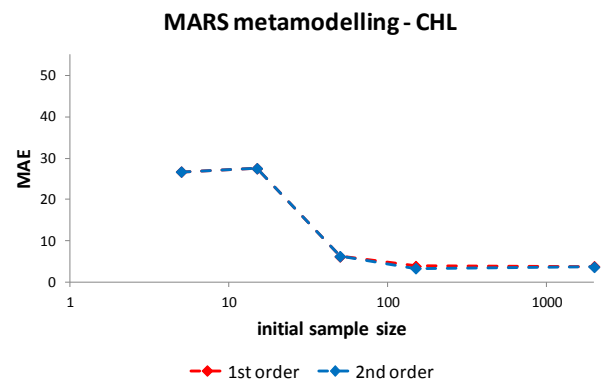
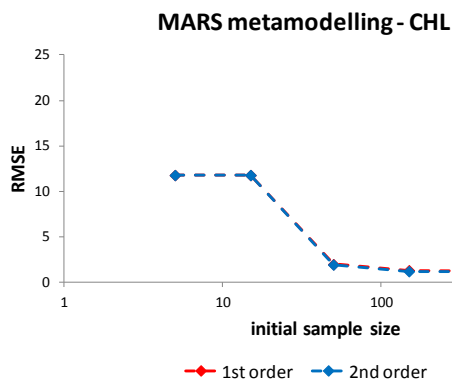


Figure 5.11: Comparison RMSE and MAE of validation data and MARS models for CHL.

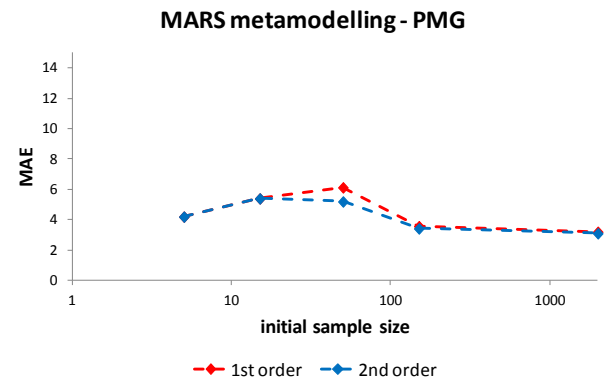
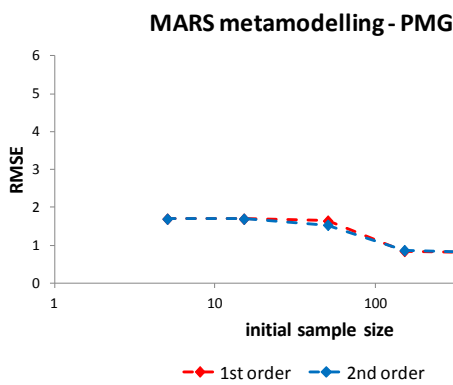


Figure 5.12: Comparison RMSE and MAE of validation data and MARS models for PMG.

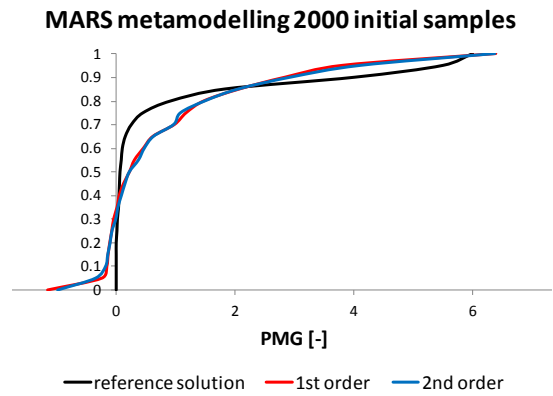
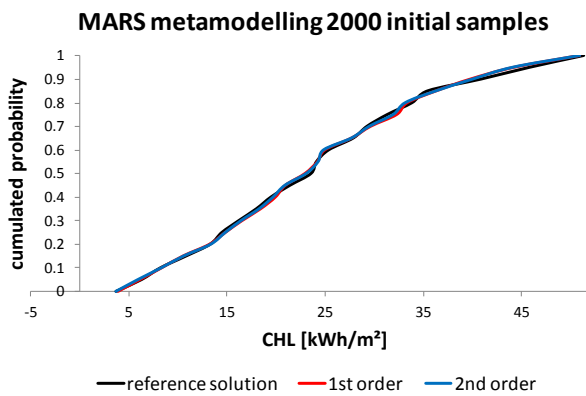


Figure 5.13: Cumulative distribution functions for reference solution and MARS metamodelling based on 2000 initial samples.

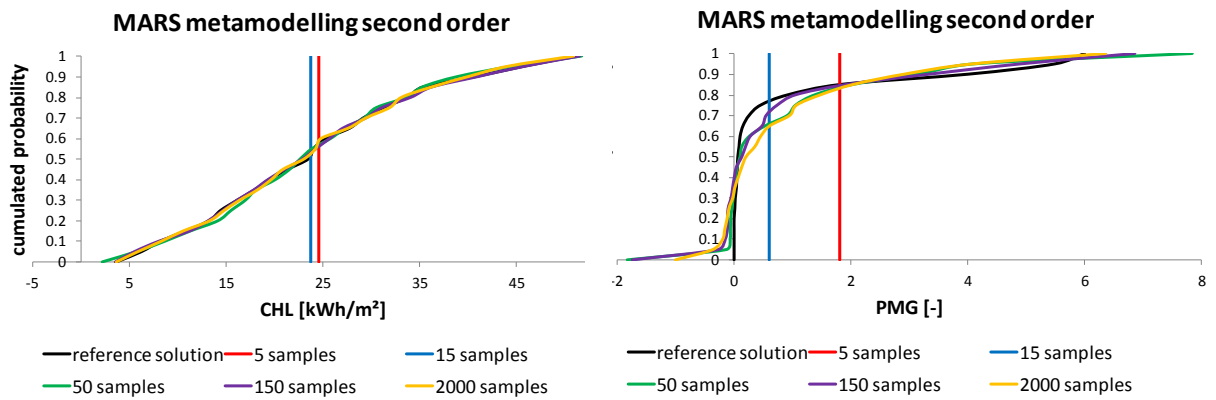


Figure 5.14: Cumulative distribution functions for reference solution and MARS metamodelling second order based on several initial sample sizes.

5.3.4.3 Kriging

For comparison of first and second order kriging models, RMSE and MAE are presented in Figure 5.15 for CHL and Figure 5.16 for PMG. Both figures show the results for several initial sample sizes. All correlation functions result in the same models; therefore, only one option per order and per sample size is shown. The coefficients can only be calculated when more samples than coefficients are available.

Figure 5.17 shows the CDFs for first and second order kriging models based on 2000 initial samples in comparison with the original model for the validation set. RMSE, MAE and CDFs all indicate that a second order kriging model is better to approximate the original model, but more initial samples are needed.

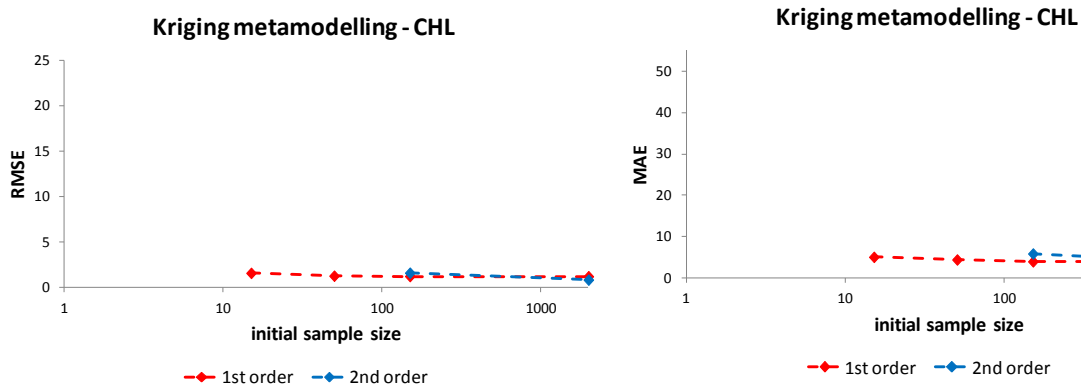


Figure 5.15: Comparison RMSE and MAE of validation data and kriging models for CHL.

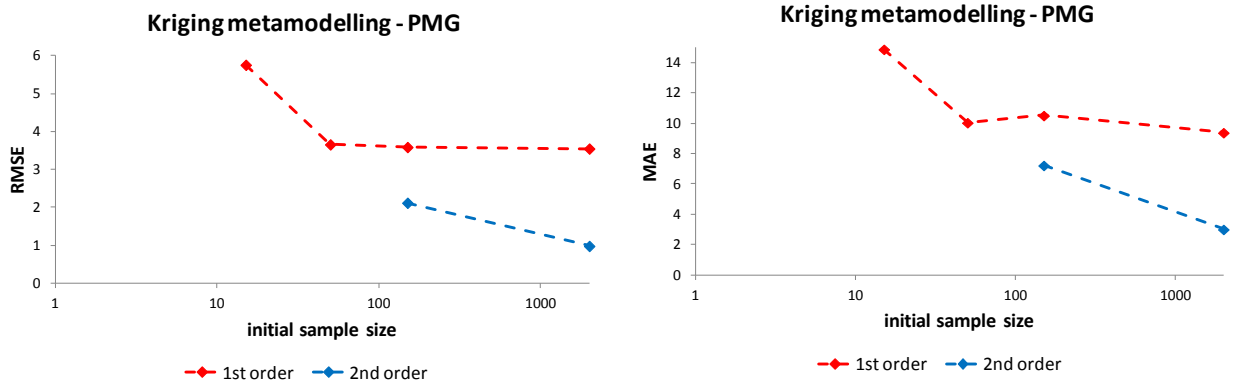


Figure 5.16: Comparison RMSE and MAE of validation data and kriging models for PMG.

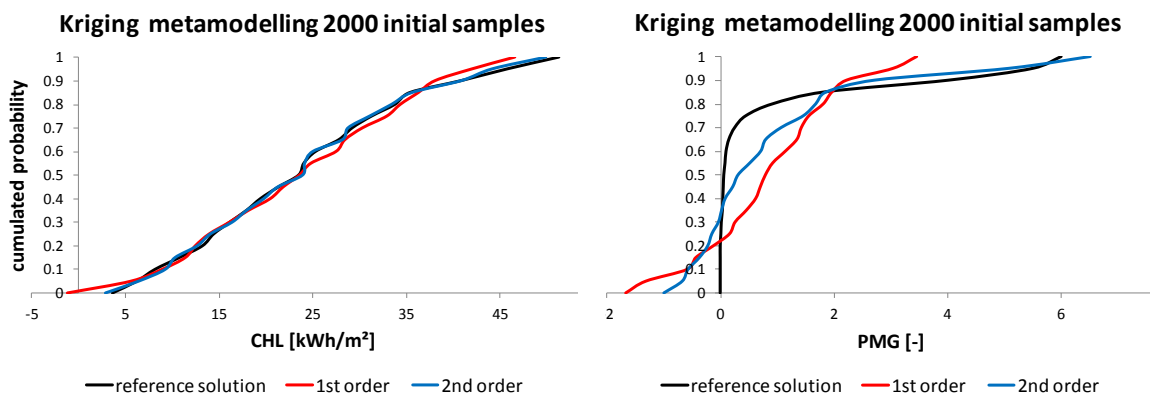


Figure 5.17: Cumulative distribution functions for reference solution and kriging metamodels based on 2000 initial samples.

Figure 5.18 shows the CDFs for second order kriging models with different initial sample sizes. The CHL model is easier to mimic than the PMG model. Against the PMG model makes an overestimation for low values.

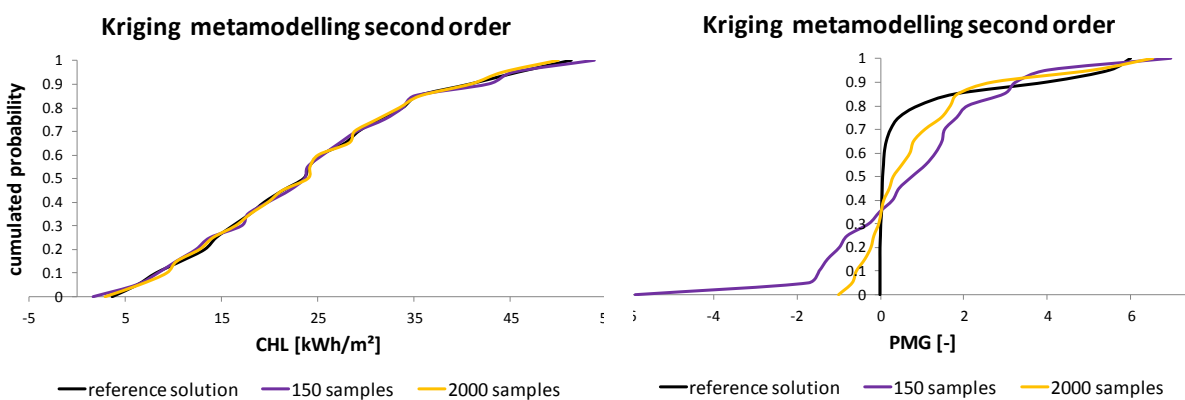


Figure 5.18: Cumulative distribution functions for reference solution and kriging metamodels based on several initial sample sizes.

5.3.4.4 Neural networks

For comparison of several neural networks, RMSE and MAE are presented in Figure 5.19 for CHL and Figure 5.20 for PMG. Both figures show the results for several initial sample sizes.

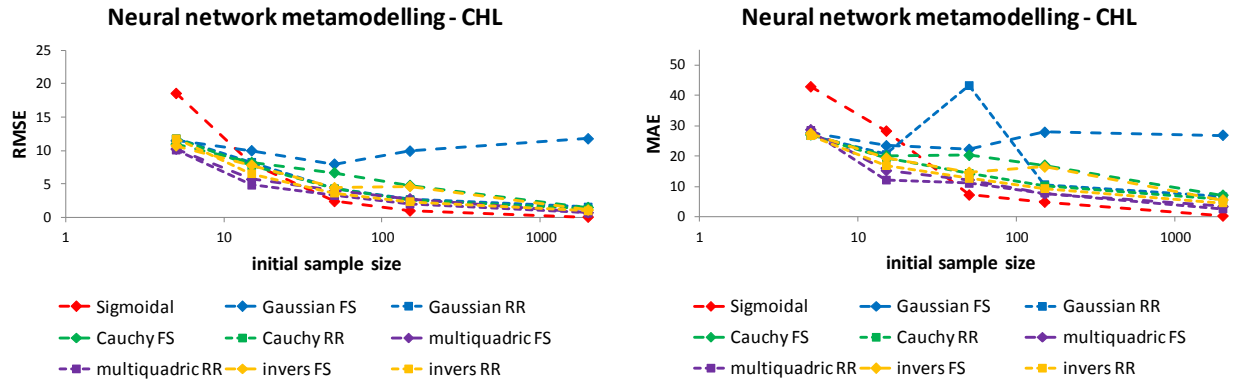


Figure 5.19: Comparison RMSE and MAE of validation data and neural networks for CHL.

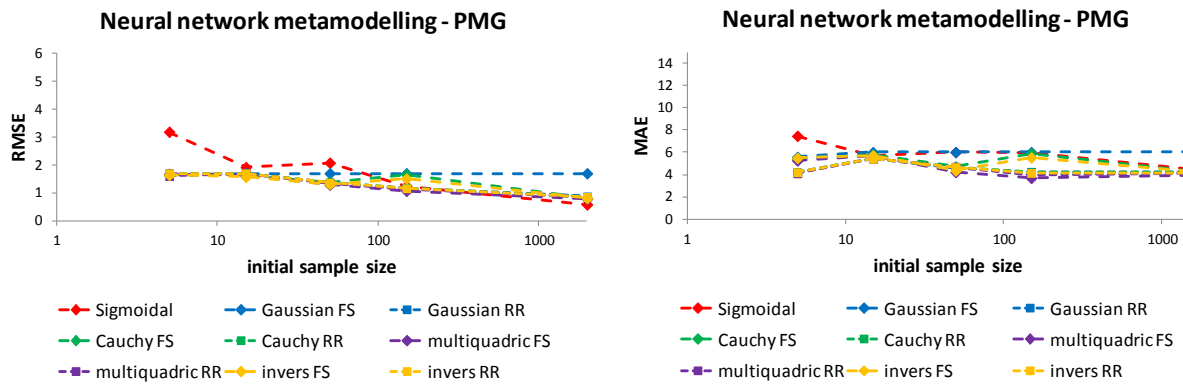


Figure 5.20: Comparison RMSE and MAE of validation data and neural networks for PMG.

Figure 5.21 shows the CDFs for the neural networks based on 2000 initial samples in comparison with the original model for the validation set. RMSE, MAE and CDFs all indicate that the sigmoidal transfer function network is better to approximate the original model.

Figure 5.22 shows the CDFs for sigmoidal transfer function networks with different initial sample sizes. More samples highly improve the model performance. The CHL model is easier to mimic than the PMG model. One can see that the PMG model makes an overestimation for low values, except for larger sample sizes.

When PMG is used in classification problems (for example if PMG above 5 is thought to result in mould damage), it is assumed the model performance can be improved. The output can be modelled as 1 if true ($PMG \geq 5$) and 0 if false. If the output is lower than 0.5, we assume it is false, either we assume it is true. The *patternet* function or the *feedforward* function in Matlab (Mathworks 2014b) can be used for that purpose.

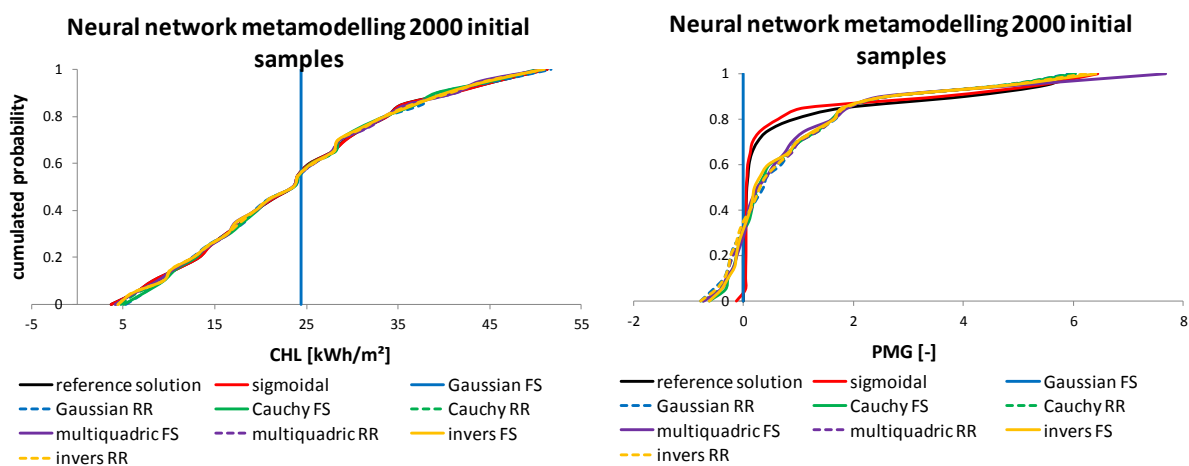


Figure 5.21: Cumulative distribution functions for reference solution and neural network metamodelling based on 2000 initial samples.

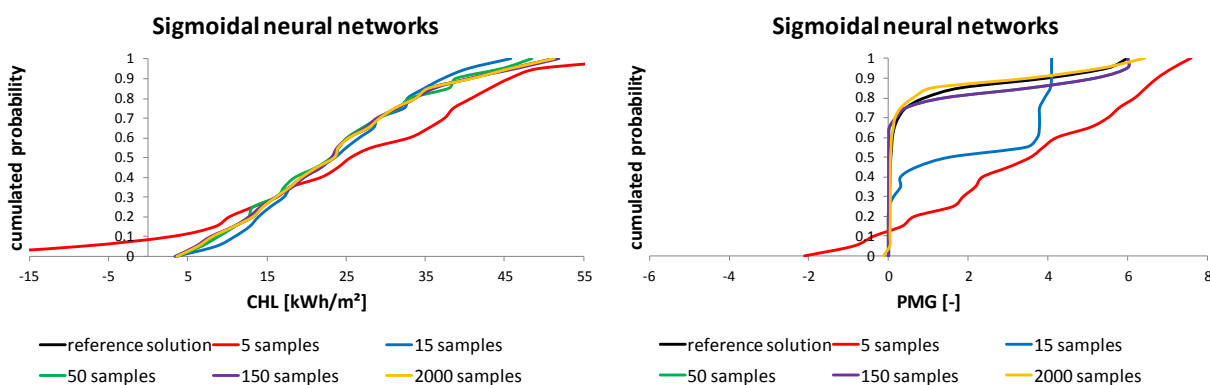


Figure 5.22: Cumulative distribution functions for reference solution and neural network metamodelling based on several initial sample sizes, using the sigmoidal neural network.

5.3.5 Comparison

Figure 5.23 shows all techniques selected in previous subsections. They all approximate the reference solution and provide similar cumulative distribution functions. Kriging methods were excluded as these techniques provide no better results than polynomial regression, but need more initial samples to train the model. 15 training samples seem to be sufficient in roughly approximating the original model for polynomial regression and neural networks, but more samples are needed to refine these approximations, especially for extremely non-linear outputs such as PMG. Figure 5.24 and Figure 5.25 confirm this.

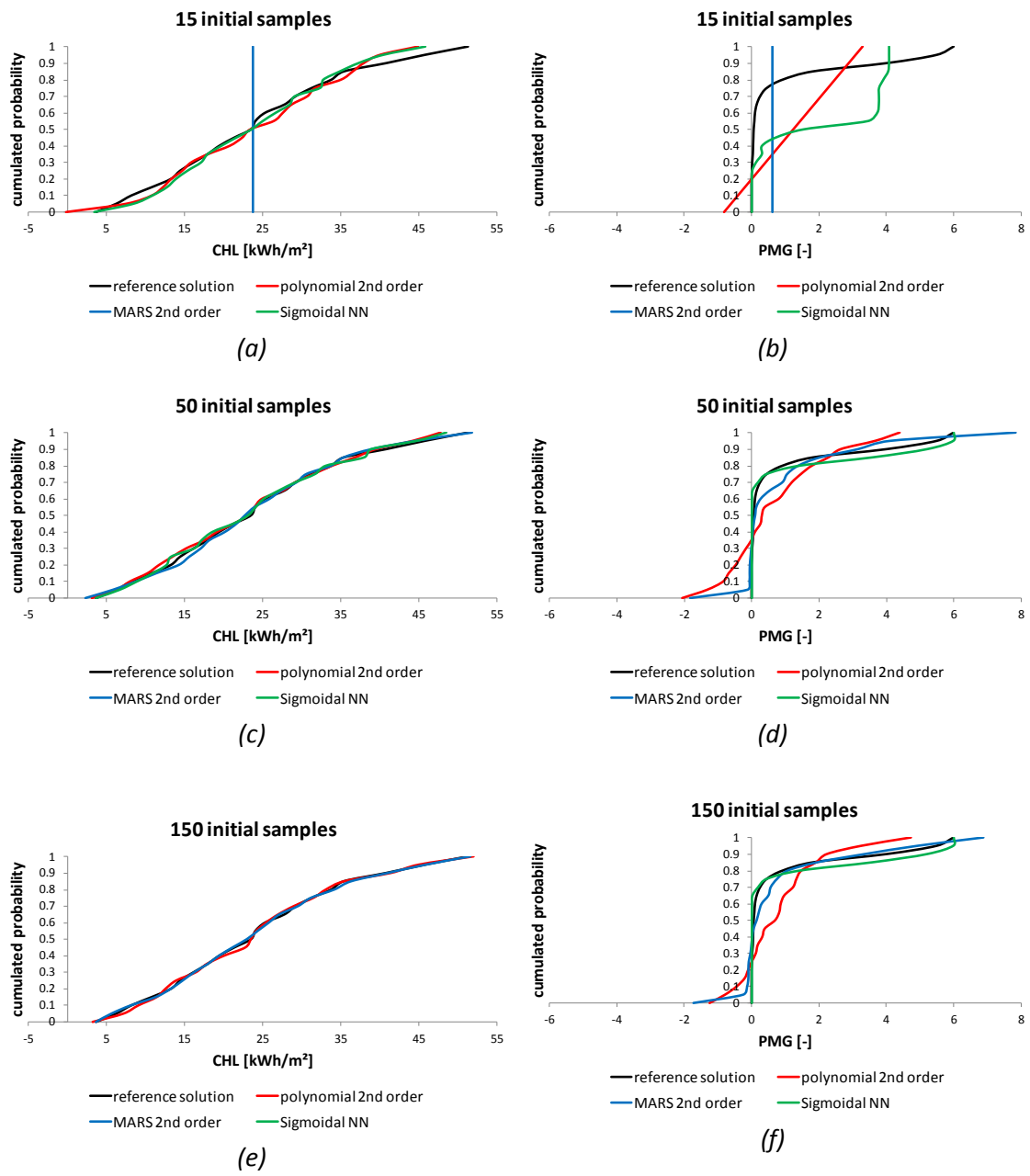


Figure 5.23: Cumulative distribution functions for reference solution of several metamodelling based on several initial sample sizes.

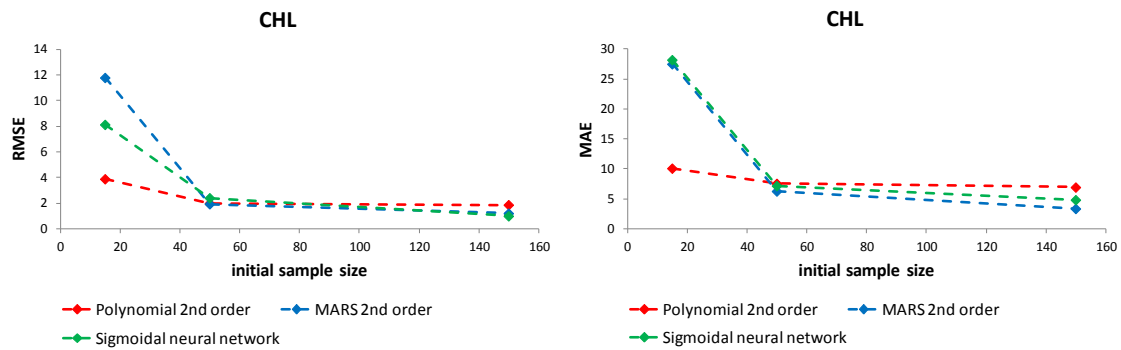


Figure 5.24: Comparison RMSE and MAE of validation data and CHL metamodelling.

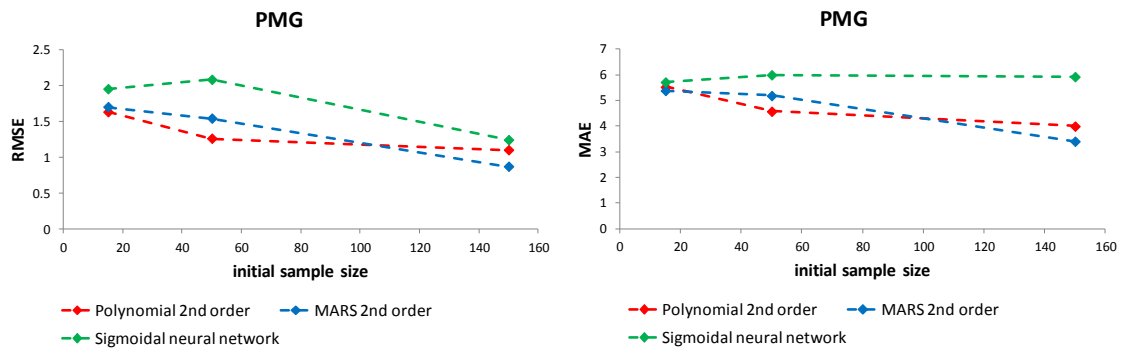
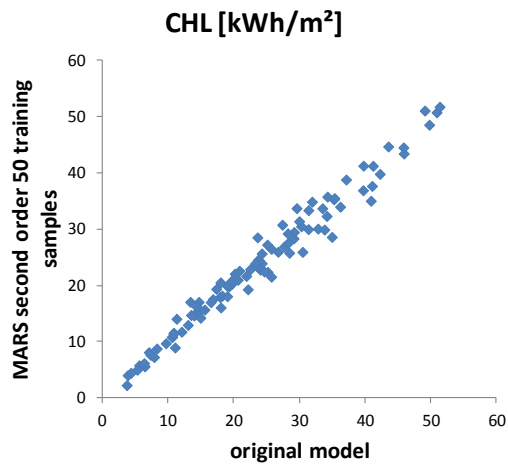


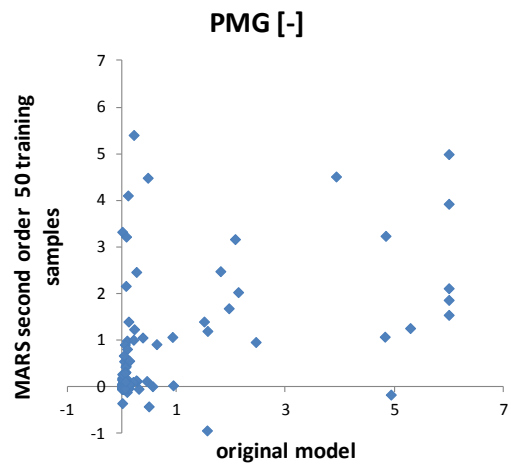
Figure 5.25: Comparison RMSE and MAE of validation data and PMG metamodelling.

For 15 samples, a second order polynomial can mimic CHL and PMG the best, but for more samples the MARS and neural network methods perform better. As models based on 50 or 150 training samples are significantly better than models on 15 training samples, Figure 5.26 shows scatter plots of the best performing metamodelling methods for 50 and 150 training samples. One can see that for CHL 50 training samples are sufficient in approximating the original model. For PMG, 150 training samples can improve the agreement, but it seems to be much harder to have very accurate metamodelling.

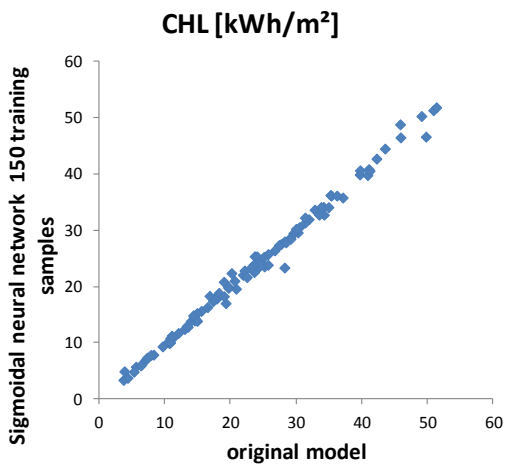
When comparing used metamodelling techniques in usability, MARS methods are slightly preferred because of their simplicity and very efficient computation time. However, depending on nonlinearity, dimension and noisy behaviour of the initial model, other techniques can provide better models (Jin et al., 2001).



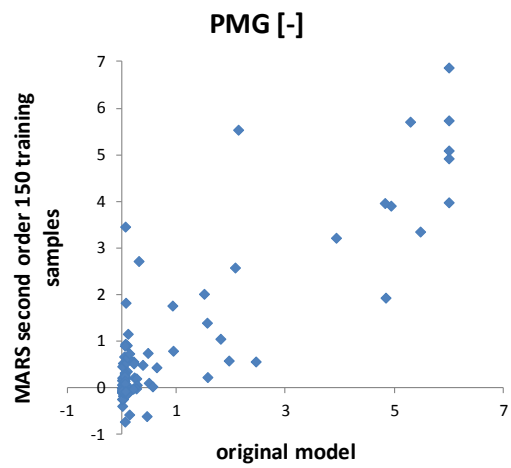
(a)



(b)



(c)



(d)

Figure 5.26: Scatter plots of reference solution and best metamodel for 50 (top) and 150 (bottom) initial samples.

5.4 Conclusions

This chapter provided an overview of metamodeling methods, applied to a hygrothermal calculation object. Four methods with several settings were extensively compared: polynomial regression, multivariate adaptive regression splines (MARS), kriging and neural networks. All models were created based on a set of input/output combinations, the training set, with five initial sample sizes: 5, 15, 50, 150 and 2000. To assess the quality of the developed metamodels, a set of 100 validation samples was used. The best modeling techniques for this calculation object were second order polynomial regression, second order MARS and sigmoidal transfer function networks. Kriging methods were excluded as these techniques provide no better results than polynomial regression. When comparing used metamodeling techniques in usability, MARS methods are slightly preferred because of their simplicity and very efficient computation time. However, depending on nonlinearity, dimension and noisy behavior of the initial model, other techniques can provide better models for other calculation objects.

Generally, the more training samples available, the better the metamodel is constrained. Unfortunately, it is not always possible to create as many samples as we want due to calculation time. For that reason, it might be important to examine how accurate the metamodel has to be. However, as that is dependent on the goal of the model, it is not straightforward either. Remember that the accuracy should be checked on validation data not used in the training and that the metamodel can only be used within the range of the training data values. Metamodels built on 50 to 150 training samples were already reasonably accurate for the considered calculation object. However, this might be dependent on the original model. It should be mentioned that the accuracy of the metamodel is at least as important as the calculation time. As long as we need less initial samples for the metamodel than we should need for a Monte Carlo analysis on the original model, we can expect that time (and thus money) will be saved.

The number of runs required for good approximating power already yields decent initial uncertainty and sensitivity estimates. Therefore, a metamodel is only useful if more samples are needed than is feasible with the original model. To that extent, highly computational sensitivity methods might benefit from metamodeling. Furthermore, calculation time for optimization problems, as illustrated in Chapter 6, can greatly be reduced by them.

Further modifications are possible to potentially improve some metamodels. A prior exclusion of less significant model parameters can help to reduce the number of coefficients in the metamodel and thus to reduce calculation time, especially for polynomial regression. Therefore, the metamodel algorithm can be improved by first calculating sensitivity indices of training samples. As seen in Section 5.3, some outputs are easier to metamodel than others. A solution might be to convert these outputs into classification problems, as discussed in Section 5.3.4.4. Additional constraints can be added to the metamodels as well and might improve them. For example, one can constrain CHL to be positive and limit PMG between 0 and 6. Dynamic metamodels of underlying physical time-dependent properties might improve the approximating power, but were beyond the scope of this chapter.

5.5 References

- D'Errico J. (2012). Matlab function 'polyfitn', <http://www.mathworks.com/matlabcentral/fileexchange/34765-polyfitn> , last accessed on April 14 2014.
- Furrer R., Nychka D. and Sain S. (2013). Matlab package 'fields'. <http://cran.r-project.org/web/packages/fields/fields.pdf>, last accessed on April 14 2014.
- Friedman J.H. (1991). Multivariate adaptive regression splines. *The Annals of Statistics* 19:1-141.
- Galkin I. and Lowell U.M. (2013). Polynomial neural networks. <http://ulcar.uml.edu/~iag/CS/Polynomial-NN.html>, last accessed on April 14 2014.
- Hastie T., Tibshirani R., Leisch F., Hornik K. and Ripley B.D. (2013). Matlab package 'mda'. <http://cran.r-project.org/web/packages/mda/mda.pdf>, last accessed on April 14 2014.
- Jekabsons G. (2011). ARESLab: Adaptive Regression Splines toolbox for Matlab/Octave, <http://www.cs.rtu.lv/jekabsons/regression.html>, last accessed on April 14 2014.
- Jin R., Chen W. and Simpson T.W. (2001). Comparative studies of metamodelling techniques under multiple modelling criteria. *Structural and Multidisciplinary Optimisation* 23:1-13.
- Johnson R.T., Montgomery D.C., Jones B. and Parker P.A. (2010). Comparing computer experiments for fitting high-order polynomial metamodells. *Journal of Quality Technology*, 42:86-102.
- Mathworks. (2013). Stepwise regression. <http://www.mathworks.nl/help/stats/stepwisefit.html>, last accessed on April 14 2014.
- Mathworks. (2014a) Tan-sigmoid transfer function. <http://www.mathworks.nl/help/nnet/ref/tansig.html>, last accessed on April 14 2014.
- Mathworks (2014b) Neural network toolbox. <http://www.mathworks.nl/products/neural-network>, last accessed on April 14 2014.
- Nielsen H.B., Lophaven S.N. and Søndergaard J. (2002). DACE: a Matlab Kriging toolbox. <http://www2.imm.dtu.dk/~hbn/dace>, last accessed on April 14 2014.
- Orr M.J.L. (1996) Introduction to Radial Basis Function Networks. Centre for Cognitive Science, University of Edinburgh, Scotland.
- Orr K.J.L. (1999). Matlab functions for Radial Basis Function Networks. <http://www.anc.ed.ac.uk/rbf/rbf.html>, last accessed on April 14 2014.
- Simpson T.W., Peplinski J.D., Koch P.N. and Allen J.K. (2001). Metamodels for computer-based engineering design : survey and recommendations. *Engineering with Computers* 17:129-150.

Wikipedia (2013). Tikhonov regularization. http://en.wikipedia.org/wiki/Ridge_regression , last accessed on April 14 2014.

Wikipedia (2014). Multivariate adaptive regression splines. http://en.wikipedia.org/wiki/Multivariate_adaptive_regression_splines, last accessed on April 14 2014.

6 ECONOMIC OPTIMISATION

Lead author

Payel Das

6.1 Introduction

6.1.1 Background

Building performance simulations can be used to calculate the impact of a design option on the energy use and indoor air quality in a dwelling, and uncertainty analyses can be used to explore the associated variation with the impact as a result of variabilities in dwelling characteristics across a stock, weather variability, economic future, and workmanship (Chapter 3). Metamodelling methods can also be used to significantly reduce the computational running time associated with carrying out uncertainty analyses (Chapter 5). There is still however the question of how to select the optimal design option from a choice of several possible options, and in particular when the building performance simulations have been carried out probabilistically.

The process of determining the optimal design option involves first defining a design parameter space to explore. Design variables typically explored in the case of the optimization of residential energy efficiency interventions include building geometry (Arumi, 1977; D’Cruz et al., 1983; Gero et al., 1983; Peippo et al., 1999; Tuhus-Dubrow and Krarti, 2010), glazing properties (Arumi, 1977; Asadi et al., 2012a; Bouchlaghem, 2000; D’Cruz et al., 1983; Diakaki et al., 2008; Fesanghary et al., 2012; Gero et al., 1983; Johnson et al., 1984; Peippo et al., 1999; Radhi, 2008; Tuhus-Dubrow and Krarti, 2010), fabric properties of the building envelope (Asadi et al., 2012a; Bouchlaghem, 2000; D’Cruz et al., 1983; Das et al., 2013; Diakaki et al., 2008; Fesanghary et al., 2012; Peippo et al., 1999; Radhi, 2008; Sambou et al., 2009; Tuhus-Dubrow and Krarti, 2010; Wang and Xu, 2006), operation of equipment such as solar shading (Johnson et al., 1984; Tuhus-Dubrow and Krarti, 2010) and heating, ventilating, and air-conditioning system parameters (Kelly and Bushby, 2012; Wright et al., 2002).

The next step is to specify performance criteria for comparing the various design options. Choosing an economically-driven performance criterion is a natural choice for energy-efficiency interventions, enabling the decision-maker to easily compare different options. It also creates a single objective optimization problem, rather than a multi-objective optimization problem in which several criteria are used to compare design options. There are studies that simply use the cost of energy savings due to changes in the heat loss through the building fabric as a measure for comparing design options (Ahern et al., 2013; Charlier and Risch, 2012; Das et al., 2013; Hesaraki and Holmberg, 2013). The energy savings can be compared directly to the initial investment required for the implementation of the scenario (Garrido-Soriano et al., 2012; Goodacre et al., 2002), or through the number of years for the initial investment to be repaid through energy savings, as given by the Payback Period criterion (Aste et al., 2012; Chan and Chow, 2010; Popescu et al., 2012; Rasouli et al., 2013; Sadineni et al., 2011). The Net Present Value gives a current ‘value’ for the intervention after a chosen number of years according to the initial investment, maintenance costs, and energy savings, all subject to a future change in energy price and inflation (Malatji et al., 2013; Turner et al., 2013). The Return on Investment (*ROI*) criterion is calculated as the ratio of the Net Present Value

criterion and a sum of the investment and maintenance costs (Kuckshinrichs et al., 2010). The Internal Rate of Return criterion is the value inflation would need to be so that the Net Present Value of an intervention after the chosen number of years is zero (Goodacre et al., 2002). Another variation is the Equivalent Annual Cost, which divides the Net Present Value of an intervention over its lifespan by the present value of an annuity or loan repayment factor (Mata et al., 2013). Life-cycle cost analysis also uses Net Present Value over the lifespan of each intervention (Fesanghary et al., 2012; Ramesh et al., 2012; Tuhus-Dubrow and Krarti, 2010), and has been modified to incorporate life-cycle assessment, which takes into account environmental impacts associated with the transport and construction of any material intervention (Gu et al., 2008).

There are several different types of algorithms for exploring the design space. These include gradient-based methods such as the Levenberg-Marquardt algorithm that looks for the point where the objective function gradient is closest to zero. They need that the objective functions have particular mathematical properties like continuity and the derivability and get stuck in local minima. There are several derivative-free direct search methods that range from a systematic evaluation of evenly-spaced points covering the design space to methods such as a pattern search in which each dimension is sequentially trialled at a coarse resolution, and then when no further improvement is possible, the interval size is halved. There are also derivative-free stochastic algorithms that range from random sampling of the design space to highly sophisticated methods, designed to deal with complex optimization problems. The most commonly employed in the optimization of retrofitting strategies is the genetic algorithm, which mimics evolutionary mechanisms to evolve a population of possible solutions to the optimal solution (Malatji et al., 2013; Sambou et al., 2009; Tuhus-Dubrow and Krarti, 2010; Wright et al., 2002). Excellent reviews have been carried out by Attia et al. (2013) and Evins (2013).

Several aspects of the schemes implemented in the literature to find the optimal energy efficiency scenario could still be improved. For example, although thermal comfort is often incorporated as an additional objective function in the optimization procedure or imposed as a constraint, the impacts of interventions on indoor air quality are hardly considered (Attia et al., 2013). Only a handful of studies treat uncertainty and variability in building characteristics and future economic scenarios when carrying out optimization procedures, as also identified by Attia et al. (Attia et al., 2013). Uncertain economic criteria are considered in the work of Rasouli et al. (Rasouli et al., 2013) and Hopfe et al. (Hopfe, 2009) investigated the propagation of uncertainty through a building design optimization algorithm to aid robustness. This Chapter will illustrate the impact of alternative formulations for determining the optimal design option in the context of a probabilistic analysis, illustrated on the attics of a typical Swedish stock of dwellings.

6.2 Presentation of methods

In this section, we introduce the economic performance criteria explored here in the assessment of design options, different methods for deriving a deterministic objective function from a non-deterministic distribution of performance criteria, and different schemes for carrying out the optimization.

6.2.1 Performance criterion

Four different economic performance criteria are investigated for assessing the performance of a particular design option, which are described in detail below. As a probabilistic approach is used, each design option will be associated with a performance criterion distribution rather than a single deterministic value.

6.2.1.1 Payback period (*PB*)

An investment that leads to a cash flow in the future can be assessed by the payback period (*PB*), which is a measure of how long it takes for the initial investment to be paid back, without a correction for inflation or change in energy costs:

$$\sum_{l=1}^{PB} \frac{\Delta K_{E,l}}{I_0} = 1 \quad (6.1)$$

where I_0 is the initial cost of the design option, $\Delta K_{E,l}$ is the change in energy costs in year l and is given by:

$$\Delta K_{E,l} = P_E \Delta E_{use,heating,l} \quad (6.2)$$

with P_E the price per kWh. and $\Delta E_{use,heating,l}$ the difference between the original and retrofitted dwelling in year l .

6.2.1.2 Net Present Value (*NPV*)

The present value of future cash flows is discounted back to the time of the investment to compare different investment alternatives. The total Net Present Value (*NPV*) after a chosen number of years, y , since a design option is defined as:

$$NPV = -I_0 - I_M + \sum_{l=1}^y \frac{\Delta K_{E,l} (1+r_E)^l}{(1+a)^l} \quad (6.3)$$

where I_0 and $\Delta K_{E,l}$ are defined above, I_M is the maintenance cost, r_E is the inflation-corrected annual increment in energy cost ($0 < r_e < l$), and a is the inflation-corrected present value factor ($0 < a < l$).

6.2.1.3 Return on investment (*ROI*)

To compare alternatives with different initial investment costs, Return on Investment (*ROI*) can be used. The *ROI* is a measure of the efficiency of the investment defined as the ratio of the *NPV* and initial investment:

$$ROI = \frac{NPV}{I_0 + I_M} \quad (6.4)$$

where *NPV*, I_0 , and I_M are defined above. Therefore it is similar to the payback period, but takes into account maintenance costs, inflation, and changes to energy prices.

6.2.1.4 Internal rate of return (*IRR*)

The Internal Rate of Return (*IRR*) is the inflation-corrected present value factor, a , for the design option where the *NPV* equals 0, i.e.

$$NPV = 0 \Rightarrow I_0 + I_M = \sum_{l=1}^t \frac{\Delta K_{E,l} (1 + r_E)^l}{(1 + a_{IRR})^l} \quad (6.5)$$

where a_{IRR} is calculated by an iterative process.

6.2.2 Objective function

A deterministic objective function needs to be extracted from the probabilistic performance criterion, but now with the advantage that the expected value takes into account uncertainty and variabilities in the model inputs, and some information regarding the shape of the whole distribution can be incorporated into its definition. Many different moments can be considered in the objective function, but in this work we explore moments that reflect a varying degree of risk.

6.2.2.1 Risk neutral

Risk-neutral decision makers are not concerned with risk and therefore the negative of the expected value of the performance criterion (denoted by y) can be directly minimized thus allowing the expected value to be maximized:

$$-E(y) \quad (6.6)$$

6.2.2.2 Risk-taking

Risk-taking decision makers are willing to take a risk that the probability of a poor performance is increased if it also means that the probability of a very good performance is also increased. In this case a weighted-sum of the negative of the expected value and the dispersion of the performance criterion distribution is minimized:

$$-E(y) + \theta\sigma(y), \theta < 0 \quad (6.7)$$

A negative θ allows the dispersion of the distribution to be maximized while the expected value is also maximized.

6.2.2.3 Risk-averse

Risk-averse decision makers are not willing to take a risk on their investment and would like to be assured of little variation in the result for a stock, or specifically that the probability of a negative performance criterion is minimized. Therefore either the following can be minimized:

$$-E(y) + \theta\sigma(y), \theta > 0 \quad (6.8)$$

or

$$-E(y) + \mu P(y < 0), \mu > 0 \quad (6.9)$$

In the former a positive θ limits the dispersion in the performance criterion distribution, while the expected value is being maximized. In the latter, a positive μ forces the probability of the performance criterion being less than 0 to be minimized, while the expected value is maximized.

The two formalisms for the objective functions in Sections 6.2.2.2 and 6.2.2.3 are essentially a form of weighted-sum multi-objective optimization with varying weights between the expected value and the dispersion of the performance criterion distribution.

6.2.2.4 Effectiveness and robustness criteria

An alternative definition of the objective function is presented here that also considers the expected value and the spread of the performance criterion distribution, but through the effectiveness ε and robustness R_P criteria. It relies on a scheme where the design options are already sampled *a priori*, for example as in the scheme proposed in Section 6.2.3.1 or 6.2.3.1 below. The effectiveness and robustness criteria can then be determined for each design option x_n as follows (Van Gelder et al. 2013, *under review*):

$$\varepsilon(x_n) = 1 - \frac{y_{\max} - y_{50}(x_n)}{y_{\max} - y_{50}} \quad (6.10)$$

$$R_P(x_n) = 1 - \frac{y_{50+\frac{P}{2}}(x_n) - y_{50-\frac{P}{2}}(x_n)}{y_{50+\frac{P}{2}} - y_{50-\frac{P}{2}}} \quad (6.11)$$

where P is the user-specified percentage of included sample points, y_k is the k^{th} percentile of the performance criterion distribution corresponding to all the design options combined, $y_k(x_n)$ is the k^{th} percentile of the performance criterion distribution associated with design option x_n , and y_{\max} is the maximum value that y takes across all design options, which is not an outlier, where an outlier is defined as a performance criterion value greater than $y_{75}(x_s) + 1.5(y_{75}(x_s) - y_{25}(x_s))$. Effectiveness is thus defined as the improvement in the median performance of a design option as a ratio of the best possible increase. The robustness is similarly defined as the improvement in the performance spread of a design option as a ratio of the spread across all design options. According to these definitions, a measure with an effectiveness and robustness of one is the best possible case, while negative values should be avoided. The criteria are also illustrated in Figure 6.1.

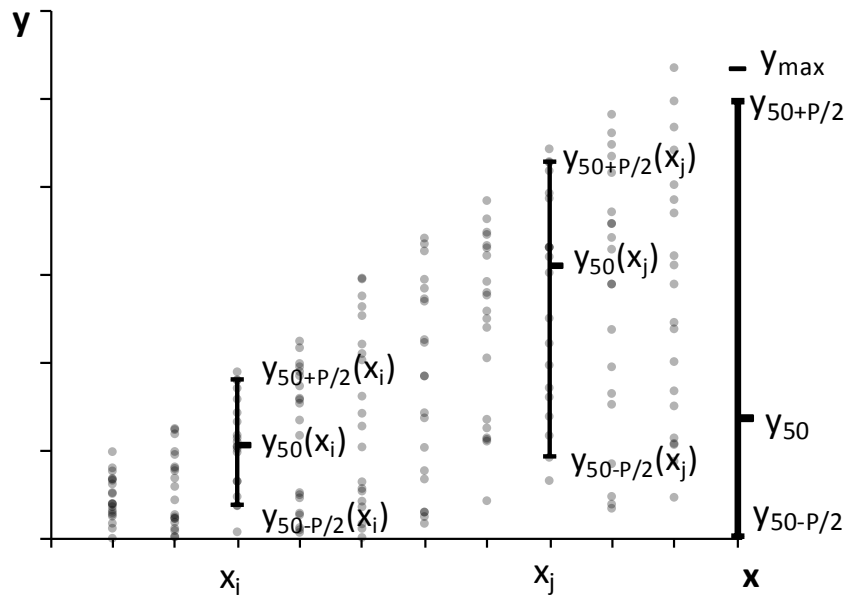


Figure 6.1: Illustration of the effectiveness and robustness criteria. x corresponds to the design option with the largest spread, while x_i and x_j are two random design options.

The objective function is taken to be the weighted sum of the effectiveness and robustness criteria:

$$w_1 \mathcal{E}(x_n) + w_2 R_p(x_n) \quad (6.12)$$

where w_1 is the weight on the effectiveness criterion, and w_2 is the weight on the robustness criterion. Therefore as with the risk-taking and risk-averse approach, a weighted-sum multi-objective optimization approach is applied in order to take into account both the expected value and the associated risk.

6.2.3 Optimization schemes

Figure 6.2 summarizes the steps involved in carrying out the optimization of retrofitting dwellings under the context of uncertainties and variabilities in model inputs. There are several different ways of generating design options. There are also alternative approaches for sampling the variations in the model used to calculate the performance criterion. The model can also be replaced by a metamodel to reduce the computational running time, and enable a higher resolution of Monte Carlo analysis to be carried out. Three different combinations for generating the design options, sampling the model variations, and using a metamodel are explored here.

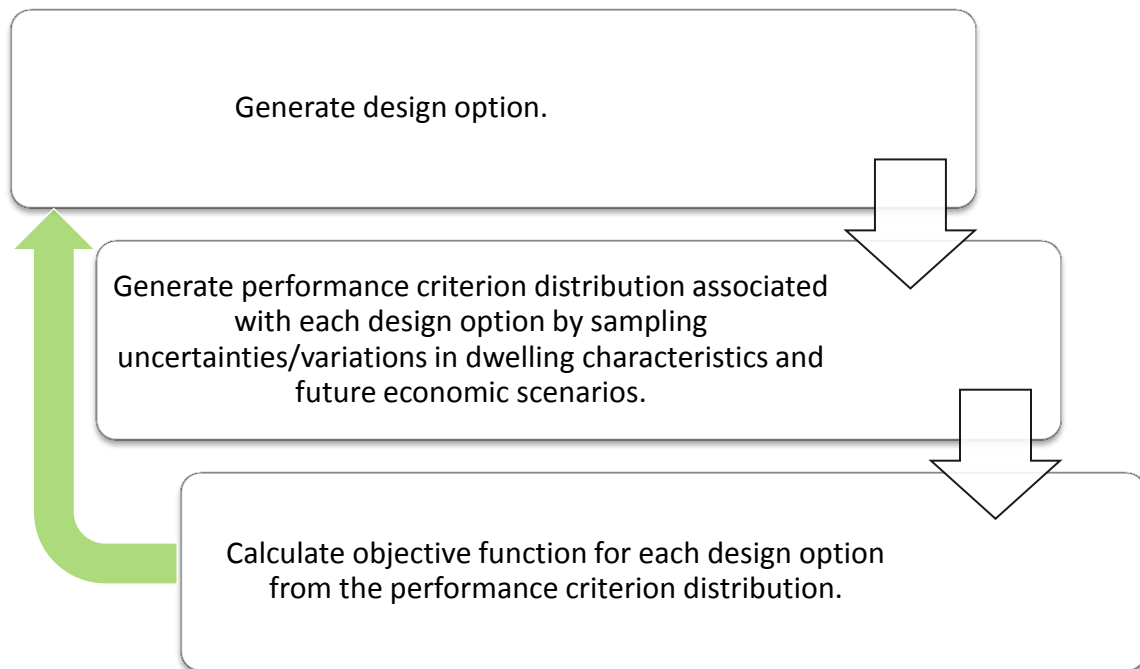


Figure 6.2: Steps involved in finding the optimal design option.

6.2.3.1 Single-layered direct approach

The parameter space of the design variables defining the design options is divided into an equally-spaced grid of multiple dimensions, where each grid space corresponds to a particular design option. The objective function is systematically evaluated for each grid space, sampling all variations simultaneously. The model is used directly rather than replacing it with a computationally faster but possibly less accurate surrogate model (see Chapter 5). The design option with the lowest objective function is defined as the optimal solution.

6.2.3.2 Multi-layered sampling scheme

The design parameter space can instead be explored using a sampling method such as the full factorial design. In the optimization scheme presented here, the sampling of design options is combined with a multi-layered sampling of the variations, according to their source. For example, there are variations associated with the dwelling stock and there are those associated with future economic scenarios, and by separating these variations, an assessment can be made as to whether the overall optimal design option is in fact the optimal design option in all economic situations.

Therefore the sampling scheme is in fact a three-layered design, used to sample the uncontrollable variations associated with the dwellings and the uncontrollable variations associated with the future economic scenarios for each controllable design option. In the first layer, all potential design options are sampled. For every design option, the future economic scenarios are sampled in a second layer. The remaining uncertainties/variabilities are sampled in a third layer. Multi-adaptive regressions splines (MARS) are used to represent the model (Chapter 5).

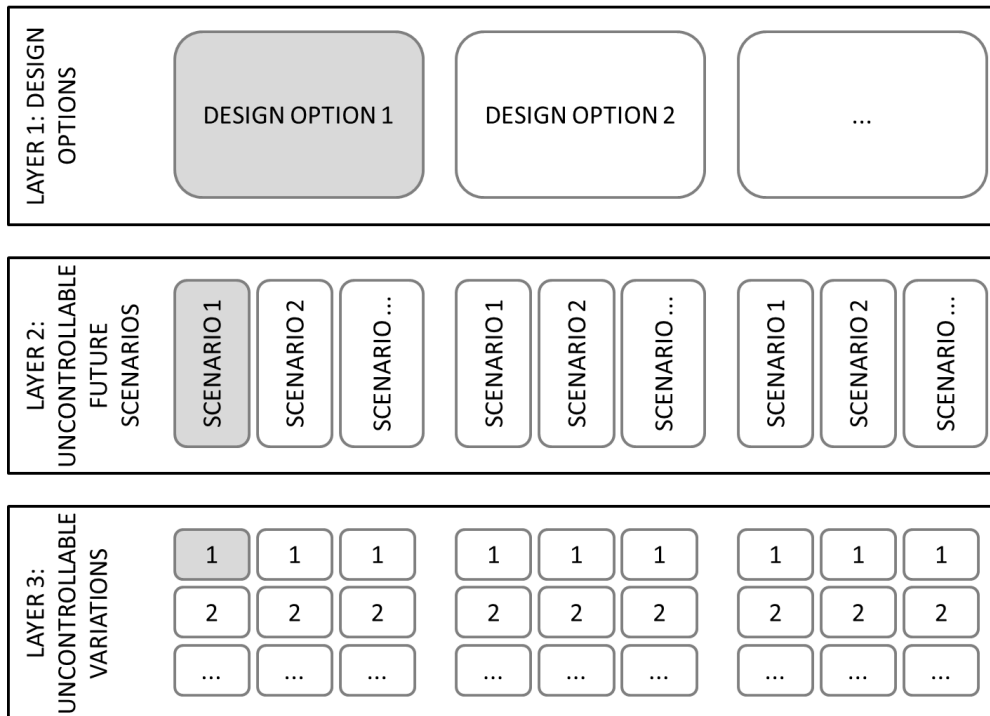


Figure 6.3: Three-layered sampling design, separating controllable variations in the design options (top layer) from uncontrollable variations in future economic scenarios (middle layer) and dwelling characteristics (bottom layer).

6.2.3.3 Single-layered hybrid genetic algorithm

This method uses the objective functions associated with previously sampled design options to help select the next design option, therefore only investigating part of the whole design parameter space in detail. The genetic algorithm initially randomly generates a population of *chromosomes*, each corresponding to a design option. The objective function is evaluated for each chromosome in the population. The new population for the next iteration is formed by randomly selecting multiple chromosomes from the current population, depending on their associated objective function, and recombining them with possible random mutations. The genetic algorithm is specified so that it stops once either a maximum number of generations has been reached or if the weighted average relative change in the minimum objective function value over a specified number of generations is less than or equal to some specified level of accuracy. The genetic algorithm is used to find the region containing the solution, and then the much more computationally efficient gradient-descent algorithm finds the precise solution. In the evaluation of the objective function, the variations are all sampled simultaneously. A neural network metamodel is used to represent the model. More details regarding this metamodel can be found in Chapter 5.

6.2.4 Application to the renovation of attics

Exploration of the various optimization formulations are carried out with regards to the renovation of attics in a neighbourhood of residential dwellings in Sweden, introduced in

section 1.3.6 of Chapter 1. Each design option is a combination of one or more of the following renovation measures:

1. Increasing the insulation level of the attic floor, i.e. reducing the U -value to a target value of $U_{c,target}$. No lower limit is assumed to the U -value that can be achieved.
2. Increasing the airtightness of the attic floor, i.e. reducing the effective leakage area of the attic floor to a target value of $A_{c,target}$. The lowest achievable effective leakage area is considered to be $5 \times 10^{-8} \text{ m}^2/\text{m}^2$.
3. Sealing the ventilation gaps at the eaves, i.e. reducing the venting area per metre eave to a target value of $A_{e,target}$. The airtightness of the attic floor has a lower limit of $2.5 \times 10^{-5} \text{ m}^2/\text{m}$.

In this case $\Delta K_{E,l}$ is defined as the change in the cumulated heat loss through the ceiling as a result of installing the selected design option. There are uncertainties with the installation of each renovation measure, and these along with their costs are shown in Table 6.1. Therefore the actual new dwelling characteristics will vary from the target dwelling characteristics.

Table 6.1: Uncertainty in the implementation of energy efficiency interventions and their costs.

Renovation measure	Old value	Target value	Actual value	Cost
Increasing attic floor insulation	$U_{c,old}$	$U_{c,target}$	$U_{c,new}$ $= N(U_{c,target}, 0.1U_{c,target})$	$8.0 + 1.2 \left(\frac{1}{U_{c,new}} - \frac{1}{U_{c,old}} \right)$ euro/m ²
Increasing airtightness of attic floor	$A_{c,old}$	$A_{c,target}$	$A_{c,new}$ $= N(A_{c,target}, 0.2A_{c,target})$	$5.0 + \frac{3 \times 10^{-7}}{A_{c,new}}$ euro/m ²
Sealing ventilation gaps at the eaves	$A_{e,old}$	$A_{e,target}$	$A_{e,new}$ $= N(A_{e,target}, 0.4A_{e,target})$	$12.0 + \frac{3 \times 10^{-4}}{A_{e,new}}$ euro/m

There is also uncertainty in the future economic scenario (Table 6.2) and a maintenance cost in case of mould damage. This is a one-off repair cost (58 euro/m²) in the case that the peak mould growth index (PMG) for the wooden underlay exceeds a value of 5 at least once within the 10 years since the initial retrofitting. No inflation-related corrections on the maintenance cost are taken into account.

Table 6.2: Uncertainty in future economic scenarios.

Economic parameter	Symbol	Distribution
Inflation-corrected present value factor	a	$N(0.07,0.015)$
Inflation corrected annual increment in energy cost	r_E	$N(0.065,0.0175)$

The conditions in the attic are modelled using the Cold Attic model (or a metamodel surrogate) introduced in Chapter 1.

6.3 Evaluation of methods

In this section, the impact of using different performance criteria, different definitions of the objective function, and a range of optimization schemes is demonstrated with the renovation of Swedish attics. The analysis is founded on the solutions for Common Exercise 5, seven of which were received, as contributed by Christoph Harreither (Vienna University of Technology, Austria), Liesje Van Gelder (KU Leuven, Belgium), Fitsum Tariku (British Columbia Institute of Technology, Canada), Simo Illomets (Tallinn University of Technology, Estonia), Pär Johansson (Chalmers, Sweden), Payel Das (University College London, UK) and Mikael Salonvaara (Owens Corning, USA). The complete solutions are not included here, instead a synthesis is made of the findings and comments only.

6.3.1 Impact of performance criterion

The impact of the choice of performance criterion is illustrated using a single-layered direct approach and the full Cold Attic model, exploring 6 target U-values, 2 target values for the leakage area of the ceiling, and 2 target values for the venting area of the attic eaves. The parameters defining inflation and energy prices are assumed to be different year to year and between each of the dwellings. The objective function is defined as the expected value of the performance criterion.

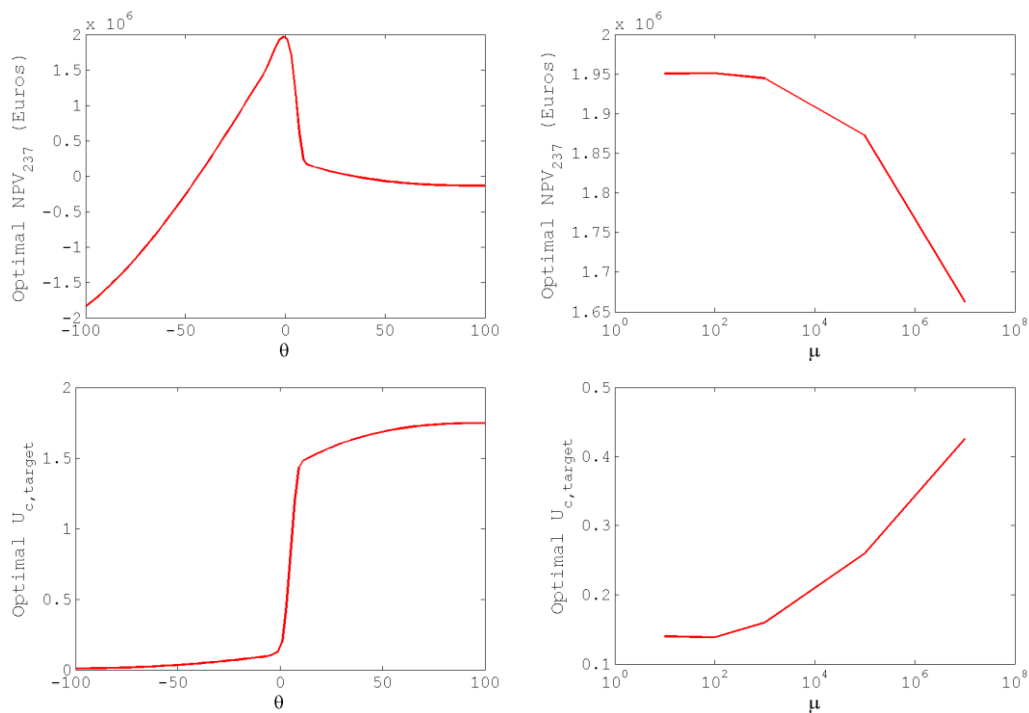
Table 6.3: Performance criteria for a range of design options.

$U_{c,target}$	$A_{c,target}$	$A_{e,target}$	$E(NPV)$	$E(ROI)$	$E(PB)$	$E(IRR)$
W/m ² /K	m ² /m ²	m ² /m	€			
0.08	5.00E-06	0.01	1,695,711	2.44	2.27	0.28
0.1	5.00E-06	0.01	1,789,123	2.87	1.87	0.33
0.15	5.00E-06	0.01	1,854,729	3.49	1.35	0.42
0.2	5.00E-06	0.01	1,804,170	3.78	1.23	0.44
0.25	5.00E-06	0.01	1,768,982	4.03	1.01	0.49
0.3	5.00E-06	0.01	1,690,626	4.07	1.00	0.49
0.08	5.00E-06	0.02	1,632,186	2.39	2.48	0.26
0.1	5.00E-06	0.02	1,737,192	2.79	2.02	0.31
0.15	5.00E-06	0.02	1,853,331	3.49	1.35	0.42
0.2	5.00E-06	0.02	1,801,427	3.78	1.23	0.44
0.25	5.00E-06	0.02	1,730,261	3.91	1.18	0.45
0.3	5.00E-06	0.02	1,684,408	4.06	1.00	0.49
0.08	1.50E-05	0.01	1,028,104	1.37	4.48	0.13

0.1	1.50E-05	0.01	1,011,005	1.51	4.47	0.13
0.15	1.50E-05	0.01	1,101,133	1.94	4.05	0.15
0.2	1.50E-05	0.01	1,219,071	2.52	3.41	0.19
0.25	1.50E-05	0.01	1,150,065	2.60	3.45	0.19
0.3	1.50E-05	0.01	1,094,659	2.69	3.44	0.19
<hr/>						
0.08	1.50E-05	0.02	1,026,481	1.37	4.49	0.13
0.1	1.50E-05	0.02	1,010,492	1.51	4.47	0.13
0.15	1.50E-05	0.02	1,074,448	1.87	4.06	0.15
0.2	1.50E-05	0.02	1,157,961	2.33	3.63	0.17
0.25	1.50E-05	0.02	1,145,470	2.59	3.46	0.19
0.3	1.50E-05	0.02	1,088,181	2.67	3.45	0.19

Assuming *NPV* as the performance criterion finds an optimal design option defined by the target variables $[U_{c,target}, A_{c,target}, A_{e,target}] = [0.15, 0.5 \times 10^{-5}, 0.01]$ while the other performance criteria prefer $[U_{c,target}, A_{c,target}, A_{e,target}] = [0.3, 0.5 \times 10^{-5}, 0.01]$. The other performance criteria are still increasing at $U_{c,target} = 0.3$, and therefore this is a lower limit as the minimum point in the curve may not have yet been reached.

6.3.2 Impact of objective function definition



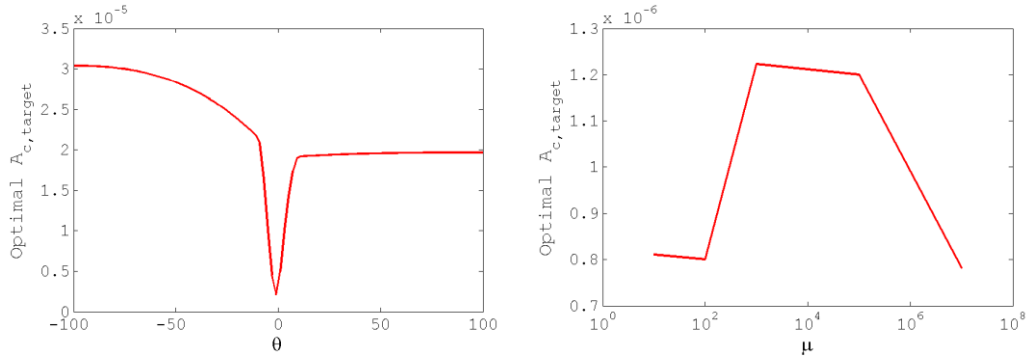


Figure 6.4: The impact of θ (the weight on the dispersion of the NPV distribution in the objective function) and the impact of μ (the weight on the probability of the NPV being less than 0 in the objective function) on the total optimal profit for a stock of 237 dwellings (top), the optimal design U_c (middle), and the optimal design A_c (bottom).

The impact of varying θ and μ in Equations (6.7-6.9) is illustrated using a single-layered hybrid genetic algorithm scheme and the neural network metamodel, and assuming the design option to be defined by $[U_{c,target}, A_{c,target}]$ only, as $A_{e,target}$ is found to have a small effect. NPV is taken to be the performance criterion. Genetic algorithm parameters assumed include a population size of 15, a maximum number of generations of 100, and a crossover fraction between generations of 0.6. The parameters defining inflation and energy prices are assumed to be different year to year but not between each of the dwellings. θ is varied between -100 and 100 and μ between 1 and 10^7 .

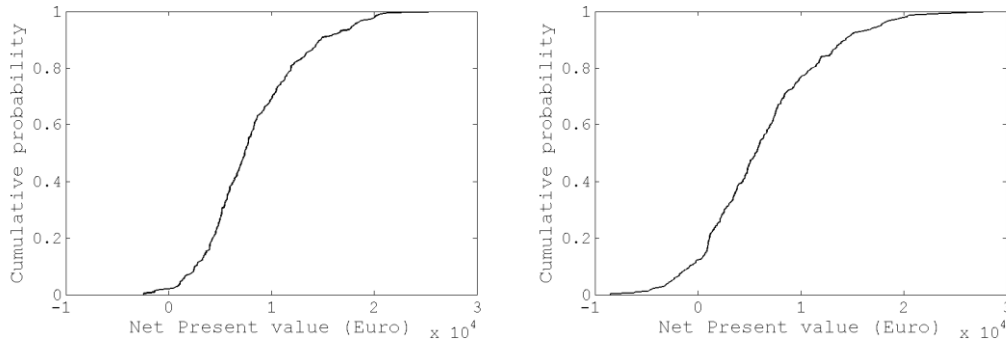


Figure 6.5: The NPV cumulative probability distribution for $\theta = 0$ (left) and $\theta = -10$ (right).

The design option with the highest profit is found at $\theta = 0$, as the only driving term in the optimization is the expected value of NPV. As $\theta \rightarrow -\infty$, the profit associated with the optimal design option falls off very quickly as a large dispersion is favoured over a high expected value. Inspecting the NPV cumulative probability distribution in more detail (Figure 6.5) shows that the risk-taker increases the probability of achieving a very high NPV in select dwellings, even though the overall profit is compromised. The optimal $U_{c,target}$ falls towards zero, and the optimal $A_{c,target}$ increases. As $\theta \rightarrow \infty$, the profit associated with the optimal design option falls initially but then levels off as a small dispersion is increasingly favoured. This shows that there is a lower limit to the dispersion achievable, which can be reached with a relative weight of about 10 on dispersion, though it significantly reduces the total profit. The optimal $U_{c,target}$ increases as a lower dispersion is sought, and the optimal $A_{c,target}$ also increases.

As $\mu \rightarrow 0$, the profit associated with the optimal design option falls off quickly as the probability of a positive *NPV* throughout dominates over its expected value. Analyzing the *NPV* cumulative probability distribution in more detail shows that the risk-taker increases the probability of achieving a very high *NPV* in select dwellings, even though the overall profit is compromised. The optimal $U_{c,target}$ increases while the optimal $A_{c,target}$ does not change much, therefore again showing that a higher $U_{c,target}$ is a lower-risk approach.

The impact of using the effectiveness and robustness criteria is demonstrated using the multi-layered sampling scheme combined with the MARS metamodel, and assuming the design options are defined by all possible design variables $[U_{c,target}, A_{c,target}, A_{e,target}]$. *NPV* is again taken to be the performance criterion. Different permutations of the objective function in Equation (6.12) are explored through a range of combinations of $[P, w_1, w_2]$, where $P = [75, 80, 80, 90, 95, 100]$, $w_1 = [1, 1.5, 2]$, and $w_2 = 1$. A direct comparison is not possible with the objective function formalisms described earlier, but the trends found can be compared. Each of the design option variables in the first layer of Figure 6.3 are assigned ten levels, of which nine are uniformly selected, and one is the initial state. All thirty design variable values are then combined in a full factorial design, resulting in 1000 design options. The uncontrollable future economic scenario variables in the second layer and uncontrollable dwelling characteristics variables in the third layer are separately sampled in a replicated maximin design of 100 samples (5x20). The distributions in the second and third layers are combined to give the *NPV* distribution for each design option, and combined for all the design options to give the total *NPV* distribution.

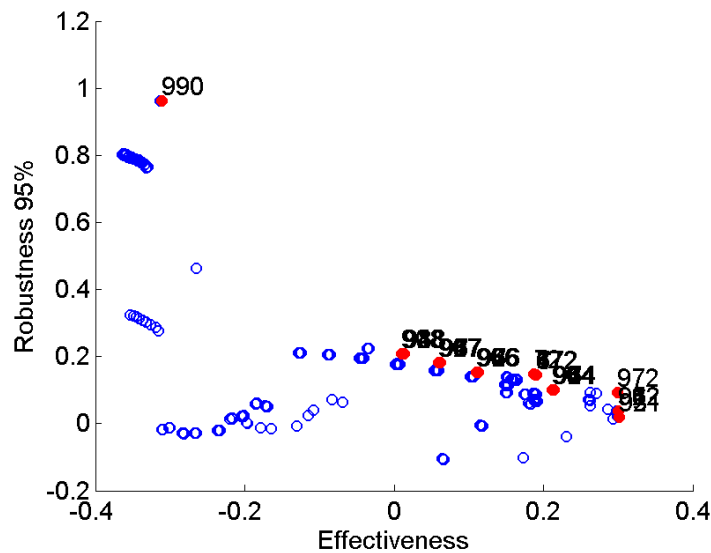


Figure 6.6: The trade-offs between robustness and effectiveness, assuming 95% of sample points are included in the robustness criteria calculation (P). The red dots illustrate the Pareto front.

Figure 6.6 shows the values of the robustness criteria versus the values of the effectiveness criteria for all design options before applying the weights, assuming 95% of sample points are included in the robustness criterion calculation in Equation (6.11). The most effective design option is given by $[U_{c,target}, A_{c,target}] = [0.2, 7.02 \times 10^{-6}]$ and the most robust solution is

given by $[U_{c,target}, A_{c,target}] = [0.2, 9.01 \times 10^{-6}]$. The design option given by $[U_{c,target}, A_{c,target}] = [0.2, 8.01 \times 10^{-6}]$ is the optimal design option for most weight factors and percentages of included data, as illustrated in Table 6.4. The optimal design options preferred no changes to be made to A_e as was found in the application of the other optimization schemes.

Table 6.4: Optimal design options for several variations of P (percentage of included sample data), w_1 (the weight factor for ϵ), and w_2 (the weight factor for R_p).

P	w_1	w_2	$U_{c,target}$	$A_{c,target}$
75	1	1	0.2	9.01E-06
80	1	1	0.2	9.01E-06
90	1	1	0.2	8.01E-06
95	1	1	0.2	8.01E-06
100	1	1	0.3	9.01E-06
75	1.5	1	0.2	8.01E-06
80	1.5	1	0.2	8.01E-06
90	1.5	1	0.2	8.01E-06
95	1.5	1	0.2	8.01E-06
100	1.5	1	0.2	7.02E-06
75	2	1	0.2	8.01E-06
80	2	1	0.2	8.01E-06
90	2	1	0.2	8.01E-06
95	2	1	0.2	8.01E-06
100	2	1	0.2	7.02E-06

6.3.3 Impact of optimization scheme

The impact of the optimization scheme is illustrated in the case where the design option is defined by $[U_{c,target}, A_{c,target}]$ only, the performance criterion is taken to be NPV , and the objective function is taken to be the expected value of NPV .

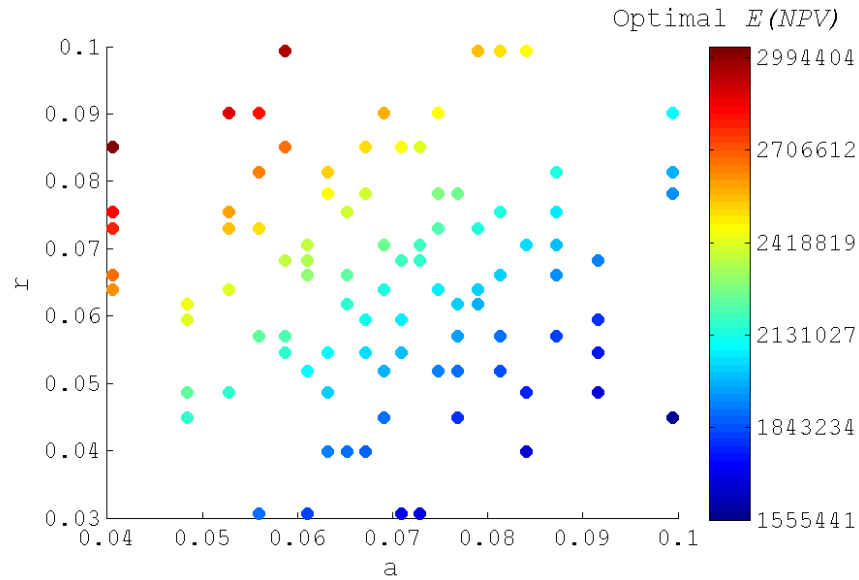


Figure 6.7: Optimal $E(NPV)$ (represented by colour) for different future economic scenarios.

The direct approach using the Cold Attic model finds a maximum $E(NPV)$ of 2,063,955€, arising from the design option $[U_{c,target}, A_{c,target}] = [0.15, 5 \times 10^{-6}]$. The genetic algorithm using the neural network metamodel finds a maximum $E(NPV)$ of 1,950,472€ arising from the design option $[U_{c,target}, A_{c,target}] = [0.14, 7.96 \times 10^{-7}]$. The multi-layered sampling scheme using the MARS metamodel finds a maximum $E(NPV)$ of 2,155,600€ arising from the design option $[U_{c,target}, A_{c,target}] = [0.2, 7.01 \times 10^{-6}]$. Therefore the schemes proposed find similar optimal values for $E(NPV)$. The various schemes all agree that the optimal scenarios prefer no change in A_e of the dwellings in the housing stock, and the target U_c and A_c for the dwellings in the stock are on the lower end of the spectrum, though they are not in exact agreement.

The multi-layered sampling scheme also enables us to compare optimal solutions between different future economic scenarios (Figure 6.3). The optimal design options are all either $[U_{c,target}, A_{c,target}] = [0.2, 7.01 \times 10^{-6}]$ or $[U_{c,target}, A_{c,target}] = [0.1, 4.03 \times 10^{-6}]$, which implies that the optimal solutions are robust against the uncertainty of the future economic scenario, though part of the lack of variation is attributable to the relatively coarse grid of design options explored. This however relates to a range of total profit of between ~1,500,00-3,000,000€, with a high r combined with a low a leading to up to a factor of two discrepancy compared to a scenario with a low r and high a .

6.4 Discussion and conclusions

This Chapter proposes several alternatives for an optimization framework, with variations in the definition of the performance criterion, the derivation of a deterministic criterion from a performance criterion distribution, and the uncertain optimization scheme employed, drawing together several methodologies developed in earlier Chapters.

NPV was found to give a different result compared to *ROI*, *IRR* and *PB*, as the latter are more closely coupled to the ratio between the initial investment and the future cash flow. This implies that it may be worth looking at more than one economic criterion in the assessment of retrofitting scenarios, and consider the most appropriate in each case. A mathematical analysis of the properties of the equations governing *NPV* and *IRR* (Osborne, 2010) found that results depend on the specification of the project and that problems arise in the case of *IRR* when positive and negative cash flows are present in the same project. The author concluded that *NPV* is a richer concept than the *IRR*, in agreement with a study comparing *NPV* with *IRR*, *PB*, amongst several other criteria (Pasqual et al., 2013). There are also other ways of defining the performance criterion that could be explored in further work. A life-cycle cost analysis would be an alternative economic performance criterion that calculates the total profit over the lifetime of the intervention. A non-economically driven approach could have used the energy savings and peak mould growth directly in a multi-objective optimization that aims to determine the Pareto optimal front in which an improvement in one objective cannot be achieved without compromising the other (Asadi et al., 2012b; Das et al., 2013).

The objective functions formulations described here tried in some way to create an objective function that considers both the overall profit and risk associated with each design option in the case of the θ formulation and the robustness/effectiveness formulation. As lowering risk becomes more important, the optimal target U-value and leakage area of the ceiling increases in the former, and in the latter, the optimal target leakage area increases only, though this may be a resolution issue. Reducing the probability of $NPV < 1$ directly does not appear to be significantly influenced by the target leakage area of the ceiling, but again is favoured by higher target U-values of the ceiling. The two formulations proposed here introduce weights that need to be selected, which could perhaps be informed by expert opinion, although weights are not required when only the Pareto-optimal front needs to be viewed. If the criteria do need to be combined, the robustness/effectiveness approach possibly unnecessarily introduces two weights, when only the relative weight is important. It has the advantage however of rating each design option's 'effectiveness' or 'robustness' as a ratio of the effectiveness and robustness of all design options together, but this requires an additional parameter to be specified P . This parameter could perhaps just be replaced by a standard deviation.

The proposed uncertain optimization schemes succeed in bringing together elements of the previous chapters by finding similar optimal design options. The main disadvantages and

advantages of the various schemes can be summarized as follows. Using the direct approach instead of a metamodeling approach avoids the problems with reproducing the peak mould growth, which is not as accurate as the metamodel for heat loss through the attic floor (Chapter 5), though it does not appear to have a big impact on the solutions found here. An obvious disadvantage of using the full model is the time required to run it, and therefore a lack of resolution in the sampling of variations and the exploration of the design space. The use of the genetic algorithm as opposed to the direct approach or sampling approach offers a very computationally efficient way of exploring the design space, therefore avoiding the issue of a high resolution of the design space. It cannot be used however in conjunction with the robustness and effectiveness criteria as they require a full exploration of the design space. Though the implementation of the multi-layered scheme essentially increases the number of simulations by a power of two, a lot more information is revealed concerning the performance of design options in different possible economic scenarios, which may be of interest to the decision maker.

The main conclusions can be summarized as:

- The optimal design options depend on the assumed economic criterion in the renovation of attics in Sweden. *ROI*, *IRR*, and *PB* give similar results however.
- The optimal design options depend on the relative weighting between the total profit and risk. Risk can be assessed by looking at the standard deviation of the performance criterion distribution or the probability it has a value in an undesired range. Robustness and effectiveness criteria offer a method of combining total profit and risk by examining the maximum possible total profit and risk.
- The genetic algorithm offers an efficient method for exploring the design space compared to a direct or sampling approach as the design options are only sampled in higher resolution close to the solution.
- A multi-layered sampling scheme of the variations is able to provide useful information on how the optimal design options may vary across a second layer of variations such as those associated with future economic scenarios.

6.5 References

Ahern C., Griffiths P. and O’Flaherty M. (2013). State of the Irish housing stock—Modelling the heat losses of Ireland’s existing detached rural housing stock & estimating the benefit of thermal retrofit measures on this stock. *Energy Policy* 55:139-151.

Arumi F. (1977). Day lighting as a factor in optimizing the energy performance of buildings. *Energy and Buildings* 1:175-182.

Asadi E., da Silva M. G., Antunes C. H. and Dias L. (2012a). A multi-objective optimization model for building retrofit strategies using TRNSYS simulations GenOpt and MATLAB. *Building and Environment* 56:370-378.

Asadi E., da Silva M. G., Antunes C. H. and Dias L. (2012b). Multi-objective optimization for building retrofit strategies:A model and an application. *Energy and Buildings* 44:81-87.

Aste N., Adhikari R. S. and Buzzetti M. (2012). ENERGY RETROFIT OF HISTORICAL BUILDINGS:AN ITALIAN CASE STUDY. *Journal of Green Building* 7:144-165.

Attia S., Hamdy M., O’Brien W. and Carlucci S. (2013). Assessing gaps and needs for integrating building performance optimization tools in net zero energy buildings design. *Energy and Buildings* 60:110-124.

Bouchlaghem N. (2000). Optimising the design of building envelopes for thermal performance. *Automation in Construction* 10:101-112.

Chan A. L. S. and Chow T. T. (2010). Investigation on energy performance and energy payback period of application of balcony for residential apartment in Hong Kong. *Energy and Buildings* 42:2400-2405.

Charlier D. and Risch A. (2012). Evaluation of the impact of environmental public policy measures on energy consumption and greenhouse gas emissions in the French residential sector. *Energy Policy* 46:170-184.

D’Cruz N., Radford A. and Gero J. S. (1983). A pareto optimization problem formulation for building performance and design. *Engineering Optimization* 7:17-33.

Das P., Chalabi Z., Jones B., Milner J., Shrubsole C., Davies M., ... Wilkinson P. (2013). Multi-objective methods for determining optimal ventilation rates in dwellings. *Building and Environment* 66:72-81.

Diakaki C., Grigoroudis E. and Kolokotsa D. (2008). Towards a multi-objective optimization approach for improving energy efficiency in buildings. *Energy and Buildings* 40:1747-1754.

Evins R. (2013). A review of computational optimisation methods applied to sustainable building design. *Renewable and Sustainable Energy Reviews* 22:230-245.

Fesanghary M., Asadi S. and Geem Z. W. (2012). Design of low-emission and energy-efficient residential buildings using a multi-objective optimization algorithm. *Building and Environment* 49:245-250.

Garrido-Soriano N., Rosas-Casals M., Ivancic A. and Álvarez-del Castillo M. D. (2012). Potential energy savings and economic impact of residential buildings under national and regional efficiency scenarios. A Catalan case study. *Energy and Buildings* 49:119-125.

Gero J. S., D’Cruz N. and Radford A. D. (1983). Energy in context:A multicriteria model for building design. *Building and Environment* 18:99-107.

Goodacre C., Sharples S. and Smith P. (2002). Integrating energy efficiency with the social agenda in sustainability. *Energy and Buildings* 34:53-61.

Gu L., Lin B., Zhu Y., Gu D., Huang M. and Gai J. (2008). Integrated assessment method for building life cycle environmental and economic performance. *Building Simulation* 1:169-177.

Hesaraki A. and Holmberg S. (2013). Energy performance of low temperature heating systems in five new-built Swedish dwellings:A case study using simulations and on-site measurements. *Building and Environment* 64:85-93.

Hopfe C. J. (2009). Uncertainty and sensitivity analysis in building performance simulation for decision support and design optimization. PhD thesis, Technische Universiteit Eindhoven, the Netherlands.

Johnson R., Sullivan R., Selkowitz S., Nozaki S., Conner C. and Arasteh D. (1984). Glazing energy performance and design optimization with daylighting. *Energy and Buildings* 6:305-317.

Kelly G. E. and Bushby S. T. (2012). Are intelligent agents the key to optimizing building HVAC system performance? *HVAC&R Research* 18:750-759.

Kuckshinrichs W., Kronenberg T. and Hansen P. (2010). The social return on investment in the energy efficiency of buildings in Germany. *Energy Policy* 38:4317-4329.

Malatji E. M., Zhang J. and Xia X. (2013). A Multiple Objective Optimisation Model for Building Energy Efficiency Investment Decision. *Energy and Buildings* 61:81-87.

Mata É., Kalagasidis A. S. and Johnsson F. (2013). A modelling strategy for energy carbon and cost assessments of building stocks. *Energy and Buildings* 56:100-108.

Osborne M. J. (2010). A resolution to the NPV-IRR debate? *The Quarterly Review of Economics and Finance* 50:234-239.

Pasqual J., Padilla E. and Jadotte E. (2013). Technical note:Equivalence of different profitability criteria with the net present value. *International Journal of Production Economics* 142:205-210.

Peippo K., Lund P. D. and Vartiainen E. (1999). Multivariate optimization of design trade-offs for solar low energy buildings. *Energy and Buildings* 29:189-205.

Popescu D., Bienert S., Schützenhofer C. and Boazu R. (2012). Impact of energy efficiency measures on the economic value of buildings. *Applied Energy* 89:454-463.

- Radhi H. (2008). A systematic methodology for optimising the energy performance of buildings in Bahrain. *Energy and Buildings* 40:1297-1303.
- Ramesh T., Prakash R. and Shukla K. K. (2012). Life cycle approach in evaluating energy performance of residential buildings in Indian context. *Energy and Buildings* 54:259-265.
- Rasouli M., Ge G., Simonson C. J. and Besant R. W. (2013). Uncertainties in energy and economic performance of HVAC systems and energy recovery ventilators due to uncertainties in building and HVAC parameters. *Applied Thermal Engineering* 50:732-742.
- Sadineni S. B., France T. M. and Boehm R. F. (2011). Economic feasibility of energy efficiency measures in residential buildings. *Renewable Energy* 36:2925-2931.
- Sambou V., Lartigue B., Monchoux F. and Adj M. (2009). Thermal optimization of multilayered walls using genetic algorithms. *Energy and Buildings* 41:1031-1036.
- Tuhus-Dubrow D. and Krarti M. (2010). Genetic-algorithm based approach to optimize building envelope design for residential buildings. *Building and Environment* 45:1574-1581.
- Turner W. J. N., Logue J. M. and Wray C. P. (2013). A combined energy and IAQ assessment of the potential value of commissioning residential mechanical ventilation systems. *Building and Environment* 60:194-201.
- Wang S. and Xu X. (2006). Simplified building model for transient thermal performance estimation using GA-based parameter identification. *International Journal of Thermal Sciences* 45:419-432.
- Wright J. A., Loosemore H. A. and Farmani R. (2002). Optimization of building thermal design and control by multi-criterion genetic algorithm. *Energy and Buildings* 34:959-972.

7

CONCLUSION

Lead authors

Hans Janssen

Staf Roels

7.1 Quantification methodology

7.1.1 Introduction

Oberkampf and co-authors (2002) state that all “realistic modelling and simulation of complex systems must include the non-deterministic features of the system and the environment”. The importance of identifying, characterising and disseminating the impact of uncertainty on analyses or designs of complex systems is indeed progressively more appreciated (Helton and Burmaster, 1996). This essentially calls for the evaluation of probabilities, and hence for the application of probabilistic techniques rather than deterministic methods. Annex 55 therefore aims at introducing probabilistic approaches in analysis and design of hygrothermal building performances. This integration of probabilistic assessment comprises four parts: 1) a global probabilistic methodology (subtask 3), 2) a suite of probabilistic tools (subtask 2), 3) input with uncertainty estimates (subtask 1), and 4) guidelines for probabilistic assessment (subtask 4).

Specifically, the prime objective of Annex 55’s Subtask 2 is to appraise the advantages and disadvantages of existing probabilistic methods for qualitative and quantitative assessment with regard to their applicability within the particular context of building performance analysis and design. Subtask 2 does hence not intend to develop new probabilistic tools, instead it aims at familiarising building physical engineers and researchers with the possibilities and limitations of existing probabilistic tools available from other fields. Five sets of tools are needed for probabilistic assessments, each with a distinct purpose:

1. *qualitative exploration*:
to identify all relevant parameters, and the relations between them;
2. *uncertainty propagation*:
to quantify the probabilistic character of the assessment’s outcome;
3. *sensitivity analysis*:
to determine the dominant and the non-dominant input parameters;
4. *metamodelling method*:
to formulate a simple surrogate model, to replace the original model;
5. *economic optimisation*:
financial criteria and optimisation schemes to attain the best solution;

These five tool sets have each been subject of a specific common exercise in Subtask 2, as well as having been the topic of a dedicated chapter in this report. In these chapters, the outcomes of the common exercises have been used to assess the capabilities and limitations of the different available methods for each of the five tool sets.

In this final chapter, all aspects are combined into a global quantification methodology. Based on the final common exercise, the five primary sets of probabilistic tools are transformed into a generic flowchart, which should be generally applicable for probabilistic assessment of building performance. This flowchart forms also the overall conclusion of this report, as it brings all previously discussed elements together. It should be noted though that the given flowchart remains fairly simple, a more complete version is discussed in Van Gelder et al. (2014).

This global quantification methodology is illustrated for the CE5 idea, where a thermal retrofit of 237 roofs of a neighbourhood is to be designed (see Section 1.3.6 and Addendum 5). To arrive at the renovation measure with the highest overall profit, three main steps can be identified in the quantification methodology (see Figure 7.1): preprocessing, uncertainty quantification, and final optimisation. These steps consecutively describe the problem, select an appropriate tool and the relevant input and output parameters (preprocessing), identify the key parameters (uncertainty quantification) and finally execute the actual probabilistic assessment (optimisation).

7.1.2 Preprocessing

In a first step a qualitative exploration identifies all possible renovation measures. For the case considered, two key mechanisms drive the heat flow from living spaces towards the attic: heat conduction through the attic floor and convective losses due to buoyancy and wind driven air pressure differences. Hence, two possible renovation measures can immediately be determined: adding attic floor insulation and/or increasing the air tightness of the attic floor. Since the magnitude of the losses is determined by the temperature differences between living spaces and attic, and assuming the comfort level in the living spaces fixed, increasing the attic temperature will also reduce the losses. This can be achieved by two additional renovation measures: increasing the roof insulation and/or reduce the ventilation rate of the attic by raising the air tightness of the roof and closing ventilation gaps of the eaves.

Besides identifying all possible renovation measures, all possible hygrothermal risks have to be identified as well, as those might introduce (moisture) damage and additional costs. The major problem for thermal renovation of unheated attics in Sweden is the risk on mould growth on the wooden roof structure. Mould germination and growth is determined by temperature and relative humidity. All identified possible renovation measures (adding insulation or changing the airtightness both of the attic floor as well as of the roof itself) will change the temperature and relative humidity conditions in the attic and thus alter the boundary conditions for mould growth. If severe mould growth occurs this will be an economic loss as the damage has to be repaired, which can counterbalance the gains due to less energy consumption.

Summarised, the qualitative exploration maps all possible renovation measures with the corresponding gains (less energy consumption) and losses (initial investments and repair of potential damage). A flowchart can help to structure all possible scenarios and detect the relevant input and output parameters. Once those determined an appropriate numerical model has to be chosen, being able to quantify the output parameters as a function of the input parameters. For the current case a Matlab-model taking into account all heat, air and moisture flows between outdoor environment, living spaces and attic is chosen. The input parameters are determined as the geometry and current state of the building (air tightness, indoor air temperature and moisture supply,...) as well as the costs for the different renovation and repair measures, evolution of energy prices,... As output the net present value over a time span of 10 years is taken.

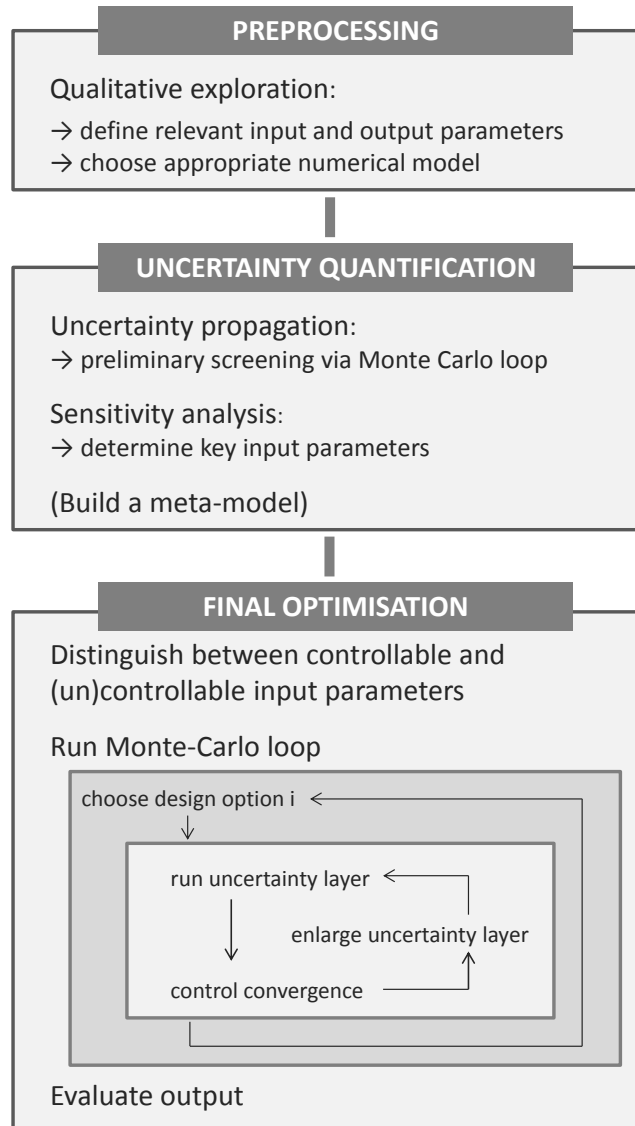


Figure 7.1: Flowchart overall quantification methodology.

7.1.3 Uncertainty quantification

Once an appropriate model is chosen and all relevant input and output parameters determined, the uncertainty quantification can be performed. Note that, at this stage the input parameters are determined, but sometimes the exact distribution is not (yet) known. In such cases, provisional distributions can be ascribed to the stochastic parameters, based on reasonable assumptions. For the current case, the uncertainty quantification, performed via a Monte Carlo loop, shows that the variabilities of the input parameters indeed strongly affect the predicted hygrothermal performances, via the spreads on heat loss and mould growth. The obtained results are used for a sensitivity analysis. Sensitivity indices are calculated to rank the input parameters from most to least influencing the output distributions. Based on this sensitivity ranking, it can be decided whether provisional distributions of influencing parameters need to be updated, while less influencing input parameters can be omitted.

As a lot of hygrothermal simulation models are time consuming, this is also the place to decide on replacing the original model with a metamodel (a faster surrogate model) before going to the actual probabilistic design and final optimisation. The runs used for the uncertainty propagation can be used to construct and validate the metamodel. To do so, the sampling sets of the uncertainty quantification, which are run in the original model, can be subdivided in training and validation sets. Common Exercise 5 showed that for the predicted heat losses through the attic floor a simple regression function suffices to reliably predict the output variable as a function of the input variables, while for the mould growth more advanced metamodels are needed.

7.1.4 Final optimisation

Before performing the final optimisation, it can be useful to subdivide the input parameters into controllable and uncontrollable factors. For instance the renovation measures such as additional attic floor insulation or air tightness are controllable parameters. They are unknown parameters in the optimisation process, but can be seen as design parameters. Once a design is selected, these input values are known. Whereas inherently uncontrollable factors such as workmanship (and hence e.g. the finally obtained airtightness) are completely uncontrollable by the decision maker as their values are neither known in the design process nor after, but can notably affect the final performance. In the probabilistic design the conceptual meaning of the different input parameters can be taken into account by performing a multi-layered sampling scheme. In a multi-layered sampling scheme all design options can e.g. be subjected to the same uncertain parameters, enabling a correct and direct comparison of the obtained output distributions. Note that a further subdivision into more layers can be desirable. Van Gelder et al. (2014) for instance further distinguish an economic scenario layer, to check whether a design option is the most profitable for all future energy price evolutions. Since such a multi-layered scheme will significantly increase the number of runs, this is an additional reason to replace the original model with a faster meta-model.

Once the decision is taken on a one-, two- or multi-layered sampling scheme and all input distributions are known, the output distributions can be calculated in a Monte Carlo loop. To obtain reliable results, all considered output indicators should converge. In a two-layered scheme typically a single design option is selected (e.g. designed U-value and airtightness of the attic floor) and the uncertainty layer values are run. Sampling sets in this layer are added until the output indicators reach convergence.

Once all outputs calculated, each design option can be associated with a performance criterion distribution. Within Common Exercise 5 the cumulative distribution function of the net present value is taken as performance criterion, but other economic performance criteria can be explored as was shown in Chapter 6. Compared to a traditional deterministic analysis, the probabilistic assessment of the design options, gives insight in the reliability of the obtained outcome (effectiveness and robustness of a design option can be evaluated) and the obtained distribution can be combined with an objective function, ranging e.g. from risk-averse to risk-taking to make the final decision.

7.1.5 Final thought

This integrated quantification methodology provides the overall framework for the five sets of probabilistic tools that have been investigated in the different chapters of this report and in the different common exercises of the subtask, and it thus concludes the final report of Subtask 2.

It should however ultimately be stated that the contents of this report on probabilistic tools is not exhaustive on all themes related to the topic. Examples of themes that have not been dealt are:

- correlations between stochastic variables
- multi-objective optimisation of designs
- extreme-value analysis of problems
- stochastic analysis of time-series
- ...

amongst others. More information on these elements can be found in the relevant literature.

7.2 References

Helton J.C. and Burmaster D.E. (1996). Guest editorial: treatment of aleatory and epistemic uncertainty in performance assessments for complex systems. *Reliability Engineering and System Safety* 54:91-94.

Oberkampf W.L., DeLand S.M., Rutherford R.M., Diegert K.V. and Alvin K.F. (2002). Error and uncertainty in modeling and simulation. *Reliability Engineering and System Safety* 75:333-357.

Van Gelder L., Janssen H. and Roels S. (2014). Probabilistic design and analysis of building performances: methodology and application example. *Energy and Buildings* 79:202-2011.

ADDENDA

Addendum 1

Instruction document of Common Exercise 1: Hazard identification and flowchart formation for wall renovation measures

Addendum 2

Instruction document of Common Exercise 2: Hygrothermal analysis of massive wall with interior insulation

Addendum 3

Instruction document of Common Exercise 3: Sensitivity analysis of hygrothermal performance of cold attic

Addendum 4

Instruction document of Common Exercise 4: Metamodelling of the hygrothermal performance of cold attic

Addendum 5

Instruction document of Common Exercise 5: Economic assessment of retrofitting measures



IEA-ANNEX 55

Reliability of Energy Efficient Building Retrofitting –
Probability Assessment of Performance and Cost
(RAP-RETRO)

SUBTASK 2, COMMON EXERCISE 1 - INSTRUCTION DOCUMENT

HANS JANSSEN / STAF ROELS, NOVEMBER 2010

COMMON EXERCISE 1: HAZARD IDENTIFICATION AND FLOWCHART FORMATION FOR WALL RENOVATION MEASURES

– INSTRUCTION DOCUMENT –
Hans Janssen, Staf Roels, November 2010

1. Objectives of Common Exercise 1

Subtask 2 aims at the development of a probabilistic methodology to predict the energy savings of retrofitting measures while simultaneously assessing the risk of potential hygrothermal failure. In the final stage of the Annex it should be possible to apply this methodology in a generic way: e.g. to make decisions on retrofitting measures for a typical building stock. In the current onset stage of the Annex, the aim is first to get familiar with probabilistic methodologies, to investigate the limits and possibilities of stochastic models for our specific problems, to investigate possible bottle necks to apply the methodology in the field of building physics, etc.

While Common Exercise 2, which runs in parallel with Common Exercise 1, aims at exploring quantitative tools, such as FORM/SORM or Monte Carlo, based on an analysis of interior insulation, Common Exercise 1 focuses on qualitative probabilistic tools on a larger scale. The objective of Common Exercise 1 is the qualitative analysis of different wall thermal upgrade measures, with respect to both energy consumption and hygrothermal damages. This allows investigating the capabilities and limitations of different qualitative methods for probabilistic risk assessment.

2. General description of the Exercise

The studied object for Common Exercise 1 is the Danish Villa, one of the cases studied in Annex 55. More specifically, the thermal upgrade of the cavity walls of this dwelling is to be analysed. The figure below shows (from left to right) the front façade of the villa, a vertical cut of the building, a magnification of the façade and the cavity wall dimensions. For this exercise, we will consider the villa as free-standing, without any significant vegetation shielding it. Further information can be found in the Case report and presentation, uploaded to the Common Exercise folder.

Three main options exist for the thermal upgrade of these cavity walls: interior insulation, exterior insulation or cavity filling. Each of these options has a different potential efficiency for reduction in building energy consumption and a different potential risk for hygrothermal damages. The overall objective of the Common Exercise 1 is to attain a flowchart for the probabilistic evaluation of the energy consumption and hygrothermal damages. This flowchart should logically connect all the potential influence factors to the final estimation of energy consumption and hygrothermal damages.

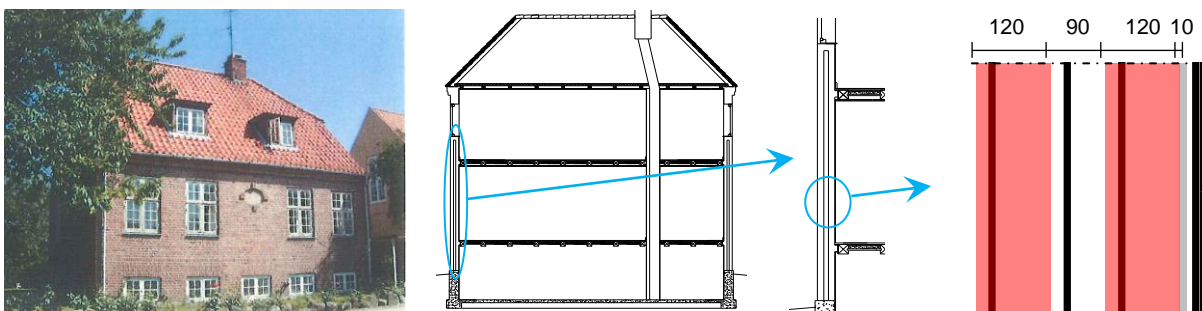


Illustration: Danish villa, vertical cut, cavity wall detail, cavity wall dimensions.

3. Task specification for the Exercise

3.1. Introduction

The final aim of any comparative study is to assess the advantages and disadvantages of different options, to finally come to a choice that is assumed to yield an optimal balance. For this case, a thermal upgrade for cavity walls, three choices are to be compared: interior insulation, exterior insulation, and cavity filling. The main grounds for comparison are the reduction in energy consumption and the minimisation of hygrothermal damages. This implies that distributions in energy consumption and hygrothermal damages are to be quantified, which requires a probabilistic assessment.

In the Probabilistic Tools Workshop, an element of the Copenhagen Working Meeting, a global methodology for probabilistic assessment was discussed and developed. The result is a two-tier approach, with a qualitative and a quantitative component. The qualitative analysis targets a 'dissection' of the problem, via a hazard identification phase and a flowchart formation phase. In the hazard identification, the main aim is to identify all potential influence factors that may affect the final aims (energy consumption and hygrothermal damages). In the flowchart formation, the logical connections between the influence factors and the final aims are outlined. Once this qualitative evaluation is finalised, the quantitative analysis aims at translating stochastic distributions of the influence factors to stochastic distributions of the final aims. More information on this can be found in the report on the Probabilistic Tools Workshop, uploaded to the Common Exercise folder. This Common Exercise 1 focuses on the qualitative aspects, while Common Exercise 2 targets the quantitative issues.

For each of the two phases within the qualitative analysis, several methodologies are available in literature. Hazards can be identified with Preliminary Hazard Analysis, Failure Modes and Effect Analysis, Hazard and Operability Studies, Risk Screening Sessions, ... Flowcharts can be formed via Event Trees, Fault Trees, Cause-Consequence Charts, Bayesian Probabilistic Nets, ... A short introduction to these can be found in the lecture notes of Michael Faber, particularly sections 4.6-4.7 and 10.1-10.5. The primary objective of this Common Exercise 1 is to assess the capabilities and limitations of those methods.

3.2. Hazard identification

Common Exercise participants are requested to apply a hazard identification method to the three possible wall thermal upgrade options, with reference to both energy consumption and hygrothermal damages. The final result of this assignment should be an overview of all possible influence factors that may affect the targeted reduction in energy consumption and minimisation of hygrothermal damages.

3.3. Flowchart formation

Common Exercise participants are requested to apply a flowchart formation method to the derived set of influence factors. The final result of this assignment should be a logical flowchart that illustrates the logical connections between the initial influence factors and the concluding final aims.

4. Requested output of the Exercise

Common Exercise participants are requested to deliver three main outcomes:

1. an overview of the influencing factors resulting from the hazard identification assignment;
2. one (or several) logical flowchart(s) resulting from the flowchart formation assignment;
3. a report describing the methodologies that were applied, and commenting on their capabilities and limitations;

We are aware that full execution of Common Exercise 1 may require significant effort, and that the results may quickly become extensive. Partial analysis of the problem, along the suggested lines, is therefore also possible as output from the Common Exercise.



IEA-ANNEX 55

Reliability of Energy Efficient Building Retrofitting -
Probability Assessment of Performance and Cost
(RAP-RETRO)

SUBTASK 2, COMMON EXERCISE 2 - INSTRUCTION DOCUMENT

HANS JANSSEN / STAF ROELS, NOVEMBER 2010

COMMON EXERCISE 2: HYGROTHERMAL ANALYSIS OF MASSIVE WALL WITH INTERIOR INSULATION

– INSTRUCTION DOCUMENT –
Hans Janssen, Staf Roels, November 2010

1. Objectives of Common Exercise 2

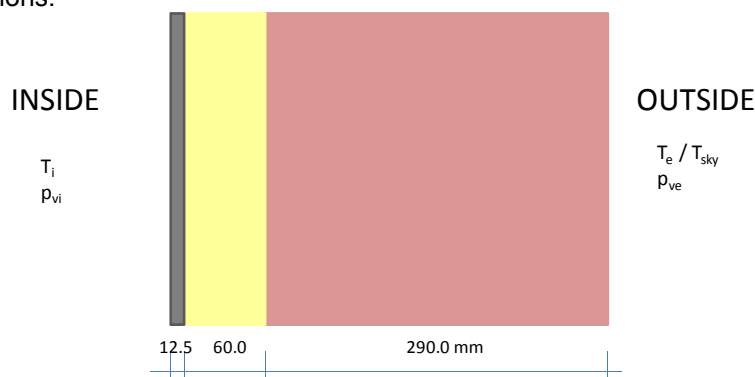
Subtask 2 aims at the development of a probabilistic methodology to predict the energy savings of retrofitting measures while simultaneously assessing the risk of potential hygrothermal failure. In the final stage of the Annex it should be possible to apply this methodology in a generic way: e.g. to make decisions on retrofitting measures for a typical building stock. In the current onset stage of the Annex, the aim is first to get familiar with probabilistic methodologies, to investigate the limits and possibilities of stochastic models for our specific problems, to investigate possible bottle necks to apply the methodology in the field of building physics, etc.

Two common exercises (CE) are described in this onset stage. While CE1, which runs in parallel with this CE2, aims at an exploration of qualitative probabilistic tools such as fault tree analysis, bayesian networks,... CE2 focuses on quantitative probabilistic tools applicable on a smaller scale.

The subject of CE2 is the probabilistic prediction of energy savings and hygrothermal risk for a specific retrofitting measure at the building component level: the application of interior insulation on an existing massive wall. This allows investigating the capabilities and limitations of different stochastic methodologies for a well-described one-dimensional HAM-problem (HAM: Heat Air and Moisture). As most probably different building envelope models will be used to assess the problem, first the deterministic case has to be calculated. This should give insight in deviations occurring from differences in the applied numerical models. Then prescribed stochastic variations are given for some of the material properties and boundary conditions. The applied probabilistic methodology to take into account these stochastic variations is free. In this way, a comparison of the obtained probability density functions of the requested performances in addition with information of the applied probabilistic tool, calculation time, etc. should give information on possibilities and limitations of different probabilistic tools in the field of HAM-analysis of building components.

2. General description of the case

To keep the hygrothermal simulations one-dimensional a simplified version of the outer walls of the 'Danish villa'- case have been used as starting point. As retrofitting measure the outer brick layer (uniform layer of 29 cm thick) is foreseen from interior insulation (6 cm) and finished at the inside with coated gypsum board. The wall is assumed to be perfectly airtight and is submitted to transient indoor and outdoor conditions.



3. Input parameters

3.1. Material properties

This section gives an overview of all necessary material properties of the different layers. First the material properties to be used in the deterministic case are described, then for each material an overview is given of those properties that have to be treated as stochastic variables with the prescribed distribution of the properties which are to be taken into account.

3.1.1. Coated gypsum board

The properties of the coated gypsum board are based on the round robin test performed within ST2 of IEA-Annex 41. For the current exercise the gypsum board has to be treated as one homogeneous layer with the following equivalent material properties:

Heat capacity of dry material:

$$\rho.c = 690 \cdot 1100 \text{ J/(m}^3 \cdot \text{K)}$$

Thermal conductivity:

$$\lambda = 0.198 \text{ W/(m.K)}$$

Sorption isotherm:

$$w(\Phi) = 53 \cdot \left(1 + (-215 \cdot \ln(\Phi))^{1.628}\right)^{\left(\frac{1-1.628}{1.628}\right)} \text{ (kg/m}^3\text{)}$$

with Φ the relative humidity (-)

Vapour diffusion:

$$\delta_p = \frac{5.65 \cdot 10^{-8}}{T} \cdot \left(1 / \mu_{dry} + 0.00003 \cdot \exp(8.25 \cdot \Phi)\right) \text{ (s)}$$

with $\mu_{dry} = 300$

Liquid moisture permeability:

$$K_l(p_c) = 0$$

In the stochastic analysis only the vapour diffusion of the coated gypsum board layer is treated as stochastic variable with the following distribution:

$$\delta_p = \text{var} \cdot \frac{5.65 \cdot 10^{-8}}{T} \cdot \left(1 / \mu_{dry} + 0.00003 \cdot \exp(8.25 \cdot \Phi)\right) \text{ (s)}$$

with var a normal distributed multiplication factor with mean value of 1.0 and stdev of 0.25.

3.1.2. Interior insulation

Mineral wool fibre is used as interior insulation with the following properties:

Heat capacity of dry material:

$$\rho.c = 50 \cdot 840 \text{ J/(m}^3 \cdot \text{K)}$$

Thermal conductivity:

$$\lambda = 0.04 \text{ W/(m.K)}$$

Sorption isotherm:

$$w(\Phi) = 0.83 * \left(1 + (-447 * \ln(\Phi))^{1.18}\right)^{\left(\frac{1-1.18}{1.18}\right)} \quad (\text{kg/m}^3)$$

Vapour diffusion:

$$\delta_p = \frac{5.65 * 10^{-8}}{T * \mu_{dry}} \quad (\text{s})$$

with $\mu_{dry} = 1.2$

Liquid moisture permeability:

$$K_i(p_c) = 0$$

In the stochastic analysis only the thermal conductivity of the mineral wool is treated as stochastic variable corresponding to a normal distribution with mean value $\lambda_{\text{mean}} = 0.04$ W/mK and stdev of 0.005.

3.1.3. Masonry wall

The original masonry wall is simplified into a single homogeneous brick layer with the following equivalent properties:

Heat capacity of dry material:

$$\rho \cdot c = 1786 * 840 \text{ J/(m}^3 \cdot \text{K)}$$

Thermal conductivity:

$$\lambda = 0.5 + 0.0045 * w \text{ W/(m.K)}$$

Sorption isotherm – water retention curve:

$$w(P_{suc}) = 206.7 * \left(\sum_{s_i=1}^{s_n} l_i \left(1 + (c_i P_{suc})^{n_i}\right)^{\left(\frac{1-n_i}{n_i}\right)}\right) \quad (\text{kg/m}^3)$$

with $s_n = 2$

$$l_1 = 0.5422; l_2 = 0.4578$$

$$c_1 = 4.57 * 10^{-5}; c_2 = 1.85 * 10^{-5}$$

$$n_1 = 5.10; n_2 = 2.677$$

Vapour diffusion:

$$\delta_p = \frac{5.65 * 10^{-8}}{\mu_{dry} * T} \frac{1 - \frac{w}{206.7}}{0.503 * \left(1 - \frac{w}{206.7}\right)^2 + 0.497} \quad (\text{s})$$

with $\mu_{dry} = 13.8$

Liquid moisture permeability:

The liquid water permeability is given as data-file (*perm.txt*) containing two columns: $\log(P_{suc})$ and $\log(K_i)$. Intermediate values have to be calculated via logarithmic interpolation. For those numerical codes using a diffusivity-approach, the same data is provided in '*diff.txt*' as moisture diffusivity D_w as a function of moisture content w .

None of the properties of the brick wall are taken as stochastic variables.

3.2. Boundary conditions

3.2.1. Outside climate and exterior properties

The outside conditions are based on the hourly values of the climatic data file of Essen, which can be found in the data file: *Essbasi01h.cli*.

Driving rain is modelled according to the British Standard, using the following relation:

$$R_{\text{wdr}} = \alpha * U * R_h * \cos(\xi) \text{ kg/m}^2\text{h}$$

with R_{wdr} the wind-driven rain ($\text{kg/m}^2\text{h}$), α the wind-driven rain coefficient (s/m), U the meteorological wind speed (m/s), R_h the horizontal rain ($\text{kg/m}^2\text{h}$) and ξ the angle between the wind direction and the normal to the wall (-). For this exercise, α is taken equal to 0.1 s/m.

The convective heat transfer coefficient at the exterior surface is taken constant at $20 \text{ W/m}^2\text{K}$, the moisture transfer coefficient at $1.54 * 10^{-7} \text{ s/m}$, the short-wave absorptivity 0.6 and the long-wave emissivity 0.9.

For the deterministic case it is assumed that the wall is facing the south direction.

For the stochastic case it is assumed that the wall can be orientated in all possible directions, equally distributed.

3.2.2. Indoor climate and interior properties

The indoor temperature is assumed to be constant at 20°C . The total heat transfer coefficient at the interior surface is $8 \text{ W/m}^2\text{K}$, the moisture transfer coefficient $3 * 10^{-8} \text{ s/m}$.

The indoor relative humidity is dependent on the outdoor vapour pressure, moisture production rate inside the dwelling and ventilation rate imposed by the inhabitants. The vapour over pressure $\Delta p_{v,i-e}$ indoor versus outdoor is based on the moisture balance of the dwelling and has to be calculated as:

$$\Delta p_{v,i-e} = 3600 * R_v * T_i * G_v / (n * V)$$

with R_v the water vapour gas constant (462 J/kg.K), T_i the indoor temperature (293 K), G_v/V the moisture production rate divided by the volume of the dwelling; taken constant as $3.86 * 10^{-7} \text{ kg/(s.m}^3)$ and n the ventilation rate per hour (1/h) which is dependent of the outside temperature θ_e ($^\circ\text{C}$):

$$n = a * (0.45 + \theta_e / 30)$$

For the deterministic case a is taken 1.0.

In the stochastic case a is taken as variable, corresponding to a normal distribution with mean $a_{\text{mean}}=1.0$ and stdev 0.15.

3.3. Initial conditions

All layers are assumed to be initially at a temperature of 20°C and in equilibrium with 50% RH.

4. Performances to be analysed

The hygrothermal response of the wall is to be calculated from July 1st until June 30th. To evaluate the performance of the wall both the heat losses through the wall and the risk on mould growth are to be analysed.

4.1. Heat flux through the wall

To evaluate the thermal performance of the wall the heat losses during January are calculated at the interior surface.

To compare the deterministic cases the evolution of the heat losses through the wall during the month of January are to be given as a function of time in W/m^2 . The hourly values of the heat flux at the

interior surface have to be filled out in the sheet '*deterministic_heat*' of the prescribed excel-file (see §5. Requested output).

For the stochastic analysis, the same data (hourly values during January in W/m²) have to be provided, but now for each simulation run in the sheet '*stochastic_heat*' of the prescribed excel-file. At the same time, for each run also the values of the stochastic variables are requested.

4.2. Risk on mould growth

The risk on mould growth is evaluated at the interface between interior insulation and masonry wall. The analysis is based on a simplified mould growth model. The simplified model is derived from the VTT mould model, but only preserves the main characteristics. The key simplifications are situated in neglecting the retarded growth in the initial and final stages (for mould indices below 1 and above 5).

The mould growth index is indicated by M (-), and the evolution of M is modelled as:

$$\text{if } (\Phi > \Phi_{\text{crit}}): \quad dM/dt = (8 \cdot 10^{-8} + 2 \cdot 10^{-8} \cdot \theta) \cdot \exp(12.5 \cdot \Phi)$$

$$\text{if } (\Phi \leq \Phi_{\text{crit}}): \quad dM/dt = -0.015$$

with Φ the relative humidity (-), Φ_{crit} the critical relative humidity (-), t the time (days) and θ the temperature (°C). The given relations can be used on a basis of hours, minutes or seconds, but such requires dividing the given dM/dt with 24, 1440 or 86400. The critical relative humidity is calculated as:

$$\Phi_{\text{crit}} = \max(0.8, (-0.00267 \cdot \theta^3 + 0.16 \cdot \theta^2 - 3.13 \cdot \theta + 100)/100)$$

As for the heat flux, the evolution of the mould growth index (M) has to be given as a function of time (daily values from July 1st, until June 30). The daily values have to be filled out in the sheet '*deterministic_mould*' of the prescribed excel-file.

For the stochastic analysis, the same data (daily values of mould growth index), but now for each simulation run has to be filled out in the sheet '*stochastic_mould*' of the prescribed excel-file. For each run also the values of the stochastic variables have to be given.

5. Requested output

Common Exercise participants are requested to deliver two documents:

1. an excel-file corresponding the prepared *ST2_CE2_country_institute.xls* containing the numerical output of both the deterministic and stochastic analysis. Note that the given excel-file *ST2_CE2_country_institute.xls* has to be renamed with the real name of the country and institute of the participant as e.g. *ST2_CE2_Belgium_KUL.xls*
2. In addition each participant shall provide a word-document (*ST2_CE2_country_institute.doc*) describing shortly the used HAM-model and giving explanation on the applied stochastic methodology. How are the variables taken into account, are simplifications introduced, number of runs for Monte Carlo-simulations, etc.



IEA-ANNEX 55

Reliability of Energy Efficient Building Retrofitting -
Probability Assessment of Performance and Cost
(RAP-RETRO)

SUBTASK 2, COMMON EXERCISE 3 - INSTRUCTION DOCUMENT

CARL-ERIC HAGENTOFT / HANS JANSSEN / STAF ROELS, JUNE 2011

COMMON EXERCISE 3: SENSITIVITY ANALYSIS ON HYGROTHERMAL PERFORMANCE OF COLD ATTICS

— INSTRUCTION DOCUMENT —

Carl-Eric Hagentoft, Hans Janssen, Staf Roels, June 2011

1. Objectives of Common Exercise 3

Annex 55's Subtask 2 'Probabilistic tools' aims at developing a probabilistic methodology to predict the energy savings of retrofitting measures while concurrently assessing the risk of potential hygrothermal failure. In the final stage of the Annex it should be possible to apply this methodology in a generic way, e.g. to make decisions on retrofitting measures for a typical building stock. In the current onset stage of the Annex, the target is first to get familiar with probabilistic methodologies, to investigate the limits and possibilities of stochastic models for our specific problems, to investigate possible bottle necks to apply the methodology in the field of building physics, etc. Two common exercises (CE) have already been executed in Subtask 2: CE1 aimed at exploring qualitative probabilistic tools like fault tree analysis, bayesian networks ..., while CE2 focused on applying quantitative probabilistic tools for the characterisation of uncertainty.

The topic of CE3 is an uncertainty and sensitivity analysis of the hygrothermal behaviour of cold attics, particularly the mould growth in the attic and the heat loss to the attic. Uncertainty analysis is a crucial step in any probabilistic assessment, as it characterises the effects of the variability of the input parameters on the simulation outcomes. Sensitivity analysis equally is an essential element, since it allows determining which parameters actually govern the investigated outcomes, to certainly be considered in a later metamodelling exercise for example. The main aims of Common Exercise 3 are hence to reintroduce methods for uncertainty analysis, and to explore approaches for sensitivity analysis. The choice of methods is free for both aspects, and CE 3 hence generally targets an overview of different methods and a comparison of their outcomes.

2. General description of the Exercise

Opposite to our earlier common exercises, a common calculation object and tool is used to avoid interference from deviations in modelling and/or simulation approaches. The given cold attic model relates the cold attic performances to 16 different input parameters, each with its specific distribution. In a first part, resulting uncertainties on mould growth and heat losses are to be quantified. The (relative) significances of the various input parameters for the performances are to be computed in the second part.

An overview of uncertainty analysis techniques has been given at the Copenhagen working meeting, and participants are referred to the presentations from that meeting. Inspiration for sensitivity analysis methodologies can be found in:

- Lomas KJ, Eppel H, 1992. Sensitivity analysis techniques for building thermal simulation programs, *Energy and Buildings* 19, 21-44;
- Hamby DM, 1994. A review of techniques for parameter sensitivity analysis of environmental models, *Environmental Monitoring and Assessment* 32, 132-154;
- Hamby DM, 1995. A comparison of sensitivity analysis techniques, *Health Physics* 68, 194-204;
- Helton JC, Davis FJ, 2002. Illustration of sampling-based methods for uncertainty and sensitivity analysis, *Risk Analysis* 22, 591-622;
- Saltelli A, Ratto M, Andres T, Campolongo F, Cariboni J, Gatelli D, Saisana M, Tarantola S, 2008. *Global Sensitivity Analysis: The Primer*, John Wiley and Sons, West Sussex, England;

The first four publications are provided together with this common exercise.

An introduction to the physical basis of the cold attic model used for this exercise is given in ‘Simulation model for hygrothermal conditions and mould growth potential in cold attics’, which can be found at the end of this document. That physical model has been implemented in Matlab, and Cold_Attic_4.m is provided. The model uses 15 different input parameters – material properties, component characteristics, geometric dimensions, climate values – to compute 2 outcomes – the yearly peak mould growth index (PMG, -) for the wooden underlay, and the cumulated heat loss through the ceiling in January (CHL, kWh/m²). For detailed analyses, hourly values of the surface temperature and surface relative humidity of the wooden underlay, mould growth index on the wooden underlay and the ceiling heat losses are also provided by the program.

The 15 different input parameters are collected in Table 1. Table 1 equally gives the related symbol in the .m-file, and the probability distribution of each parameter. Two types of distributions are used: uniform distributions $U(x_{low}, x_{upp})$, and normal distributions $N(x_{avg}, x_{std})$. In the former, x_{low} and x_{upp} indicate respectively the lower and upper limit of the uniform distribution; in the latter, x_{avg} and x_{std} indicate the average and standard deviation respectively of the normal distribution. For all normally distributed parameters, a lower limit of 0 is moreover implicitly assumed. For the external climate data, 30 years are provided, of which one year is selected for a single simulation. This particular uniform distribution is hence restricted to the integers between 1 and 30 only.

Table 1: variable input parameters, .m-file symbol, probability distribution

input parameter	symbol	distribution
Height of building H (m)	H	U(4,8)
Area of ceiling and roof A (assumed equal) (m ²)	Area	U(50,200)
Orientation of one of eave sides (-)	BSangle	U(0,180)
Venting area per meter eave A _e (m ² /m)	Ae	U(0.001,0.05)
Length of building (eave side) L (m)	Length	U(7,20)
Thickness of wooden underlay d (m)	d	U(0.010,0.020)
Vapour diffusivity of wood δ_v (m ² /s)	deltav	$N(10^{-6}, 2 \cdot 10^{-7})$
Initial relative humidity of wood ϕ_0 (-)	startRH	U(0.5,0.9)
Thermal conductivity of wood λ_{roof} (W/mK)	lambda	N(0.13,0.02)
Resistance of roof insulation R _r (m ² K/W)	Rr	U(0,1)
Leakage area per m ² of ceiling A _c (m ² /m ²)	Ac	U(0.001,0.05)
U-value of the ceiling U _c (W/m ² K)	Ufloor	U(1,5)
Indoor temperature T _i (°C)	Ti	N(20,1.5)
Indoor moisture supply (kg/m ³)	MS	N(0.005,0.002)
Year of climate data used (-)	Year	U(1,30)*

*only discrete integer values are allowed

3. Task specification for the Exercise

3.1 Deterministic result

As an introductory step, participants are requested to provide the resulting PMG and CHL values when all input parameters are taken equal to their respective means, and year 5 is imposed as fixed external climate data. The results are to be provided in the predefined .xls-file.

3.2 Uncertainty analysis

Participants are requested to analyse the spread on PMG and CHL resulting from the variability of the different input parameters. If Monte Carlo is employed to this aim, results to be provided are input parameters and simulation outcomes for all runs, inserted into the predefined .xls-file. These will later on be compiled into cumulative probability distributions. If alternative uncertainty quantification techniques are applied, results should be inserted in the predefined .xls-file directly as a cumulative probability distributions. A short text in the predefined .doc-file should document the general details from the Monte Carlo analysis (number of runs, sampling strategy, stopping criterion, ...). If alternative uncertainty quantification techniques are applied, the short text should generally describe that approach.

3.2.1 Fixed external climate

In a first variant, the external climate data are fixed, and year 5 is used for all simulations.

3.2.2 Variable external climate

In the second variant, the variability of the external climate data is superimposed on the other 14 variable input parameters, with the year to be selected based on the U(1,30) distribution.

3.3 Sensitivity analysis

Participants are requested to quantify the (relative) significances of the different variable input parameters on the simulation outcomes PMG and CHL. The result of this sensitivity analysis is to be expressed in a numeric format, which can later on be used to rank the parameters according to the sensitivity of PMG/CHL upon them. Moreover, a short text documenting the applied sensitivity analysis technique(s) is to be supplied as well.

3.3.1 Fixed external climate

In a first variant, the external climate data are fixed, and year 5 is used for all simulations.

3.3.2 Variable external climate

In the second variant, the variability of the external climate data is superimposed on the other 14 variable input parameters, with the year to be selected based on the U(1,30) distribution.

4. Requested output of the exercise

Common Exercise 3 participants are requested to deliver two documents:

1. a .xls-file corresponding to the predefined *ST2_CE3_country_institute.xls*, containing the numerical output of both the deterministic, the uncertainty and the sensitivity analysis.
2. additionally, a .doc-file corresponding to the predefined *ST2_CE2_country_institute.doc*, shortly describing the used uncertainty and sensitivity analysis methods;

Note that the given *ST2_CE2_country_institute.xls* and *ST2_CE2_country_institute.doc* have to be renamed to the participant's actual country and institute name, as e.g. *ST2_CE3_Belgium_KUL.xls*. The two files are to be sent to Hans Janssen: haj@byg.dtu.dk. **Deadline** for submission of your results is **September 30 2011**.

Simulation model for hygrothermal conditions and mould growth potential in cold attics

Carl-Eric Hagentoft¹

1 INTRODUCTION

Problems with high humidity levels in cold attics have been remarkably increasing in Sweden over the last decade. Beside clear evidence – the significant mould growth on the wooden parts of cold attics, which is recently confirmed in about 60-80 % single-family houses in Västra Götaland region (largely the Gothenburg region; Ahrnens C & Borglund E, 2007.), mould odours in indoor air seem to be one of the most frequent side effects. Thus, cold attics are together with crawl spaces singled out as the two worst constructions in existing Swedish buildings with large existing and future mould problems.

The high humidity levels are to a large extent a consequence of the increasing demand on energy efficiency. Houses are frequently retrofitted with additional attic insulation, which leads to a colder attic space and hence a higher humidity (Hagentoft 2008). Leaks of indoor air up to the attic through the attic floor, and the under cooling of the roof due to sky radiation, increase the problem (Holm and Lengsfeld 2006, Sanders et. al 2006, Essah et. al 2009). The moist air might condensate at the underlay and small droplets of liquid water can build up. The water will then be absorbed and accumulated in the surface area. High moisture content can even lead to rot.

Another important moisture source influencing the attic hygrothermal condition is the water vapour in the surrounding outdoor air. The advice given to the building sector in Sweden today is to have a not too high or not too low ventilation rate, by outdoor air, of the attic. A too high ventilation rate, in combination with under cooling, results in high relative humidity (Sasic 2004). Too low ventilation is also risky in case of construction damp or leaky attic floor (Arfvidsson and Harderup 2005, Sanders 2006, Essah 2009). The optimal air exchange rate varies with the outdoor climate, and fixed ventilation through open eaves and/or gable and ridge vents are not always the best choice (Hagentoft et. al 2008, 2010).

2 THERMAL MODEL OF ATTIC

In the modelled attic the roof underlay consists of wooden boards with a water and moisture tight membrane facing the exterior. The attic floor is thermally insulated with varying airtightness towards the living space underneath.

The attic is ventilated through openings at the gables. The model assumes a common resultant attic air temperature. The heat capacity is located in the roof underlay; i.e. the remaining heat capacity of materials in the attic is neglected. The attic temperature is determined by the heat exchange with the outdoor air through ventilation and indoor air through air leakage and heat transmission through the attic floor. The temperature, T , of the underlay is determined by the heat exchange with the attic air temperature, the exterior equivalent temperature and the heat storage by the material itself. In this simple model differences due to the two different oriented sides of the roof are neglected. Basically this corresponds to a low sloped roof.

¹ Chalmers University of Technology, Gothenburg, Sweden, carl-eric.hagentoft@chalmers.se

Indoor temperature is T_i , the exterior temperature T_e and the equivalent temperature for the roof is T_{eq} . Using thermal conductances K (W/K), the following ordinary differential equation can be found for the wooden roof underlay temperature:

$$A d\rho c \frac{dT}{dt} = (T_{res} - T) \cdot K'_{res} + (T_{eq} - T) \cdot K^e \quad (1)$$

Here

$$T_{res} = \frac{K_v^e \cdot T_e + K_{floor} \cdot T_i + K_v^i \cdot T_i}{K_{res}} \quad K_{res} = K_v^e + K_{floor} + K_v^i \quad (2)$$

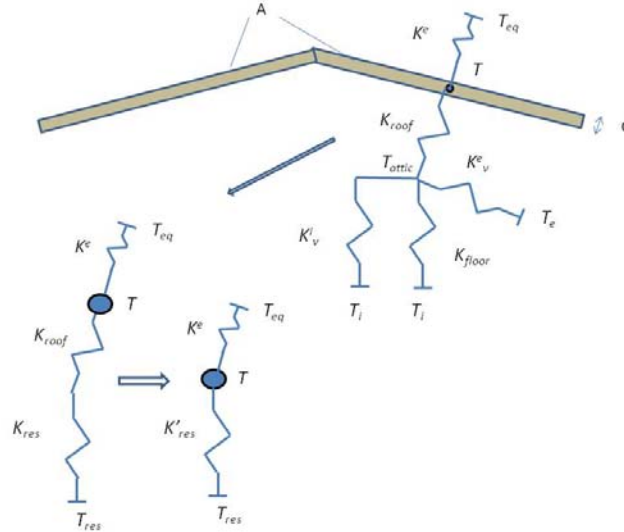


Figure 1. Thermal network of attic using thermal conductances K (with the unit W/K) and a node representing the heat capacity (J/K) of the wooden roof underlay. The second and third network (down left) shows reduced networks.

Here, d (m) represents the thickness of the wooden roof underlay layer, ρc (J/m³K) the volumetric heat capacity of wood, and A (m²) is the total roof surface area. Reduction of two serial coupled conductances gives (Hagentoft 2001):

$$1 / K'_{res} = 1 / K_{res} + 1 / K_{roof} \quad (3)$$

The conductances (W/K) are given by the following expressions:

$$\begin{aligned} K_{floor} &= A \cdot U_{floor} \\ K_v^e &= \rho_a c_{pa} \cdot R_a^e \quad K_v^i = \rho_a c_{pa} \cdot R_a^i \\ K^e &= \frac{A}{1/(\alpha_c + \alpha_r) + R_r + d/2 / \lambda_{roof}} = \frac{A}{R_{se} + R_r + d/2 / \lambda_{roof}} \quad K_{roof} = \frac{A}{R_{si} + d/2 / \lambda_{roof}} \end{aligned} \quad (4)$$

Here, R_a refers to the ventilation flow rate (m³/s) and the indices refer to if it is air from the exterior, e , or the interior, i (air leakage from the room below). The volumetric heat capacity of air, at constant pressure, is denoted $\rho_a c_{pa}$ (J/m³K). The thermal conductivity of wood is denoted λ_{roof} (W/mK). The heat transfer coefficients for long wave radiation and convection are denoted α_r and α_c (W/m²K) respectively. The total surface resistances at the interior and exterior side of the roof are denoted R_{si} and R_{se} (m²K/W) respectively.

The wind will generate the ventilation of the attic. The wind speed used in the calculations is:

$$w = a \cdot H^k \cdot w_0 \quad a = 0.52 \quad k = 0.2 \quad (5)$$

Here w_0 is the wind speed registered at the meteorological station and H is the actual height of the considered building. Since we will consider a rather flat roof, this height will also be used later for the stack effect.

The air pressure at two opposite eaves of the attic is:

$$P_1 = C_{w1} \frac{\rho_a w^2}{2} \quad P_2 = C_{w2} \frac{\rho_a w^2}{2} \quad (6)$$

Here, the density of the air ρ_a will be considered to be constant 1.245 kg/m^3 . The shape factors C_w (-) for an average urban-rural surrounding are given by the vector:

$$[0.2750 \quad -0.3500 \quad -0.5500 \quad -0.3500 \quad -0.4500 \quad -0.3500 \quad -0.5500 \quad -0.3500 \quad 0.2750 \\ -0.3500 \quad -0.5500 \quad -0.3500 \quad -0.4500 \quad -0.3500 \quad -0.5500 \quad -0.3500 \quad 0.2750]$$

For the angle of (in degrees):

$$[-360 \quad -315 \quad -270 \quad -225 \quad -180 \quad -135 \quad -90 \quad -45 \quad 0 \\ 45 \quad 90 \quad 135 \quad 180 \quad 225 \quad 270 \quad 315 \quad 360]$$

The wind direction equal to 0 corresponds to wind from North (90° East 180° South 270° West).

For a rectangular building orientation the orientation, $\varphi_{\text{building surface}} = 0^\circ$ corresponds to a South facing wall, -90° for a East facing wall and $+90^\circ$ for a West facing one. The pressure becomes:

$$P_1 = C_w (\varphi_{\text{building surface}} - (\text{wind angle} - 180^\circ)) \frac{\rho_a w^2}{2} \quad (7)$$

For a building where the eaves are facing west and east and the wind is coming from East the pressure at the eaves become:

$$P_1 = C_w (\varphi_{\text{building surface}}^{\text{west}} - (\text{wind angle} - 180)) \frac{\rho_a w^2}{2}$$

$$P_2 = C_w ((\varphi_{\text{building surface}}^{\text{west}} - 180) - (\text{wind angle} - 180)) \frac{\rho_a w^2}{2}$$

$$P_1 = C_w (90 - (90 - 180)) \frac{\rho_a w^2}{2} \quad P_2 = C_w ((90 - 180) - (90 - 180)) \frac{\rho_a w^2}{2} \quad (8)$$

$$P_1 = C_w (180) \frac{\rho_a w^2}{2} \quad P_2 = C_w (0) \frac{\rho_a w^2}{2}$$

$$P_1 = -0.45 \frac{\rho_a w^2}{2} \quad P_2 = 0.275 \frac{\rho_a w^2}{2}$$

Using mass conservation (assuming constant density of the air) the air pressure in the attic will become:

$$P_{\text{attic}} = \frac{P_1 + P_2}{2} \quad (9)$$

The ventilation rate of outdoor air becomes:

$$R_{ae} = L \cdot A_e \sqrt{\frac{P_1 - P_{\text{attic}}}{\rho_a / 0.845}} \quad R_{ae} \geq 0.001 \text{ m}^3/\text{s} \quad (10)$$

Here, L (m) is the length of the building as well as the length of one eave side and we have used Dicks' formula where A_e (m²/m) represents an effective leakage area per meter eave ventilation. For a typical Swedish cold attic eaves ventilation gap we have approximately $A_e = 0.026$ m²/m i.e. a rectangular hole with the width of 0.026 m (and length of 1 m).

For the leakage of indoor air up to the attic we will assume a building envelope with evenly distributed leakages and a shape factor C_{wi} . The wind generated indoor pressure becomes:

$$P_i = C_{wi} \frac{\rho_a W^2}{2} \quad C_{wi} = -0.3 \quad (11)$$

The stack effect gives an overpressure at the height of the ceiling. Assuming the neutral layer to be in the middle of the building it becomes:

$$P_s = \frac{H}{2} 3456 \left(\frac{1}{T_e} - \frac{1}{T_i} \right) \quad T \text{ in Kelvin} \quad (12)$$

The air leakage from the interior up to the attic becomes:

$$R_{ai} = A_c \sqrt{\frac{P_i + P_s - P_{attic}}{\rho_a / 0.845}} \quad R_{ai} \geq 0 \quad (13)$$

Here, A_c (m²) represents an effective leakage area of the ceiling. Rewriting (3) we get:

$$\begin{aligned} \frac{dT}{dt} &= -T_{factor} \cdot T + T_{e,factor} \cdot T_e + T_{eq,factor} \cdot T_{eq} + T_{i,factor} \cdot T_i \\ T_{factor} &= \frac{1}{A d\rho c} (K'_{res} + K^e) \quad T_{e,factor} = \frac{1}{A d\rho c} K^e \frac{K'_{res}}{K_{res}} \\ T_{eq,factor} &= \frac{K^e}{A d\rho c} \quad T_{i,factor} = \frac{1}{A d\rho c} (K_{floor} + K_v) \cdot \frac{K'_{res}}{K_{res}} \end{aligned} \quad (14)$$

This general way of writing the differential equation will be handy when using our mathematical solver.

The attic air temperature is given by:

$$T_{attic} = \frac{K_{roof} \cdot T + K_{res} \cdot T_{res}}{K_{roof} + K_{res}} \quad (15)$$

The underlay surface temperature is:

$$T_{surf} = T + (T_{res} - T) \frac{K'_{res}}{A_{roof}} \frac{d}{2\lambda} \quad (16)$$

The external equivalent temperature is determined by the exterior air temperature, T_e , the global solar radiation, I_g (W/m²) and the long wave radiation, I_{lw} (W/m²).

$$T^{eq} = T_e + R_{se} \cdot (I_g \cdot \alpha_{sol} + \alpha_r \cdot (T^r - T_e)) \quad T^r = \sqrt[4]{\frac{I_{lw}}{\sigma}} - 273.15 \quad (^\circ\text{C}) \quad (17)$$

Here, T^r represents the apparent sky temperature, and σ is the Stefan-Boltzmann constant. The solar absorptance of the roof surface is denoted α_{sol} .

4 MOISTURE MODEL OF ATTIC

The moisture model assumes that the whole moisture storage capacity of the roof is within the roof underlay material and that the roof surface is perfectly moisture tight. The diffusion of moisture through the attic floor is neglected. The only way for moisture to come in to the attic is by ventilation and air leakages.

The mass balance of the underlay, assuming no condensation at the roof underlay surface, gives:

$$\frac{dM}{dt} = K_{res}^v (v_{res} - v) = K_{res}^v \left(\frac{v_i \cdot R_a^i + v_e \cdot R_a^e}{R_a^i + R_a^e} - v \right) = K_{res}^v \cdot \frac{v_i \cdot R_a^i}{R_a^i + R_a^e} + K_{res}^v \cdot \frac{v_e \cdot R_a^e}{R_a^i + R_a^e} - K_{res}^v \cdot v \quad (18)$$

Here, M (kg), is the total moisture weight of the roof underlay and, v (kg/m^3), is its humidity by volume.

$$R_{a,res} = R_a^i + R_a^e$$

$$v_{res} = \frac{v_i \cdot R_a^i + v_e \cdot R_a^e}{R_a^i + R_a^e} \quad 1/K_{res}^v = \frac{1}{R_{a,res}} + \frac{1}{A/Z} \quad Z = Z_{si} + \frac{d}{2\delta_v} \quad (19)$$

Here, Z (s/m), is the vapour resistance between the air and the centre of the underlay layer and δ_v (m^2/s) is the vapour permeability of wood. The interior and exterior humidity by volume are denoted v_i and v_e (kg/m^3) respectively.

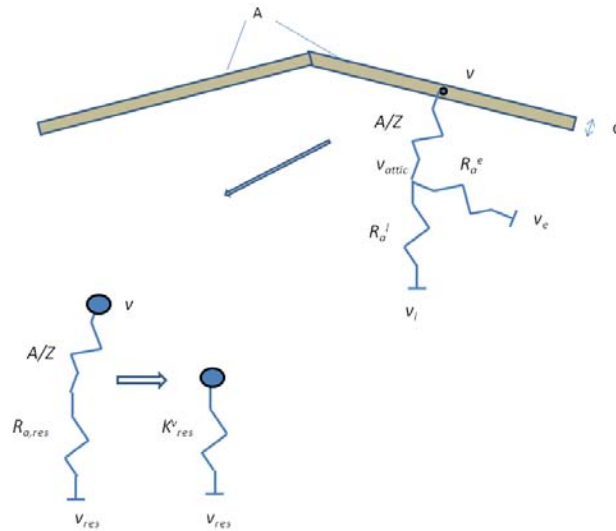


Figure 2. Moisture network of attic using vapour transfer conductances (with the unit m^3/s) and a node representing the moisture capacity of the wooden roof underlay. The second and third ones show reduced networks.

For the case of condensation we get:

$$\frac{dM}{dt} = \overline{K}_{res}^v \cdot (v_{res} - v_{sat}(T_{surf})) \quad v_{res} - v_{sat}(T_{surf}) \geq 0$$

$$\frac{dM}{dt} = \overline{K}_{res}^v \cdot \frac{v_i \cdot R_a^i}{R_a^i + R_a^e} + \overline{K}_{res}^v \cdot \frac{v_e \cdot R_a^e}{R_a^i + R_a^e} - \overline{K}_{res}^v \cdot v_{sat}(T_{surf}) \quad (20)$$

$$1/\overline{K}_{res}^v = \frac{1}{R_{a,res}} + \frac{1}{A/Z_{si}}$$

Here, v_{sat} , denotes the humidity at saturation. We assume that the condensed water on the surface of the underlay is absorbed by the layer. Assuming a known slope, $\zeta(\varphi)$ (-), of the sorption isotherm $w(\varphi)$ (kg/m^3) we can write:

$$\frac{dM}{dt} = Ad\xi \frac{d\varphi}{dt} \quad \xi = \frac{dw}{d\varphi} \quad (21)$$

Combining it with (12) and using the definition of relative humidity we have for the case with no condensation:

$$\frac{d\varphi}{dt} = \left(-\varphi_{factor} \cdot v_{sat}(T) \cdot \varphi + v_{i,factor} \cdot v_i + v_{e,factor} \cdot v_e \right) \frac{1}{\xi} \quad v_{res} - v_{sat}(T_{surf}) < 0 \quad (22)$$

$$\varphi_{factor} = K_{res}^v \frac{1}{A_{roof}d} \quad v_{i,factor} = K_{res}^v \frac{R_a^i}{R_a^i + R_a^e} \frac{1}{Ad} \quad v_{e,factor} = K_{res}^v \frac{R_a^e}{R_a^i + R_a^e} \frac{1}{Ad}$$

, and with condensation:

$$\frac{d\varphi}{dt} = \left(-\bar{\varphi}_{factor} \cdot v_{sat}(T_{surf}) + \bar{v}_{i,factor} \cdot v_i + \bar{v}_{e,factor} \cdot v_e \right) \frac{1}{\xi} \quad v_{res} - v_{sat}(T_{surf}) \geq 0 \quad (23)$$

$$\bar{\varphi}_{factor} = \bar{K}_{res}^v \frac{1}{A_{roof}d} = \frac{\bar{K}_{res}^v}{K_{res}^v} \cdot \varphi_{factor} \quad \bar{v}_{i,factor} = \frac{\bar{K}_{res}^v}{K_{res}^v} \cdot v_{i,factor} \quad \bar{v}_{e,factor} = \frac{\bar{K}_{res}^v}{K_{res}^v} \cdot v_{e,factor}$$

The exterior humidity by volume, v_e , is obtained from weather data. The interior one comes from:

$$v_i = v_e + \Delta v \quad (24)$$

Here, the second term represents the indoor moisture supply (kg/m^3), which will be a random variable:

$$\Delta v = N(\mu_{\Delta v}, \sigma_{\Delta v}) \quad (25)$$

These random numbers are limited to the minimum physically realistically values.

5. MOULD GROWTH MODEL

A fundamental uncertainty lies in how to evaluate the calculations for the temperature and the relative humidity. What we really want to do is to estimate the probability or risk for mould growth in the attic. There are several studies on this subject. However, there is no standardized or widely accepted method for the evaluation of the mould growth risk. Here, we will base the risk assessment on the method developed by (Hukka, Viitanen,1999) to calculate the mould growth index which varies between 0 and 6.

6. INPUT DATA

To be varied:

Height of building H (m)

Area of ceiling floor and roof A (m^2)

$\varphi_{building\ surface}$ Building surface angle for one of the eave sides (0-180°)

Effective leakage area per meter eave ventilation A_e (m^2/m)

Length of building (eave side) L (m)

Thickness of wooden underlay d (m)

Vapour diffusion coefficient of wood δ_v (m^2/s) (around $2 \cdot 10^{-6}$)

Initial relative humidity of wood φ_0 (-).

Thermal conductivity of wood λ_{roof} (W/mK)

Thermal resistance of insulation layer on top of the moisture tight roof membrane R_r ($\text{m}^2\text{K/W}$).

Effective leakage area of attic floor/ceiling A_c (m²)
U-value of the ceiling floor, U_c (W/m²/K)

Indoor temperature T_i (°C).

Mean and standard deviation of indoor moisture supply $\mu_{\Delta v} \sigma_{\Delta v}$ (kg/m³)

Year number for weather data, 1-30 (-)

Fixed data:

The climate data is given for 30 years. Its yearly simulation starts the first of July.

The data contains the equivalent outdoor temperature assuming:

$$\alpha_{sol} = 0.7 \quad \alpha_r = 4 \text{ W/m}^2\text{K}$$

Surface resistance at the inside and outside of attic

$$R_{se} = 0.04 \text{ m}^2\text{K/W} \quad R_{so} = 0.13 \text{ m}^2\text{K/W} \quad Z_{si} = 360 \text{ s/m}$$

Initial temperature of wood 15 °C.

7. OUTPUT DATA

1. [Peak Mould Growth index of the year (-) Heat loss through the attic floor during January (kWh)]

2. Hourly values of:

[Attic temperature (°C) Relative humidity (-) Mould growth index (-) Heat loss through ceiling (W)]

The temperature and relative humidity is for the surface of the roof underlay.

REFERENCES

Ahrenens, C., Borglund E. 2007. Fukt på kallvindar. Master thesis 2007:11. CTH, Building Physics.

Alexandersson, H., 2006. Klimat i förändring: En jämförelse av temperatur och nederbörd 1991-2005 med 1961-1990. Faktablad i Meteorologi nr 29 Oktober 2006. SMHI, SE-601 76 Norrköping, Sweden, 8 pp.

Arfvidsson, J. and Harderup, L-E. 2005. Moisture Safety in Attics Ventilated by Outdoor Air. 7th Symposium in Building Physics, Reykjavik, Island.

Essah, E.A. 2009. Modelling and measurements of airflow and ventilation within domestic pitched roofs. Doctoral thesis. Glasgow Caledonian University, Scotland, UK.

Hagentoft C E 2001, Textbook: Introduction to Building Physics. Studentlitteratur, ISBN 91-44-01896-7.

Hagentoft C.E., Sasic Kalagasidis A., Nilsson S.F., Thorin M. Mould growth control in cold attics through adaptive ventilation. 8th Symposium on Building Physics in the Nordic Countries, Copenhagen, Denmark, June 2008.

Hagentoft C-E, Sasic Kalagasidis A. Mould Growth Control in Cold Attics through Adaptive Ventilation. Validation by Field Measurements. 12th International Conference on Performance of the Exterior Envelopes of Whole Buildings, 2010, Clearwater Beach, Florida.

Holm, A., Lengsfeld, K. 2006. Hygrothermal performance of unfinished attics (ventilated roofs) – an experimental study. Research in Building Physics and Building Engineering. Proceedings from the third International Building Physics Conference, Montreal, Canada.

Hukka E., Viitanen H.A., 1999. A mathematical model of mould growth on wooden material. *Wood Science and Technology* 33, Springer-Verlag.

Samuelson, I. 1995. Hygrothermal performance of attics. In Swedish. SP Report 1995:68, Sweden.

Sanders, C.H. 2006. Modelling condensation and airflow in pitched roofs – Building Research and Establishment (BRE) information paper, IP 05/06. BRE Press, Garston, Watford – UK. ISBN 1-86081-912-5, pp. 1-7

Sasic Kalagasidis A. 2004. HAM-Tools. An Integrated Simulation Tool for Heat, Air and Moisture Transfer Analyses in Building Physics. Doctoral thesis. Chalmers University of Technology, Sweden.

IEA, Annex 14. Condensation and Energy, Catalogue of Material Properties Vol 3, IEA-ECBCS. K.U Leuven, Belgium 1992.



IEA-ANNEX 55

Reliability of Energy Efficient Building Retrofitting -
Probability Assessment of Performance and Cost
(RAP-RETRO)

SUBTASK 2, COMMON EXERCISE 4 - INSTRUCTION DOCUMENT

HANS JANSSEN / STAF ROELS, DECEMBER 2011

COMMON EXERCISE 4: METAMODELLING OF THE HYGROTHERMAL PERFORMANCE OF COLD ATTICS

– INSTRUCTION DOCUMENT –

Hans Janssen, Staf Roels, December 2011

1. Objectives of Common Exercise 4

Annex 55's Subtask 2 'Probabilistic tools' aims at developing a probabilistic methodology to predict the energy savings of retrofitting measures while concurrently assessing the risk of potential hygrothermal failure. In the final stage of the Annex it should be possible to apply this methodology in a generic way to e.g. make decisions on retrofitting measures for a typical building stock. The subtask's prime target is to get familiar with probabilistic methodologies, to investigate the limits and possibilities of stochastic models for our specific problems, to consider possible bottle necks for applications in the field of building physics, etc. Three common exercises (CE) have already been executed within Subtask 2: CE1 aimed at exploring qualitative probabilistic tools, CE2 focused on quantitative uncertainty analysis, and CE3 targeted methods for sensitivity analysis.

The topic of CE4 is the metamodelling of the hygrothermal performance of cold attics, particularly the mould growth in the attic and the heat loss to the attic. Metamodelling techniques are an essential element of probabilistic tools, since the execution time for the deterministic core model often is a restrictive factor. This implies that only a small number of runs are actually feasible, which hinders the application of standard methods for uncertainty and sensitivity analysis or for performance and robustness optimization. To resolve this, an approximate surrogate model – or metamodel – is fitted on the limited Monte Carlo set, which is then used instead of the original model for the further exploration and/or optimization. The primary aim of CE4 is thus to explore approaches for metamodelling. As simulation time is a primary motivation for metamodelling though, the influence of the initial sample size forms an important focus point in this CE. The choice of methods is free, and CE 4 hence generally targets an overview of different metamodelling methods and a comparison of their efficiency.

2. General description of the Exercise

As was done in the previous common exercise, a common calculation object and tool is used, to avoid interference from deviations in modelling and/or simulation approaches. The given cold attic model determines the cold attic performances – heat loss & mould growth – in function of 15 different input parameters, each with its specific distribution.

An introduction to the physical basis of the cold attic model has been given earlier, in the instruction for CE3, and you are referred to that instruction document for further information. The physical model has been implemented in Matlab, and `Cold_Attic_4.m` is provided. The model uses 15 different input parameters – material properties, component characteristics, geometric dimensions, climate values – to compute 2 outcomes – the yearly peak mould growth index (PMG, -) for the wooden underlay, and the cumulated heat loss through the ceiling in January (CHL, kWh/m²). For detailed analyses, hourly values of the surface temperature and surface relative humidity of the wooden underlay, mould growth index on the wooden underlay and the ceiling heat losses are also provided by the program.

The 15 different input parameters are collected in Table 1. Table 1 equally gives the related symbol in the .m-file, and the probability distribution of each parameter. Two types of distributions are used: uniform distributions $U(x_{low}, x_{upp})$, and normal distributions $N(x_{avg}, x_{std})$. In the former, x_{low} and x_{upp} indicate respectively the lower and upper limit of the uniform distribution; in the latter, x_{avg} and x_{std} indicate the average and standard deviation respectively of the normal distribution. For all normally distributed parameters, a lower limit of 0 is moreover implicitly assumed: all samples resulting in values lower than 0 are to be replaced by 0.

Important in the table is the range for the U-value of the ceiling: since the resulting metamodel must be applicable for the cold attic before as well as after the application of (extra) floor insulation, a wide range of values is put forward. Other important changes in relation to CE3 are:

- the range for the 'leakage area per m² of ceiling A_c' is reoriented to more realistic values;
- the 'year of climate data used' is to be fixed on year 5, thus excluding climate variations;

Table 1: variable input parameters, .m-file symbol, probability distribution

input parameter	symbol	distribution
Height of building H (m)	H	U(4,8)
Area of ceiling and roof A (assumed equal) (m ²)	Area	U(50,200)
Orientation of one of eave sides (-)	BSangle	U(0,180)
Venting area per meter eave A _e (m ² /m)	Ae	U(0.001,0.05)
Length of building (eave side) L (m)	Length	U(7,20)
Thickness of wooden underlay d (m)	d	U(0.010,0.020)
Vapour diffusivity of wood δ _v (m ² /s)	deltav	N(10 ⁻⁶ ,2 10 ⁻⁷)
Initial relative humidity of wood φ ₀ (-)	startRH	U(0.5,0.9)
Thermal conductivity of wood λ _{roof} (W/mK)	lambda	N(0.13,0.02)
Resistance of roof insulation R _r (m ² K/W)	Rr	U(0,1)
Leakage area per m ² of ceiling A _c (m ² /m ²)	Ac	U(10 ⁻⁵ ,5 10 ⁻⁵)
U-value of the ceiling U _c (W/m ² K)	Ufloor	U(0.2,5)
Indoor temperature T _i (°C)	Ti	N(20,1.5)
Indoor moisture supply (kg/m ³)	MS	N(0.005,0.002)
Year of climate data used (-)	Year	fixed value: 5

In this CE, the main aim of the metamodeling efforts is 'design space approximation': the goal is to obtain a quicker approximate model to stand in for the original model. The approximate model therefore must mimic the original model as good as possible over the entire parameter space.

In all cases, the quality of the developed metamodels will be assessed by comparison with the original model at 100 reference points in the parameter space. The input parameters' values for all reference points are given, **but these samples should in no way be used to guide the metamodeling.**

To (virtually) account for limitations on calculation time, the metamodeling is to happen based on four different initial sample sizes, consisting of 5, 15, 50 and 150 points. The actual sampling designs can be freely chosen. The small sample sizes allow evaluation of supersaturated metamodeling designs, while the larger sample sizes permit assessment of actual metamodeling methods. Only information obtained from a single sample set can be used in the metamodeling process: no information of independent analyses may be imported.

A first introduction to metamodeling techniques and approaches can be found in literature. Exemplary publications are:

- Simpson TW, Peplinski JD, Koch PN, Allen JK, 2001. Metamodels for computer-based engineering design: survey and recommendations, *Engineering with Computers* 17, 129-150;
- Jin R, Chen W, Simpson TW, 2001, Comparative studies of metamodeling techniques under multiple modelling criteria, *Structural and Multidisciplinary Optimisation* 23, 1-13;
- Kleijnen JPC, Sargent RG, 2000. A methodology for fitting and validating metamodels in simulation, *European Journal of Operational Research* 120, 14-29;
- JohnsonRT, Montgomery DC, Jones B, Parker PA, 2010. Comparing computer experiments for fitting metamodels, *Journal of Quality Technology* 42, 86-102;

These four publications are provided together with this common exercise.

3. Task specification for the Exercise

3.1 Metamodeling on 5 initial samples

Make 5 initial simulations with the provided cold attic model. Use these 5 sets of input parameters and simulation outcomes to develop a metamodel for the cold attic's CHL and PMG. Calculate the metamodel's output for the 100 reference points (coordinates given in the excel file).

3.2 Metamodelling on 15 initial samples

Make 15 initial simulations with the provided cold attic model. Use the 15 sets of input parameters and simulation outcomes to develop a metamodel for the cold attic's CHL and PMG. Calculate the metamodel's output for the 100 reference points (coordinates given in the excel file).

3.3 Metamodelling on 50 initial samples

Make 50 initial simulations with the provided cold attic model. Use the 50 sets of input parameters and simulation outcomes to develop a metamodel for the cold attic's CHL and PMG. Calculate the metamodel's output for the 100 reference points (coordinates given in the excel file).

3.4 Metamodelling on 150 initial samples

Make 150 initial simulations with the provided cold attic model. Use these 150 sets of input parameters and simulation outcomes to develop a metamodel for the cold attic's CHL and PMG. Calculate the metamodel's output for the 100 reference points (coordinates given in the excel file).

4. Requested output of the exercise

Common Exercise 4 participants are requested to deliver two documents:

1. a .xls-file corresponding to the predefined *ST2_CE4_country_institute.xls*, containing the numerical results: in each of the four worksheets, the input parameters and the simulation outcomes for the 5/15/50/150 initial modelling simulations are to be provided, as well as the 100 simulation outcomes from the final metamodelling simulations for the given reference points.
2. additionally, a .doc-file corresponding to the predefined *ST2_CE4_country_institute.doc*, shortly describing the methodologies applied for the different metamodelling exercises;

Note that the given *ST2_CE4_country_institute.xls* and *ST2_CE4_country_institute.doc* have to be renamed to the participant's actual country and institute name, as e.g. *ST2_CE4_Belgium_KUL.xls*. The two files are to be sent to Hans Janssen: hans.janssen@bwk.kuleuven.be. **Deadline** for submission of your results is **March 30 2012**.



IEA-ANNEX 55

Reliability of Energy Efficient Building Retrofitting -
Probability Assessment of Performance and Cost
(RAP-RETRO)

SUBTASK 2, COMMON EXERCISE 5 - INSTRUCTION DOCUMENT

HANS JANSSEN / STAF ROELS, JUNE 2012

COMMON EXERCISE 5: **ECONOMIC ASSESSMENT OF RETROFITTING MEASURES**

– INSTRUCTION DOCUMENT –

Hans Janssen, Staf Roels, June 2012

1. Objectives of Common Exercise 5

Annex 55's Subtask 2 'Probabilistic tools' deals with developing a probabilistic methodology to predict the energy savings of retrofitting measures while concurrently assessing the risk of potential hygrothermal failure. The subtask's prime target is to get familiar with probabilistic methodologies, to investigate the limits and possibilities of stochastic models for our specific problems, to consider possible bottle necks for applications in the field of building physics, etc. Four common exercises (CE) have already been executed within Subtask 2: CE1 aimed at exploring qualitative probabilistic tools, CE2 focused on quantitative uncertainty analysis, CE3 targeted methods for sensitivity analysis and CE4 dealt with metamodelling.

In the final stage of the Annex it is the aim to apply the developed methodology in a generic way by making decisions on retrofitting measures for a typical building stock. Hence, this last common exercise within ST2, CE5, will continue and combine the work done so far: stochastic modeling of benefits and risks, but now on a larger scale and from an economic perspective. To limit the work load, we stick to the Swedish attic model (see ST2-CE3 and CE4). Global objective is to determine the most profitable attic renovation measure for a neighbourhood of 237 dwellings. Instead of the earlier cumulated heat loss and peak mold growth indicators (see CE3 and CE4), now the overall cost is assumed the performance criterion.

So you can imagine yourself being a consultant for an ESCO (Energy Saving Company) that will renovate the attics of all 237 dwellings. Different renovation measures (such as adding attic floor insulation, increasing air tightness of ceiling, closing ventilation gaps,...) can be applied (and if relevant combined), but of course each renovation measure corresponds to a certain cost, will result in certain benefits (energy savings) and may result in hygrothermal risks (mould growth). Your task is to come up with the renovation measure (applicable to all dwellings) that results in the **largest overall profit within a timespan of ten years**.

2. General description of the Exercise

As was done in the previous common exercise, a common calculation object and tool is used, to avoid interference from deviations in modelling and/or simulation approaches. The cold attic model, used in CE3 and CE4, has been reoriented to tackle different renovation measures. An introduction to the physical basis of the cold attic model has been given earlier, in the instruction for CE3, and you are referred to that instruction document for further information. The updated physical model has been implemented in Matlab, and Cold_Attic_5.m is provided. Compared to the previous version, now a series of subsequent 10 years will be calculated, starting at the year indicated in the input file.

The model allows the following scenarios for renovation:

1. Increasing the insulation level of the attic floor
2. Increasing the airtightness of the attic floor
3. Sealing the ventilation gaps at the eaves.

As said, different scenarios can be combined. The expected outcome is the pdf's of the overall profit over ten years for the different scenarios.

As in CE4, the Swedish attic model uses 15 different input parameters: material properties, component characteristics, geometric dimensions, climate values, to compute 2 outcomes for each year: the yearly peak mould growth index (PMG, -) for the wooden underlay, and the heat loss through the ceiling cumulated over the heating season (CHL, kWh). The results are provided as one column with 20 values: 10 yearly PMG's, followed by 10 yearly CHL's.

The 14 different input parameters for the original state of the dwellings are collected in Table 1. Table 1 equally gives the related symbol in the .m-file, and the probability distribution of each parameter. Two types of distributions are used: uniform distributions $U(x_{low}, x_{upp})$, and normal distributions $N(x_{avg}, x_{std})$. In the former, x_{low} and x_{upp} indicate respectively the lower and upper limit of the uniform distribution; in the latter, x_{avg} and x_{std} indicate the average and standard deviation respectively of the normal distribution. For all normally distributed parameters, a lower limit of 0 is moreover implicitly assumed: all samples resulting in values lower than 0 are to be replaced by 0.

Table 1: variable input parameters, corresponding .m-file symbol and probability distribution for the original state of the dwellings

input parameter	symbol	distribution
Height of building H (m)	H	U(4,8)
Area of ceiling and roof A (m ²)	Area	U(50,200)
Orientation of one of eave sides (-)	BSangle	U(0,180)
Venting area per meter eave A _e (m ² /m)	Ae	U(0.01,0.05)
Length of building (eave side) L (m)	Length	U(7,20)
Thickness of wooden underlay d (m)	d	U(0.01,0.02)
Vapour diffusivity of wood δ_v (m ² /s)	deltav	N(10^{-6} , $2 \cdot 10^{-7}$)
Initial relative humidity of wood ϕ_0 (-)	startRH	U(0.5,0.9)
Thermal conductivity of wood λ_{roof} (W/mK)	lambda	N(0.13,0.02)
Resistance of roof insulation R _r (m ² K/W)	Rr	U(0,1)
Effective leakage area per m ² of ceiling A _c (m ² /m ²)	Ac	U(10^{-5} , 10^{-4})
U-value of the ceiling U _c (W/m ² K)	Uc	U(1,3)
Indoor temperature T _i (°C)	Ti	N(20,1.5)
Indoor moisture supply (kg/m ³)	MS	N(0.005,0.002)

For the different renovation measures the following input parameters change:

1. Increasing the insulation level of the attic floor will reduce the U-value of the ceiling (no lower limits of **Ufloor** are given). Due to uncertainties in workmanship the finally obtained U-value has a normal distribution around the target value with a standard deviation of 10% of the target value.

$$\text{U-value of the ceiling } U_c^{\text{new}} \text{ (W/m}^2\text{K)} \quad U_c \quad N(U_{c,\text{target}}, 0.1 * U_{c,\text{target}})$$

2. Increasing the airtightness of the attic floor means reducing the effective leakage area of the ceiling **Ac** to a new distribution. The lowest achievable effective leakage area is considered to be $5 \cdot 10^{-8}$ m²/m². The finally obtained leakage area has a normal distribution around the target value with a standard deviation of 20% of the target value.

$$\text{Effective leakage area of ceiling } A_c^{\text{new}} \text{ (m}^2\text{)} \quad A_c \quad N(A_{c,\text{target}}, 0.2 * A_{c,\text{target}})$$

3. Sealing the ventilation gaps at the eaves diminishes the venting area per meter eave **Ae**. As for the airtightness of the attic floor, there is a lower limit on the achievable closing of the venting gaps: $2.5 \cdot 10^{-5}$ m²/m. The finally obtained venting area per meter eave has a normal distribution around the target value with a standard deviation of 40% of the target value.

$$\text{Venting area per meter eave } A_e^{\text{new}} \text{ (m}^2\text{/m)} \quad A_e \quad N(A_{e,\text{target}}, 0.4 * A_{e,\text{target}})$$

Of course, each renovation scenario corresponds to a certain cost. Table 2 gives for each scenario mean and spread on the expected costs.

Table 2: costs related to the different renovation measures

renovation measure	cost	
1.insulating attic floor	$8.0+1.2*(1/U_c^{new} - 1/U_c^{old})$	euro/m ²
2. increasing air tightness of attic floor	$5.0+3.0*10^{-7}/A_c^{new}$	euro/m ²
3.sealing ventilation gaps at the eaves	$12.0 + 3.0*10^{-4}/A_e^{new}$	euro/m
Repair cost if PMG > 5	58.0	euro/m ²

The largest overall profit within the timespan of 10 years is evaluated based on the net present value (NPV), simplified as:

$$NPV = -I_0 - I_M + \sum_{i=1}^{10} \frac{\Delta K_E (1 + r_E)^i}{(1 + a)^i}$$

in which I_0 corresponds to the initial investment of the renovation measure, I_M is the maintenance cost, ΔK_E the change in annual energy costs due to the renovation measure, r_E the inflation corrected mean annual increment in energy cost ($0 < r_E < 1$) and a the inflation corrected present value factor ($0 < a < 1$). Note that no corrections on the maintenance cost are taken into account, but that the maintenance cost is simplified as an overall repair cost which has to be taken into account in case the peak mould growth index (PMG, -) for the wooden underlay exceeds a value of $PMG \geq 5$ within 10 years (see Table 2). This overall repair costs corresponds to drying up the roof construction, renovation of the roof from mould and installation of a controlled ventilation system to avoid mould in the future. Therefore, it is assumed that this repair cost has to be taken into account **only once** even if the PMG exceeds a value of 5 multiple times.

The inflation corrected present value factor and mean annual increment in energy cost have to be treated as normal distribution with mean and standard deviation given in Table 3. The annual change in energy costs corresponds to:

$$\Delta K_E = P_E \Delta E_{use,heating}$$

with P_E the price per kWh (see Table 3) and $\Delta E_{use,heating}$ the difference in yearly cumulated heat loss through the ceiling between original state and after applying the renovation measure.

Table 3: probability distribution functions for the present value factor, mean annual increment in energy cost and energy price

	symbol	distribution
Inflation corrected present value factor	a	N(0.07,0.015)
Inflation corrected mean annual increment in energy cost	r_E	N(0.065,0.0175)
Energy price per kWh	P_E	0.10 euro/kWh

To limit the scope of the exercise, we will not take possible climate change into account. As in ST2-CE4, 30 years of climate data are provided, all of them assumed equally realistic for the near future. The provided Matlab-code calculates over 10 subsequent years, starting at the year indicated in the input file. Hence, the first 21 years of provided climate data may be treated as a uniform distribution:

Year of climate data used (-)	Year	U(1,21)
-------------------------------	------	---------

Note, that for this uniform distribution, of course only discrete integer values are allowed.

3. Task specification for the Exercise

3.1 Optimal insulation thickness for scenario 1

Increasing the insulation level of the attic floor (scenario 1) can be seen as the first and easiest choice for an ESCO to apply. Therefore, as an introductory step, participants are requested to determine the optimal U-value of the ceiling $U_{c,target}$ for scenario 1: increasing the insulation level of the attic floor without changing the air tightness of the ceiling or closing venting gaps. The optimal $U_{c,target}$ is determined as the U-value resulting in the maximum total net present value (NPV_{total}) (timespan of ten years) when applied to all 237 dwellings. For each $U_{c,target}$ the NPV_{total} can be calculated as the integral of the pdf of NPV over the dwelling distribution. To compare results, the NPV_{total} as a function of $U_{c,target}$, as well as the cdf of the NPV for the optimal $U_{c,target}$ are to be provided in the predefined .xls-file. Two cases are to be considered:

- a) In a first case only the benefits are investigated. This means that the risks on mould growth can be neglected (repair cost $I_M=0$).
- b) In a second step, both benefits and risks are taken into account. If the PMG reaches a value of 5 in a year, the repair cost of Table 2 has to be incorporated in the NPV.

3.2 Optimal solution

Participants are requested to determine the optimal solution, by applying one of the three given scenarios or a combination of them. For each of the scenarios the level of improvement can be varied. The optimal solution corresponds to the solution with the maximum NPV_{total} . So, the NPV_{total} for the different scenarios are to be provided and if available, the pdf's of the NPV for the different scenarios can be given as well in the predefined .xls-file. In addition, a short text in the predefined .doc-file should document the applied approach.

4. Requested output of the exercise

Common Exercise 5 participants are requested to deliver two documents:

1. a .xls-file corresponding to the predefined *ST2_CE5_country_institute.xls*, containing the numerical output of the NPV_{total} as a function of the insulation thickness and pdf's of the NPV over ten years when applying only extra attic floor insulation (see 3.1) and presenting the results for the optimal solution (see 3.2).
2. additionally, a .doc-file corresponding to the predefined *ST2_CE5_country_institute.doc*, shortly describing the used methods: variations taken into account, applied technique: Monte Carlo-analysis, number of runs, sampling strategy, metamodeling,....

Note that the given *ST2_CE5_country_institute.xls* and *ST2_CE5_country_institute.doc* have to be renamed to the participant's actual country and institute name, as e.g. *ST2_CE5_Belgium_KUL.xls*. The two files are to be sent to Staf Roels: staf.roels@bwk.kuleuven.be. Deadline for submission of the results is October 15th 2012.